

# **Landslide Dam Hazard Modelling in the West Coast Region, New Zealand**

A thesis submitted in fulfilment for the degree

of

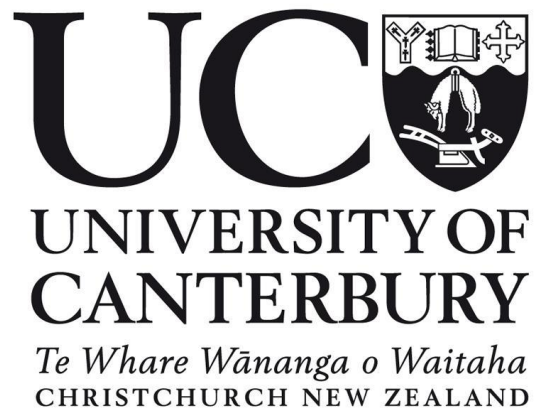
**Master of Science**

at the University of Canterbury

by

**Jane McMecking**

October 2022



## Abstract

Landslide dams are common in mountainous regions with steep narrow valleys and can expose downstream communities and critical infrastructure to large intense outburst floods. Large earthquakes such as the M 7.8 Kaikōura earthquake in New Zealand in 2016 and the M 7.9 Wenchuan earthquake in China in 2008 can form hundreds of landslide dams in a single event. As a result, we have considerable information on the locations where landslide dams occur after a large earthquake, and in particular there is extensive research on where landslide dams formed during the Kaikōura earthquake. However, there is limited research predicting where potential landslide dams may form in future, particularly on a regional scale.

In New Zealand, the West Coast Region is prone to large earthquakes due to the presence of the plate boundary that forms the Alpine Fault and has experienced large landslide dams in the past, however there is limited understanding of where landslide dams may form in the future. This study developed a regional model to identify where landslide dams are most likely to form and applied it to the West Coast Region. The model combined valley width with local relief for mapped landslide dams in the Kaikōura Region as a result of the 2016 earthquake to identify the types of locations in which landslide dams occurred. This showed that 98% of landslide dams formed in locations where local relief was equal to or exceeded local valley width.

This simple relationship was then applied to the West Coast Region with the addition of upstream area to act as a proxy for the size of any potential lake in order to determine the most high hazard locations on the West Coast Region. Overall, the Haast, Hokitika, and Whataroa catchments were shown to have the most considerable landslide dam hazard, with the Haast catchment being particularly hazardous. Larger catchments with wide floodplains such as the Buller and Grey catchments had lower landslide dam hazard despite their size.

Outburst flood modelling was then undertaken at four high hazard sites in the Haast, Hokitika, and Whataroa catchments for nominal dam heights of 10 m and 50 m, to determine the critical infrastructure exposed to outburst floods. This showed that, of the four sites, outburst flooding in the Hokitika catchment could affect the most people and infrastructure in total, however outburst flooding could be more devastating to local communities in the

Haast catchment due to a higher relative exposure. Combining the potential for large earthquakes from the Alpine Fault and the vulnerability of the West Coast Region suggests the hazard and risk from landslide dams and potential outburst flooding is high across the entire region. There is therefore an urgent need to understand the local vulnerability and prepare emergency response plans and mitigation actions prior to a major earthquake in the West Coast Region.

## Acknowledgements

Firstly, a huge and most important thank you to my main supervisor Dr Tom Robinson for his ongoing support and advice throughout this project and sharing his knowledge.

To my co-supervisors, Dr Andrea Wolter and Dr Tim Stahl, thank you for your support, expertise and guidance on this journey.

To my funders, Toka To Ake (EQC), QuakeCoRE and Mason Trust thank you for providing this opportunity and being able to contribute to research in this field.

Special thank you to Livvy for helping with fieldwork on the West Coast and your amazing positive attitude while being eaten alive by sandflies.

Thank you to my family and friends who backed my decision to return to university, I wouldn't have been able to do this without you.

Finally thank you to everyone in the School of Earth and Environment and especially the Disaster Risk and Resilience Group for the encouragement, support, friendships, and ongoing opportunities. I've really enjoyed working with you all.

## Table of Contents

Abstract.....	2
Acknowledgements.....	4
1 Introduction.....	10
1.1 Landslide Dam Overview.....	10
1.2 Where do landslide dams form?.....	11
1.3 New Zealand.....	12
1.3.1 Kaikōura earthquake.....	13
1.3.2 The West Coast Region.....	14
1.4 Research overview.....	18
1.4.1 Research Objectives.....	18
1.4.2 Research Aims.....	19
1.4.3 Research Questions.....	19
1.4.4 Thesis Structure.....	20
2 Literature review.....	21
2.1 Overview of Landslide Dams.....	21
2.1.1 Description, formation, and triggers.....	21
2.1.2 Failure styles and outburst flooding.....	24
2.2 Landslide dam hazard modelling.....	27
2.2.1 Dam formation and stability.....	27
2.2.2 Outburst flood modelling.....	30
2.3 Global Landslide Dams and Outburst floods.....	31
2.3.1 Distribution and global hotspots.....	31
2.3.2 International Case Studies.....	32
2.4 Landslide dams in New Zealand.....	35
2.4.1 2016 Kaikōura earthquake and landslide dams.....	35
2.5 West Coast Region.....	39
2.5.1 Poerua River Landslide Dam.....	41
2.5.2 Ram Creek Landslide Dam.....	44
2.5.3 Callery River, Westland.....	45
3 Methods.....	47
3.1 Conceptual Overview.....	47
3.2 Valley width.....	48
3.2.1 Identification of valley bottoms.....	50
3.2.2 Measuring Valley Bottom Width.....	52
3.2.3 Valley Width Validation.....	54

3.2.4	Landslide volume proxy – local relief.....	57
3.2.5	Aggregated Landslide Dam Hazard .....	59
3.3	Outburst Flood Hazard.....	60
3.3.1	Exposure.....	60
4	Results.....	62
4.1	Kaikōura Region Analysis .....	62
4.2	Comparison between West Coast and Kaikōura Regions .....	63
4.3	Catchment Scale Analysis.....	66
4.4	Selection of outburst flooding locations.....	72
4.5	Outburst flooding.....	77
4.6	Summary of key findings.....	84
5	Discussion.....	85
5.1	How does landslide dam potential in the West Coast region compare globally? .....	85
5.2	How can we determine where the most high hazard locations are in the West Coast Region? .....	87
5.3	What critical infrastructure is exposed to outburst flood hazard from landslide dams? .....	92
5.4	What is the risk from landslide dams on the West Coast of New Zealand?.....	94
5.5	Recommendations for future work .....	96
6	Conclusions .....	97
	References .....	98

## Table of Figures

Figure 1- Schematic diagram of key landslide dam features and the processes that can result in their failure. Adapted from (Liu et al., 2019). .....	11
Figure 2- Worldwide known landslide dam locations summarised by country (Zheng et al., 2021).....	12
Figure 3- Map of New Zealand showing active fault lines. The Ocean Basemap highlights the subduction zones to the south and north-east of New Zealand. ....	13
Figure 4- West Coast Region with major towns, State Highways and the Alpine Fault. ....	15
Figure 5- Median annual total rainfall (1981-2010) for the West Coast Region illustrating the high rainfall experienced in the region (Macara, 2016). ....	17
Figure 6- Mapped existing and past landslide dams in the West Coast region of New Zealand Morgernstern et al (in Prep). ....	18
Figure 7- Formation of a landslide dam lake – modified from (Shrestha et al., 2012). ....	22
Figure 8- Geomorphometric landslide dam classification (Fan et al., 2020). ....	23
Figure 9- Flooded homes immediately upstream of the 2014 Jure landslide dam in Nepal following the controlled breach and draining of the resulting lake. Sediment deposits on top of the houses shows they were completely submerged by the upstream flooding from the blockage.....	27
Figure 10- Schematic plot of the Morphological Obstruction Index showing the non-formation line and the formation line. Landslide volume is on the y axis and valley width on the x axis (Tacconi Stefanelli et al., 2020). ....	29
Figure 11- Worldwide distributions of existing landslide inventories and recent large landslide dams in different regions. The yellow stars are landslide dam locations, the circles relate to countries, and the numbers inside the brackets are the total number of landslide dams (Fan et al., 2020). ....	32
Figure 12: Helicopter view of the Tangjiashan landslide dam and scarp (Xu et al., 2009). ....	34
Figure 13- The 28 July 1987 Val Pola rock avalanche with the impounded lake, looking downstream (Crosta et al., 2004). ....	35
Figure 14- The location of significant landslides (pink polygons) and landslide dams (red crosses) generated during the 2016 Kaikōura Earthquake (epicentre shown by red star), overlain onto the mean Peak Ground Acceleration (PGA) experienced in the region. Areas with light to moderate (green dash) and severe (black dash) landslide damage are shown. Surface fault ruptures are shown by solid black lines (Morgenstern et al., 2020). ....	37
Figure 15 - Landslide dam on the Leader River. The landslide is a slump/block slide in a siltstone unit. The landslide dam overtopped and partially breached on the 15 <sup>th</sup> of November 2016 within 24 hours after the earthquake, with the full breach occurring on the 13 <sup>th</sup> – 14 <sup>th</sup> of February 2017 (Dellow et al., 2017a).....	38
Figure 16 - a) Hapuku River Landslide dam showing source area, landslide dam and valley downstream of dam. This is a greywacke dam with internal flows apparent as water is flowing through the dam (Dellow et al., 2017a). b) Greywacke Landslide dams visible in the Conway River. Neither of these overtopped, however developed flow through the permeable rock (Dellow et al., 2017a). ....	38
Figure 17- The location of landslide dammed lakes and former landslide dams in New Zealand updated from (Korup, 2004), (Morgenstern et al., 2020). ....	40
Figure 18 Aerial view of the Poerua landslide dam and lake on the 8th of October 1999, the day after overtopping (Hancox et al., 2005). ....	41
Figure 19- Oblique aerial photos of the Poerua River fan showing the effects of the dam break flood. October 1999, 2 days after the dam breach (Hancox et al., 2005). ....	43

Figure 20- Oblique aerial photos of the Poerua River fan showing the effects of the dam break flood. August 2001, after 22 months of sediment aggradation and erosion (Hancox et al., 2005). ....	43
Figure 21 Waiho river flowing from the Southern Alps and looking south. C and Red Lines = Callery catchment; W = Waiho catchment; T = Tatara river; TC = Tatara catchment; WL = Waiho Loop; FJ = Franz Josef township; O = oxidation ponds; LM = Lake Mapourika. Dashed line = Alpine fault. Franz Josef glacier at top right. White lines = stopbanks. Arrow = anticipated course of future avulsion. Inset – location map (Davies et al., 2013). .....	46
Figure 22- Flow Chart of method for identifying the hazard and exposure of the West Coast Region to landslide dam outburst flooding. ....	48
Figure 23- Conceptual graph of relief vs valley width. Red areas have the highest landslide hazard potential, with narrow valleys and high relief, while orange areas still have landslide dam potential, however due to low relief or wide valleys is not as significant. Green areas are unlikely to be a landslide dam hazard. ....	49
Figure 24 Comparison of the two measuring valley bottom approaches a) Jones Method b) TPI method. The TPI method is more accurate as it takes into account the smaller order 1, 2 and 3 streams and visually matches river valleys. ....	52
Figure 25- Valley width mapping using GIS for the Whataroa River catchment showing valley width points, transects, river network and the TPI Valley layer.....	53
Figure 26: Fieldwork locations a) Mid Whataroa (Mid Catchment) b) Lower Whataroa (Lower Catchment) c) Little Man River (Upper Catchment).....	54
Figure 27: Laser Telemeter in use for measuring distance and height (Nikon, 2011). ....	55
Figure 28: Fieldwork locations in the Whataroa catchment, Little Man River= Yellow, Lower Whataroa= Blue and Mid Whataroa = Green. ....	56
Figure 29: Field Measurements vs valley width model in the Whataroa catchment with vertical uncertainty bars.....	57
Figure 30- Kaikōura Region with valley width measurements overlaid with valley points (green) located within 100m of a historic landslide dam (Morgenstern et al., in prep).....	58
Figure 31- Kaikōura valley points, with orange points representing historical dams from the Morgenstern et al. (in prep) dataset. ....	62
Figure 32- Valley width method applied to the West Coast Region and Kaikōura Region. This highlights the spatial variation as the West Coast Region is significantly larger than the Kaikōura Region. The West Coast Region also has a higher percentage of large valley widths (yellow lines) primarily due to the broad alluvial plains west of the Alpine fault. ....	64
Figure 33- Modelled valley widths in the region surrounding the Whataroa catchment highlighting the typically narrow valley widths east of the Alpine Fault compared to the much wider valley widths west of the Alpine Fault. ....	64
Figure 34- Valley width frequency for the West Coast Region vs Kaikōura Region. For both regions valley widths increase until 75-99 m, then rapidly decrease, forming a similar bell curve. The longer tail for the West Coast Region indicates the larger catchment area and high frequency of floodplains. Valley width frequency on the East of the Alpine Fault follows a similar bell curve to Kaikōura, while West of the Alpine Fault appears more bi-modal, with a much higher frequency of wide (>300 m) valleys.....	65
Figure 35- West Coast Region Valley Points with orange points representing known dam sites from the Morgenstern et al. (in prep) dataset. The reference line shows locations where local relief equals local valley width. 86% of known landslide dams occur above this threshold, notably lower than observed in Kaikōura Region (Figure 31). ....	65
Figure 36- Location and extent of the eight major catchments evaluated within the West Coast Region. Note that part of the Buller catchment extends into Tasman Region, which was not included in	



this study. Values quoted throughout correspond to only the catchment area within the West Coast Region. ....	66
Figure 37- Frequency of valley points for the eight major catchments in the West Coast Region, demonstrating a similar bell curve for each catchment, where valley widths increase to 75-99 m, then rapidly decrease. The Whataroa catchment has the highest frequency curve, with the Grey catchment having the lowest frequency curve and a long tail, with a bi-modal distribution. ....	67
Figure 38- Bubble plots of the major eight catchments in the West Cost Region a) Buller, b) Grey, c) Haast, d) Hokitika, e) Taramakau, f) Waiho, g) Wanganui, h) Whataroa . ....	70
Figure 39- Relative Landslide Dam Hazard Map. This graph shows locations where local slope relief is >350 m, valley width is <150 m and upstream area is >20,000m. The colours represent valley width, with darker red representing short valley widths. Upstream area, or the size of a potential lake is represented by bubble size, with the largest upstream areas having the largest bubbles. Therefore, the greatest landslide dam hazard locations are where large red bubbles are located. ....	73
Figure 40- Relative Landslide Dam Hazard Map of the Haast Region, indicating where the most hazardous landslide dam locations occur. The larger red bubbles occur in the Landsborough river and the Gates of Haast. ....	74
Figure 41- Relative Landslide dam hazard map of the Hokitika region, indicating where the most hazardous locations occur. The largest red bubbles occur in the Hokitika River. ....	74
Figure 42- Sites selected for Outburst Flood modelling in the West Coast Region from the relative landslide dam hazard map. ....	75
Figure 43- Bubble graph for the Haast Catchment showing locations of Landsborough River and Gates of Haast locations selected for outburst flood modelling. ....	76
Figure 44- Bubble graph for the Hokitika catchment showing locations of the Hokitika river selected for outburst flood modelling. ....	76
Figure 45- Bubble graph for the Whataroa catchment showing location of the Perth river selected for outburst flood modelling. ....	77
Figure 46- Outburst flood inundation map for the Gates of Haast at 10m and 50m landslide dam heights showing downstream exposure. ....	80
Figure 47- Outburst flood inundation map for the Haast Landsborough catchment at 10 m and 50 m landslide dam heights showing downstream exposure. ....	81
Figure 48- Outburst flood inundation map for Hokitika for 10m and 50m landslide dam heights showing downstream exposure. ....	82
Figure 49 - Outburst flood inundation map for Whataroa at 10m and 50m landslide dam heights showing downstream exposure. ....	83
Figure 50- Threshold plot for relative landslide dam hazard indicating the different reference lines and how they relate to historic landslide dam locations from the Morgenstern et al (in prep) dataset. ....	88
Figure 51- Cumulative Distribution Figure for dam locations with the West Coast Region and Kaikōura Region combined. ....	89
Figure 52- Density Plot for the West Coast region indicating a clear correlation between where valley measurements are taken and where mapped landslide dams are located. ....	90
Figure 53- Density Plot for the Kaikōura Region indicating a clear correlation between where valley measurements are taken and where mapped landslide dams are located. ....	90

# 1 Introduction

## 1.1 Landslide Dam Overview

A landslide dam is a natural river damming event that occurs when a landslide partially or completely blocks a river. Generally, landslide dams are caused by earthquakes or high intensity and/or duration rainfall that triggers a landslide that deposits into a river. This results in the downstream flow slowing or ceasing completely and a lake forms behind the blockage (Figure 1). The lake continues to increase in size, flooding the upstream valley behind the dam, until the water level reaches the top of the blockage. Landslide dammed lakes can be gigantic, at times exceeding depths of 100 m and extending many 10s of kilometres upstream as water backs up.

Landslide dams are different to artificial or earth dams used for hydro power as they are made from poorly consolidated material and are comparatively unstable (Costa & Schuster, 1988). Given there is no engineered water barrier, no constructed spillways and no outlet to control water they are prone to failure and can cause large unpredictable outburst floods (O'Connor & Beebee, 2009). In comparison with 'normal' hydrometeorological floods, they carry large amounts of boulders and woody debris and often occur with little warning to communities (Becker et al., 2007). In the event of failure, landslide dam outburst flooding can damage critical infrastructure both upstream and downstream (Tacconi Stefanelli et al., 2015). The majority of landslide dams that fail, do so rapidly, often within 24 hrs of forming, meaning there is rarely sufficient time to fully quantify their hazard and risk (Costa & Schuster, 1988; Peng & Zhang, 2012a).

Large earthquakes can exacerbate the hazard from landslide dams by triggering 10s to 100s simultaneously across large areas of mountainous terrain (Dellow et al., 2017a). Therefore, they can occur on extraordinary large scales and are a major hazard for communities and infrastructure exposed to potential outburst flooding. Given the significant impacts of landslide dams, and their often rapid failure, it is essential we understand and model the hazard before they occur.

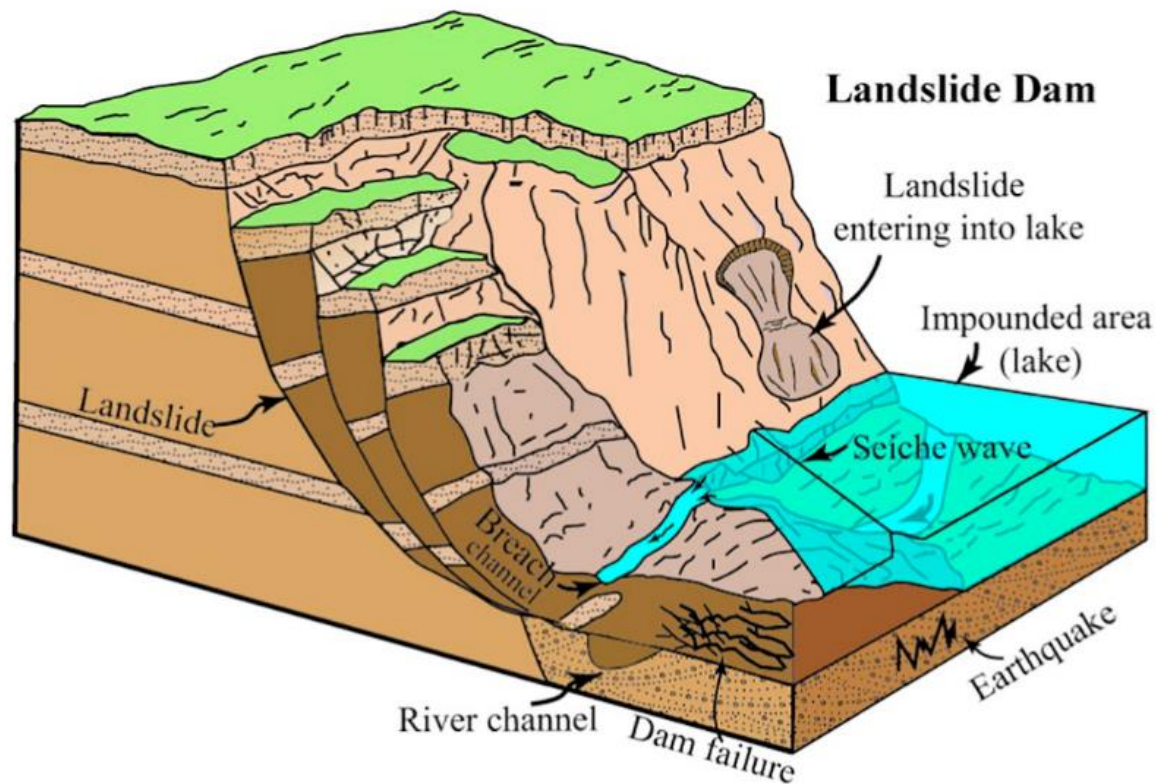


Figure 1- Schematic diagram of key landslide dam features and the processes that can result in their failure. Adapted from (Liu et al., 2019).

## 1.2 Where do landslide dams form?

Landslide dams form in mountain rivers that are steep, short, and narrow and especially prone to blockage (Korup, 2005). Therefore, landslide dams are most common in mountainous countries that are tectonically active (Wu et al., 2022; Zheng et al., 2021). Consequently, mountainous regions of countries such as China, Italy, USA, Japan and New Zealand are considered international landslide dam hotspots (Figure 2). The chances of a landslide dam forming is dependent on having a landslide volume over a certain threshold to obstruct the valley floor (Tacconi Stefanelli et al., 2020). The conditions associated with dam formation can be determined by combining river width and landslide volume using the Hydromorphological Dam Stability Index, which determines where a landslide dam is likely to form or not form (Tacconi Stefanelli et al., 2016).

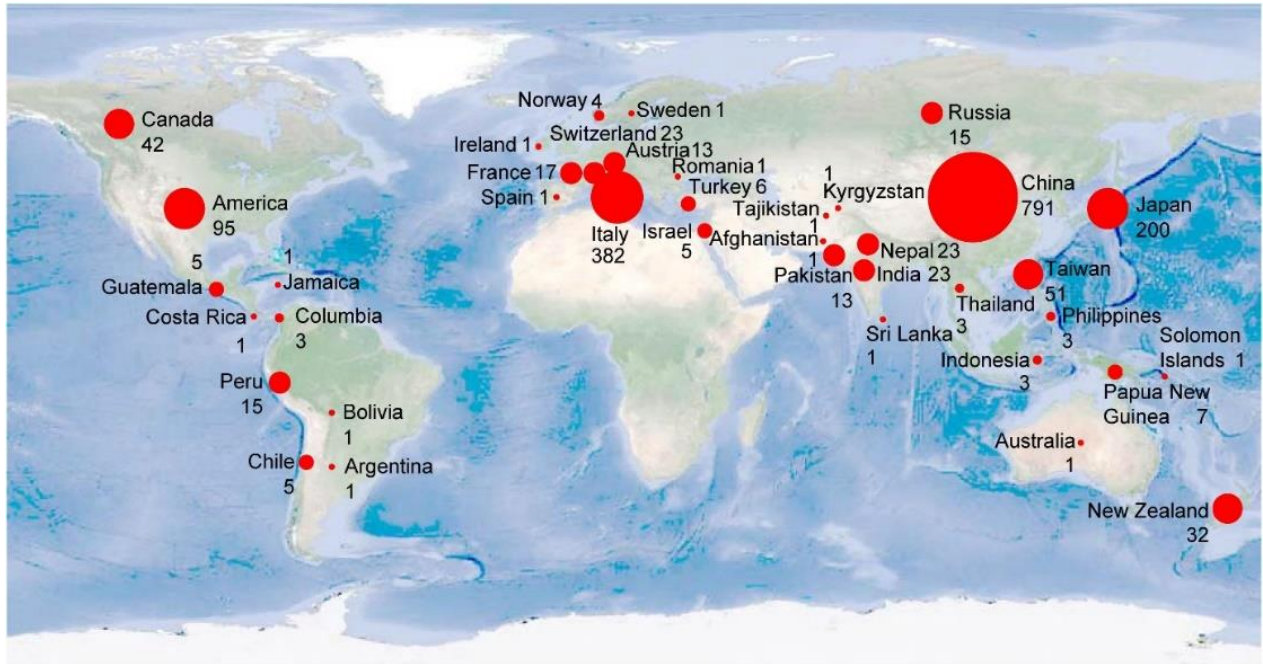


Figure 2- Worldwide known landslide dam locations summarised by country (Zheng et al., 2021).

### 1.3 New Zealand

New Zealand is particularly prone to landslide dams due to its high tectonic activity, heavy rainfall and an active mountainous landscape. New Zealand is situated on the active plate boundary between the Indo-Australian and Pacific Plates, which is one of the most active tectonic plate boundaries on earth (Robinson & Davies, 2013). With offshore subduction zones to the north-east and south, New Zealand is defined by major active fault lines and earthquakes are common (Figure 3). Given a large earthquake can trigger hundreds of landslides and landslide dams at once, New Zealand is especially susceptible to landslide dam hazards on a regional scale.

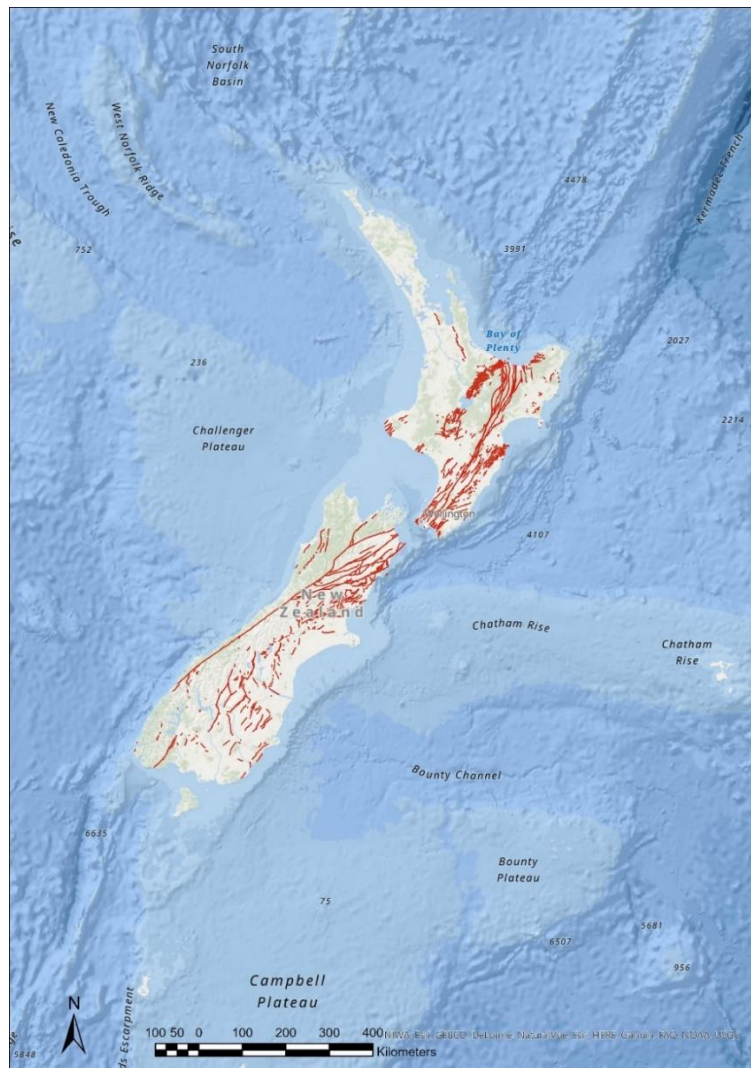


Figure 3- Map of New Zealand showing active fault lines. The Ocean Basemap highlights the subduction zones to the south and north-east of New Zealand.

### 1.3.1 Kaikōura earthquake

On the 14<sup>th</sup> November 2016, a M 7.8 earthquake occurred in the North Canterbury region of New Zealand. This earthquake caused widespread damage to buildings and infrastructure and triggered up to 30,000 landslides and at least 196 landslide dams over an area of 10,000 km<sup>2</sup> (Dellow et al., 2017a). Seven of these dams were identified as hazardous and exposing downstream communities and properties to flooding (Dellow et al., 2017a). There was a major concern that aftershocks would result in dam failure and outburst flooding (Massey et al., 2018). One of the landslide dams on the Clarence River failed within 16 hours of the earthquake, resulting in a rapid flood wave and a warning being sent to downstream residents. Fortunately, due to the area affected by landslides and landslide dams being

sparsely populated, only a small number of buildings were affected and there were no fatalities (Dellow et al., 2017a). However, the recovery from secondary impacts of the earthquake such as landslide dams resulted in damages in excess of \$2 Billion (Kiernan, 2016).

The Kaikōura earthquake demonstrated the impacts a large earthquake can have in New Zealand in mountainous areas, particularly in terms of secondary hazards such as landslides and landslide dams. Hundreds of landslides and landslide dams were generated within just a few minutes of shaking, highlighting the significant implications of having populations and infrastructure directly below tectonically active mountain areas. A future earthquake in a more populated mountainous region could therefore have devastating consequences.

### 1.3.2 The West Coast Region

The West Coast Region is a remote region of the South Island of New Zealand occupying a narrow strip of coastal land bounded to the west by the Tasman Sea and to the east by the Southern Alps (Figure 4). The West Coast Region covers an area of 23,246 km<sup>2</sup> and is dissected by the Alpine Fault. There are large mountains to the east of the fault and wider flood plains to the west, although in the north the Paparoa Ranges west of the Alpine Fault extend north from Greymouth.

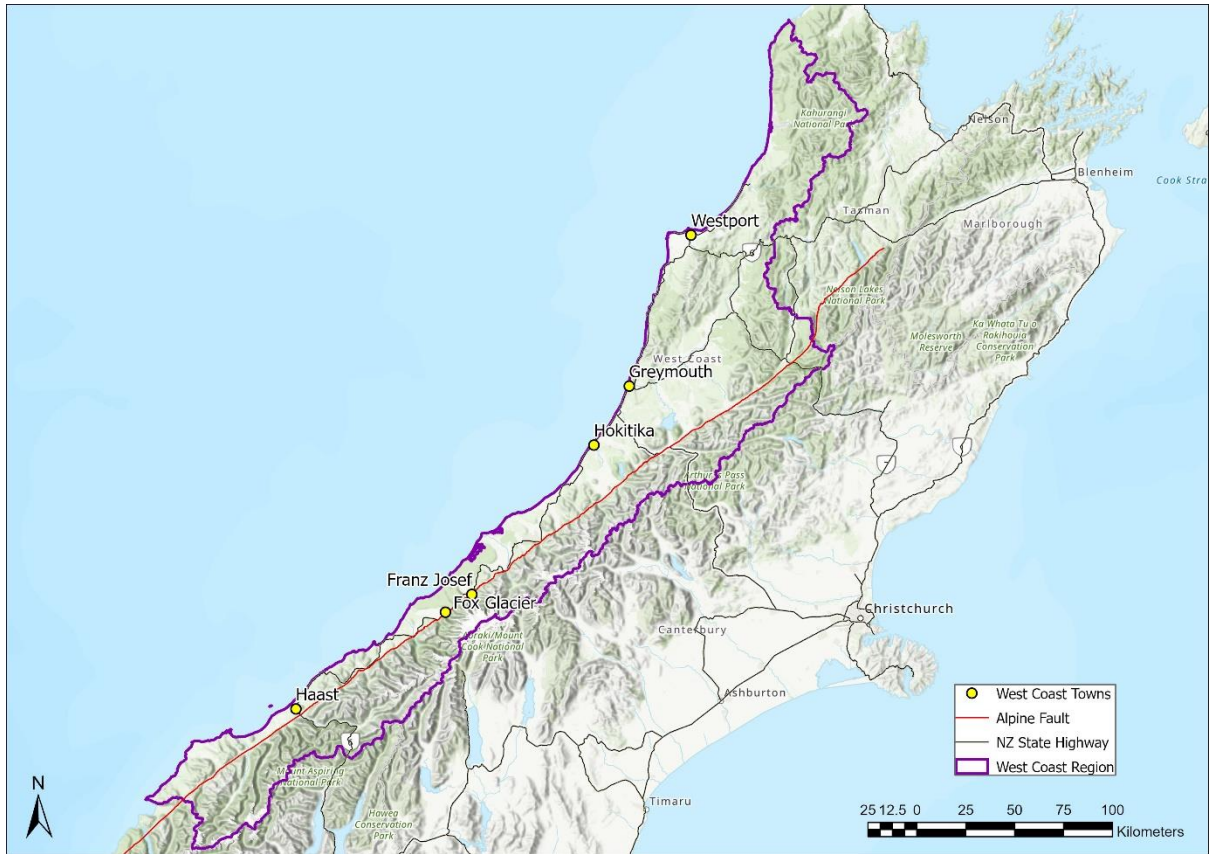


Figure 4- West Coast Region with major towns, State Highways and the Alpine Fault.

The West Coast Region has a relatively small population of 31,575 according to the 2018 census (Statistics NZ, 2018). The majority of people reside in the major townships of Hokitika, Greymouth and Westport, which account for 12% of the total population with the remaining people located in numerous small townships spread across the region (Statistics NZ, 2018). The region is heavily reliant on three major industries: tourism, dairy farming, and mining, which account for 30% of GDP (Infometrics, 2021; West Coast Emergency Management Group, 2016). The region and its population are isolated from the rest of New Zealand due to limited road and rail access, as well as from each other, with only one major highway (SH6) connecting the small townships south of Hokitika. The few infrastructure links the do connect with the West Coast Region must cross the Southern Alps through narrow mountain passes, meaning there is little redundancy in the infrastructure connections, making both day-to-day and emergency access difficult. Lewis Pass (SH7) and Arthur’s Pass (SH73) are particularly vulnerable to extreme conditions and often inaccessible during major storm events. Consequently, the West Coast Region is incredibly remote and during strong weather events

it is often isolated if roads become inaccessible due to landslides and air flight routes becoming unsafe. Given the remoteness of the West Coast Region, the people living and travelling there are highly vulnerable and can be easily isolated from the rest of New Zealand and each other.

The Alpine Fault has resulted in fast moving uplift and erosion of the Southern Alps, therefore the West Coast Region is defined by high mountains and steep, narrow river valleys that are prone to blockage. The Alpine Fault defines the active plate boundary between the Indo-Australian and Pacific plates and is a major strike-slip fault running up the majority of the South Island (Korup, 2005; Robinson & Davies, 2013). At 600 km in length, it is the largest slipping fault in the South Island and acknowledged as the most threatening seismic hazard for the region (Howarth et al., 2021; Townend et al., 2013). The Alpine Fault produces large M 8.0 earthquakes regularly and is estimated to move horizontally up to 10 m during an earthquake (Orchiston et al., 2016). An earthquake of this scale would initiate a complex range of geomorphic responses over thousands of square kilometres (Robinson and Davies, 2013). Potential geomorphic and hydrologic hazards from the initial earthquake and aftershocks include landslides, landslide dams, landslide dam outburst floods, avalanches, lake tsunamis, liquefaction, river aggradation and river flooding (Orchiston et al., 2016). The last known Aline Fault earthquake was in 1717 (Stirling et al., 2012). With a recurrence interval estimated at 300 years, the probability of an Alpine Fault earthquake occurring is high, with a 75% probability of occurring with 50 years with an 82% probability of a Magnitude 8 earthquake (Howarth et al., 2021; Robinson et al., 2016).

Due to the orographic effect from the Southern Alps and proximity of New Zealand to the Southern Ocean, the West Coast Region receives considerable amounts of rainfall annually. Consequently, the West Coast Region is the wettest in New Zealand (Figure 5), experiencing up to 6+ m of rain on average each year (Macara, 2016). Rapid uplift and high precipitation has resulted in an active, erosional landscape defined by frequent landsliding (Korup, 2005). As a result, earthquakes, landslides, storms and flooding are common occurrences in the West Coast Region (Becker et al., 2007; Korup 2002; Kourp 2005). These complex factors result in landslides and landslide dams being common in the West Coast Region (Figure 6).



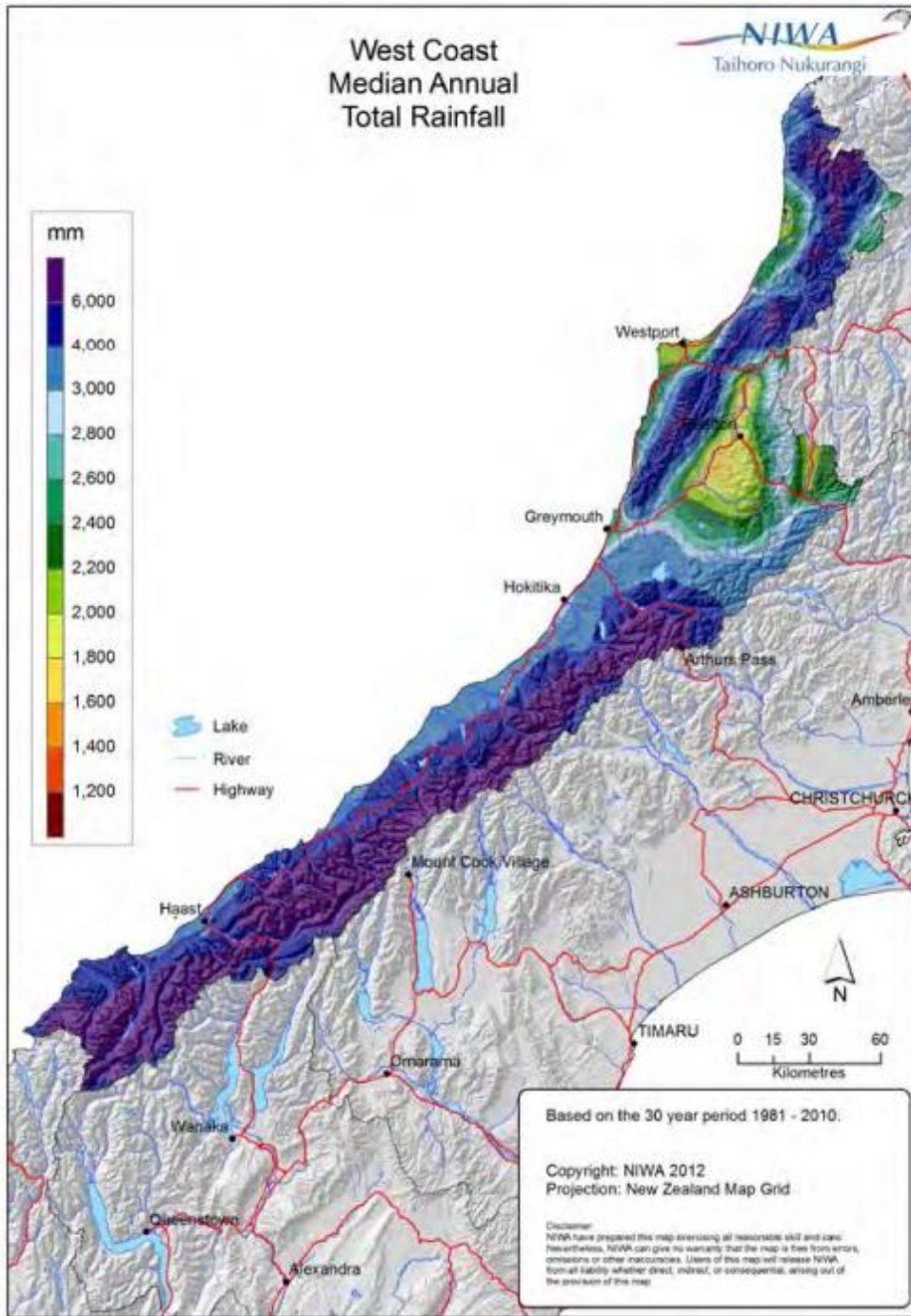


Figure 5- Median annual total rainfall (1981-2010) for the West Coast Region illustrating the high rainfall experienced in the region (Macara, 2016).

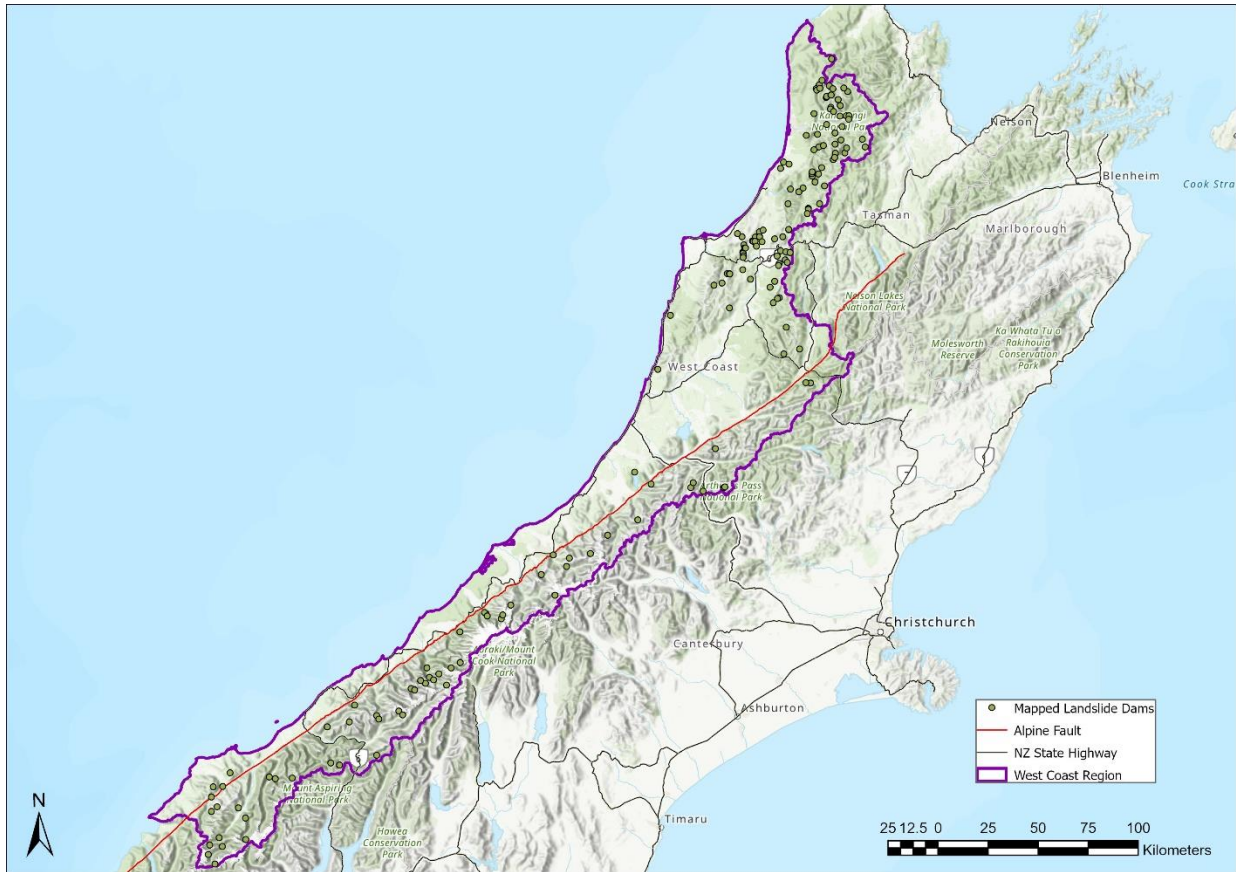


Figure 6- Mapped existing and past landslide dams in the West Coast region of New Zealand Morgerstern et al (in Prep).

## 1.4 Research overview

### 1.4.1 Research Objectives

The hazard from landslide dams in general is well researched. The Kaikōura earthquake in 2016 demonstrated the risk of multiple, simultaneous landslide dams and the potential impacts on downstream communities and utilities. Previous research has determined where landslides are likely to form in the Southern Alps in a large Alpine Fault event (Robinson & Davies, 2013). Therefore, we have a good understanding of where landslides are likely to form and where landslide dams have occurred in the past. However, limited investigation has sought to model the areas that could be affected by future landslide dams and outburst flooding. There is particularly limited understanding of the potential landslide dam hazard and exposure in the West Coast Region. With the most recent major landslide dam in the West Coast Region occurring >20 yrs ago in 1999, awareness of landslide dam risk in the region is limited. Therefore, further research is required to investigate the potential for

landslide dam formation in the West Coast region and to determine the landslide dam outburst flood hazard.

The goal of this research is to develop a regional scale model of landslide dam potential and apply it to the West Coast for the first time. Using the results, the outburst flood hazard at key high blockage potential sites will be explored. Firstly, this project will identify potential landslide dam sites using a model to estimate valley width at a regional scale. Valley width will then be combined with local relief and upstream area to determine the relative landslide dam hazard for all investigated sites across the entire West Coast Region. This dataset will be compared with the historic landslide dam databases for the Kaikōura and West Coast Region to determine a threshold for potential landslide dam formation. These results will be used to determine the most hazardous locations for landslide dams. Secondly, a series of high hazard locations will be selected for outburst flood modelling, to explore the potential downstream exposure. Outburst flood models will be run for 10 m and 50 m dam heights to provide example exposure maps for downstream critical infrastructure. Developing a model to identify potential landslide dam hazard sites regionally and outburst flooding exposure maps will provide a greater understanding of the hazard and exposure from landslide dams in the West Coast Region. Modelling landslide dam hazard and exposure before an event occurs will provide local councils and communities with essential information that may enable them to improve resilience prior to and following an event, such as an Alpine Fault earthquake.

#### 1.4.2 Research Aims

- 1) Develop a method to model landslide dam hazard at a regional scale
- 2) Determine the landslide dam potential in the West Coast Region
- 3) Undertake outburst flood modelling at key high hazard locations and evaluate downstream exposure of population and critical infrastructure

#### 1.4.3 Research Questions

- 1) How does landslide dam potential on the West Coast Region compare globally?
- 2) How can we determine the highest hazard locations in the West Coast Region?
- 3) What critical infrastructure is exposed to outburst flood hazard from landslide dams?

#### 1.4.4 Thesis Structure

Chapter 3 provides a summary of the existing published literature on landslides dams in New Zealand and globally, as well as previous approaches for modelling landslide dam formation and outburst floods. Chapter 4 provides an overview of the methods applied, as well as model validation and uncertainty estimates. Chapter 5 details the results of modelling landslide dam hazard at a regional scale and exposure of critical infrastructure to outburst floods at selected high hazard locations. Chapter 6 presents a discussion of the results of landslide dam identification and outburst flooding exposure, comparing the hazard globally and to the Kaikōura Region, along with recommendations for future work. Finally, Chapter 7 provides a final conclusion and summary of the high-level findings from this study.

## 2 Literature review

### 2.1 Overview of Landslide Dams

#### 2.1.1 Description, formation, and triggers

A landslide dam is a natural river damming event caused by mass movement. Landslide dams form when debris from a landslide partially or completely blocks a river, causing the downstream flow to slow or cease and a lake to form behind the blockage (Figure 7). Landslides triggered by heavy precipitation or earthquakes are the most common cause of landslide dams, accounting for 90% of all recorded landslide dams (Costa & Schuster, 1988; Korup, 2002; Zheng et al., 2021), however occasionally there may be no clear trigger. A single high intensity rainstorm or earthquake can result in many hundreds of landslide dams simultaneously: the Wenchuan earthquake in 2008 caused over 800 landslide dams, and the Kaikōura earthquake in 2016 resulted in at least 196 landslide dams (Cui et al., 2009; Dellow et al., 2017a). Natural river damming events can also be induced by other factors such as volcanic eruptions, moraine emplacement, and glacier-ice dams (Costa & Schuster, 1988; Fan et al., 2020; Morgenstern et al., 2020), however those formed by large landslides are the most common and the most hazardous to people and property (Costa & Schuster, 1988; Fan et al., 2020). Previous work has shown that landslide dams are most likely to form in narrow, steep valleys surrounded by high mountains, and dam breaches may be triggered through overtopping, high precipitation or tectonic activity amongst other factors (Costa & Schuster, 1988; Korup, 2005). In extreme cases, landslide dams can have debris volumes exceeding  $10^9$  m<sup>3</sup> and landslide dammed lakes can be over 1000 m deep (Korup, 2002; O'Connor & Beebee, 2009).

Landslide dams are typically categorised geomorphically by their relationship with the valley floor. Costa and Schuster (1988) originally proposed a classification scheme based on the type of mass movement and resulting deposit from 184 landslide dams categorised from around the world, but this has since been updated by Hermanns et al. (2011) and Fan et al., (2020) (Figure 8).

The majority of landslide dams are made up of the most hazardous Type II (44%) and Type III (41%) dams, where the whole valley width is blocked (Costa & Schuster, 1988). In contrast, Type I dams are small, shallow and less hazardous (11%), while types IV (<1%), V (<1%) and VI

(3%) are rare (Costa & Schuster, 1988). The modified classification by (Hermanns et al., 2011) (Figure 8), includes 4 further classes of landslide dams, however these refer to very specific and rare cases at river confluences and drainage divides (Fan et al., 2020).

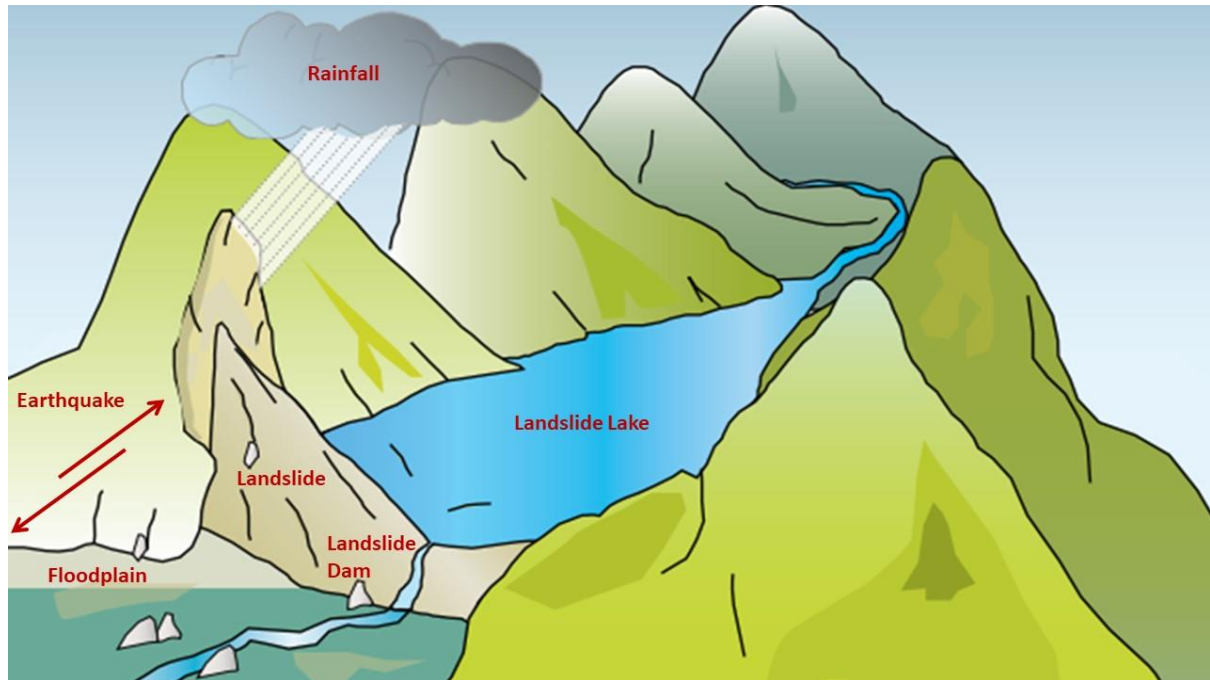

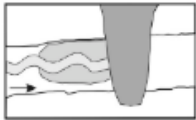
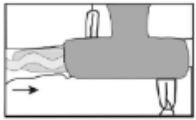
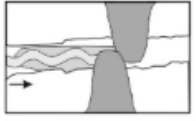
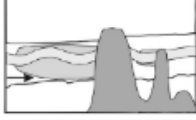
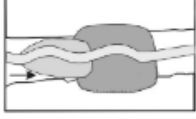

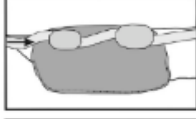

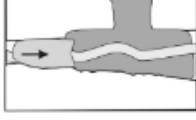



Figure 7- Formation of a landslide dam lake – modified from (Shrestha et al., 2012).

Geomorphometric landslide dam classifications.

Sketch	Description	Type (Costa and Schuster, 1988)	Type (Hermanns et al., 2011b)
	Small dams relative to the valley size that does not reach the opposite slope	I	II c
	Large dams, but still small compared to the valley dimensions. This is one of the most widespread types, and they are frequently formed by rotational or translational landslides	II	II a
	Very large dams that fill the valley from side to side. The collapsed materials are distributed both upstream and downstream from the release area, at times with a T-shaped deposit. Casagli and Ermini (1999) introduced a distinction in this class, separating the phenomena in which the dam also affects the tributary valleys of the main one (III a) from those in which these are not involved (III b).	III	IV a
	Those very rare dams are formed from the contemporary movement of two landslides detached from opposite sides of the same valley.	IV	II b
	Several dams are formed by multiple tongues of a singular landslide. They are not very common for landslides but may form by glaciers (glacier tongues).	V	III b
	Landslides with sub-channel rupture surfaces.	VI	II d
	Supra-landslide lakes on landslide deposits are frequent on larger rockslide deposits, but can occur on all types of landslides. They are not connected to located within the channel of the dammed river.	-	I
	Sub-type of plan view distribution of multiple landslide dams in a single valley in a line formed by a single landslide. Another type is III b.	-	III a
	Type of a landslide dam affecting water divides; with the landslide deposit depositing directly in the drainage divide.	-	V a
	Single landslide dam having different forms distinguished between a rockslide crossing the valley partially or entirely, a rockslide involving the valley floor, and rockslides which, after impacting the valley bottom, spread in an up- and down valley direction (almost the same as III of Costa and Schuster).	-	II e
	More complex multi-river geometries, focusing on the morphological relations of the dam in relation to the river valley	-	IV b-e, VII a-b, VIII, IX




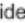

Legend:  Landslide dam  Lake  River  Tributary  Flow direction

Figure 8- Geomorphometric landslide dam classification (Fan et al., 2020).

## 2.1.2 Failure styles and outburst flooding

Landslide dams are different from artificial earth dams as they are often formed from poorly consolidated landslide debris and have no engineered water barrier, no constructed spillways, and no outlet for the controlled flow of water (Costa & Schuster, 1988; O'Connor & Beebee, 2009). Therefore, landslide dams can be highly dangerous and unpredictable. In the event of catastrophic failure, they can initiate large outburst floods and debris flows causing damage to properties, infrastructure and lifelines both upstream and downstream (Argentin et al., 2021; Tacconi Stefanelli et al., 2015). Their failure can release flood waves far in excess of hydrometeorological floods (Korup, 2002), often being colloquially described as inland tsunamis. Further, dam break floods can have a rapid onset with little warning and carry larger boulders and woody debris compared with standard floods (Becker et al., 2007).

### 2.1.2.1 Failure Mechanisms

There are four factors that determine the durability of a landslide dam (Morgenstern et al., 2020):

- 1) Initial landslide source material, failure mechanism and debris runout distance
- 2) Geometry of the valley and dam (shape, height and volume)
- 3) Characteristics of the water course (catchment area and stream power)
- 4) Impounded lake volume

These factors are highly variable and determine the persistence of a landslide dam, which may last from hours to indefinitely (Morgenstern et al., 2020). The underlying geology of the landslide source material is a key factor in determining landslide dam durability (Dellow et al., 2017a; Morgenstern et al., 2020). For example, landslide dams formed with 'soft' sedimentary rocks such as sandstone and siltstone are typically considered more likely to fail, while 'hard rock' compositions of strong metamorphic rock such as granite or gneiss can be more resistant to failure (Costa & Schuster, 1988; Massey et al., 2020). However, dam stability is complex, and under the right conditions dams in 'soft' rock may remain stable while those in 'hard' rock fail soon after formation.

The majority of landslide dams that do fail, do so within a week of formation resulting in limited inventories on both existing and historic landslide dams (Argentin et al., 2021; M. Peng



& Zhang, 2012; Tacconi Stefanelli et al., 2015). Generally, landslide dam failure is induced by overtopping, progressive failure or slope failure such as slumping (Morgenstern et al., 2020; Takayama et al., 2021; Zheng et al., 2021). Overtopping is the most common failure mode, accounting for ~90% of failures and occurs when the lake level exceeds the dam height and an overtopping flow erodes a channel through the dam triggering a positive feedback loop that often leads to catastrophic failure (Takayama et al., 2021). This process can often be exacerbated by heavy rainfall as it increases river flow and reduces the time required for the lake to fill (Costa & Schuster, 1988; Fan et al., 2019; Korup, 2002; Morgenstern et al., 2020; Zheng et al., 2021; Zhou et al., 2013). Progressive failure accounts for ~8% of failures and occurs when a partial collapse at the toe of the dam, typically caused by piping, progressively retrogresses towards the dam crest, eventually resulting in collapse (Costa & Schuster, 1988; Takayama et al., 2021). Slope failure is the sliding of the upper section of a landslide dam inducing the release of the impounded lake and is the cause of ~1% of failures (Takayama et al., 2021). Seepage through the dam due to the lack of an internal impermeable layer may also occur and result in failure, however this is considered less common (Zheng et al., 2021).

#### *2.1.2.2 Outburst Flooding*

Landslide dams create the potential for two different types of flooding. Firstly, upstream flooding as the reservoir fills and secondly, downstream flooding as a result of failure of the dam (Costa & Schuster, 1988). Upstream flooding can cause significant damage, as the impounded lake will continue to grow in size until it reaches the lowest section of the blockage (Figure 9), which can be 10s to 100s of meters above the valley floor, inundating lifelines and buildings (Costa & Schuster, 1988; Korup, 2005; Liu et al., 2019). Rapid failure of a landslide dam results in a sudden release of stored water, causing an outburst flood that can travel significant distances (Fan et al., 2013; Morgenstern et al., 2020). Outburst flooding can have significant consequences for downstream communities and lifelines, resulting in large floodwaves carrying significant amounts of debris that can devastate anything in their path (Fan et al., 2019; Korup, 2004; Morgenstern et al., 2020; Zheng et al., 2021; Zhou et al., 2019). Characteristics of outburst flooding is dependent on discharge, flow type, depositional features, the type of breach and interactions with the channel and valley (O'Connor & Beebe, 2009). Importantly, for catastrophic outburst floods to occur a significant amount of water needs to be contained in a landslide lake, with outburst flooding from small lakes

quickly attenuating downstream (Korup, 2005; Zheng et al., 2021). Outburst flooding from landslide lakes with significant volumes have the ability to be hundreds of times above maximum recorded hydrometeorological floods, and pose serious threats to any lives and properties in the region (Fan et al., 2014; Zheng et al., 2021).

Outburst flooding caused by a sudden release of water has resulted in the majority of the largest floods recorded on earth (Baker, 2002; Costa & Schuster, 1988; Liu et al., 2019; O'Connor & Beebee, 2009). For example, in China, outburst floods associated with landslide dams are recorded as the most widespread cause of infrastructure damage and loss of life in the region (Liu et al., 2019). Liu et al. (2019) studied 287 landslide dam events in China and found the maximum outburst flood discharge recorded was  $1.2 \times 10^5 \text{ m}^3/\text{s}$  at Yingong Tibet, while the minimum discharge was  $1200 \text{ m}^3/\text{s}$ . The flow recorded at Yingong, Tibet resulted from catastrophic failure from a 55 m high landslide dam in June 2000 (O'Connor & Beebee, 2009). A global compilation of 340 landslide dams found 75% have breached and resulted in downstream outburst flooding (Costa, 1991a), while (Ermini & Casagli, 2003) showed that from 282 landslide dams, 67% resulted in significant downstream flooding (O'Connor & Beebee, 2009). By comparison, Korup, (2004) studied 232 landslide dams in New Zealand and found that just 37% had breached, however this analysis did not account for pre-historic short-lived blockages for which there may be little evidence remaining.



*Figure 9- Flooded homes immediately upstream of the 2014 Jure landslide dam in Nepal following the controlled breach and draining of the resulting lake. Sediment deposits on top of the houses shows they were completely submerged by the upstream flooding from the blockage.*

## 2.2 Landslide dam hazard modelling

### 2.2.1 Dam formation and stability

Modelling of landslide dam formation and stability is most commonly undertaken at a local scale. Investigations typically include identifying where landslide dams have already occurred or are likely to occur (Davies & Scott, 1997), or modelling dam formation after an event to understand stability (Crosta et al., 2004; Dai et al., 2005; Li et al., 2011). In particular, modelling the stability of landslide dams after they have occurred is well researched. For example, Dong et al. (2011); Shan et al. (2020) and Zhong et al. (2021) modelled landslide dam stability of case studies after they occurred. Regional-scale models of dam formation and potential however, are a relatively new area of research. For instance, recent research investigating dam formation potential from active landslides has used logistic regression models to try and understand landslide dam hazard across large regions (Jin et al., 2022).

However, so far, methods for effective assessment of river obstruction and dam stability at regional scales have not been widely adopted (Tacconi Stefanelli et al., 2016).

Fan et al., (2014) used an empirical method to estimate the landslide volume threshold required to dam a river, comparing damming and non-damming landslides from the Wenchuan earthquake. Argentin et al. (2021) used slope classification from lower and upper slopes to determine thresholds for stable and unstable criteria, that were then used to identify landslide areas and volumes required to form a landslide dam in the Austrian Alps. In New Zealand, Robinson et al. (2018) undertook empirically-based statistical modelling for the 2016 Kaikōura earthquake to quantify relative landslide hazard and identify potential landslide dam locations, combining landslide susceptibility models with simplified runout estimates to identify potential dam sites. Dal Sasso et al. (2014) used a combination of empirical and physics-based approaches to estimate landslide dam formation at the basin scale in the Basilicata region of Italy. While each of these methods has been shown to provide reasonable accuracy in modelling landslide dam locations, they each have limitations that mean none have so far been widely adopted. The Argentin et al. (2021), Dal Sasso et al. (2014), Fan et al. (2019) methods all require complex numerical modelling requiring expensive software and multiple approaches that increase complexity, while the Robinson et al., (2018) method is known to overestimate hazard and has not been applied outside of New Zealand.

The most commonly used tool to assess landslide dam formation and stability is the Dimensionless Blockage Index (DBI) which integrates dam height, landslide volume and the catchment area, with dam height determining the stability of a dam to overtopping and piping (Ermini & Casagli, 2003; Tacconi Stefanelli et al., 2016). Tacconi Stefanelli et al. (2016) introduced two new indexes: The Morphological Obstruction Index (MOI) for landslide dam formation and the Hydromorphological Dam Stability Index (HDSI) for landslide dam stability. The MOI contains landslide volume and valley width and classifies landslide dams into 3 domains: formed, not formed, and uncertain (Tacconi Stefanelli et al., 2020). The limits of these domains are defined by two straight lines (Figure 10) and show that when a landslide reaches a valley floor, blockage likelihood depends on the volume of landslide material and the width of the valley floor (Tacconi Stefanelli et al., 2020). The stability of any resulting dam can then be determined by the DBI (Tacconi Stefanelli et al., 2016). A minimum landslide volume of  $10^4 \text{ m}^3$  is typically required to block a valley capable of forming a dam, with volumes

below this threshold unlikely to block the river, regardless of the valley width (Tacconi Stefanelli et al., 2020). Narrower valleys require smaller landslide volumes ( $10^4$ - $10^5$  m<sup>3</sup>), which occur more frequently than larger ( $>10^6$  m<sup>3</sup>) landslides, making narrow valleys far more likely to be blocked than wider sections of a river (Tacconi Stefanelli et al., 2016). Therefore, empirical relationships such as MOI provide an opportunity to identify potential future landslide dam sites at a regional scale.

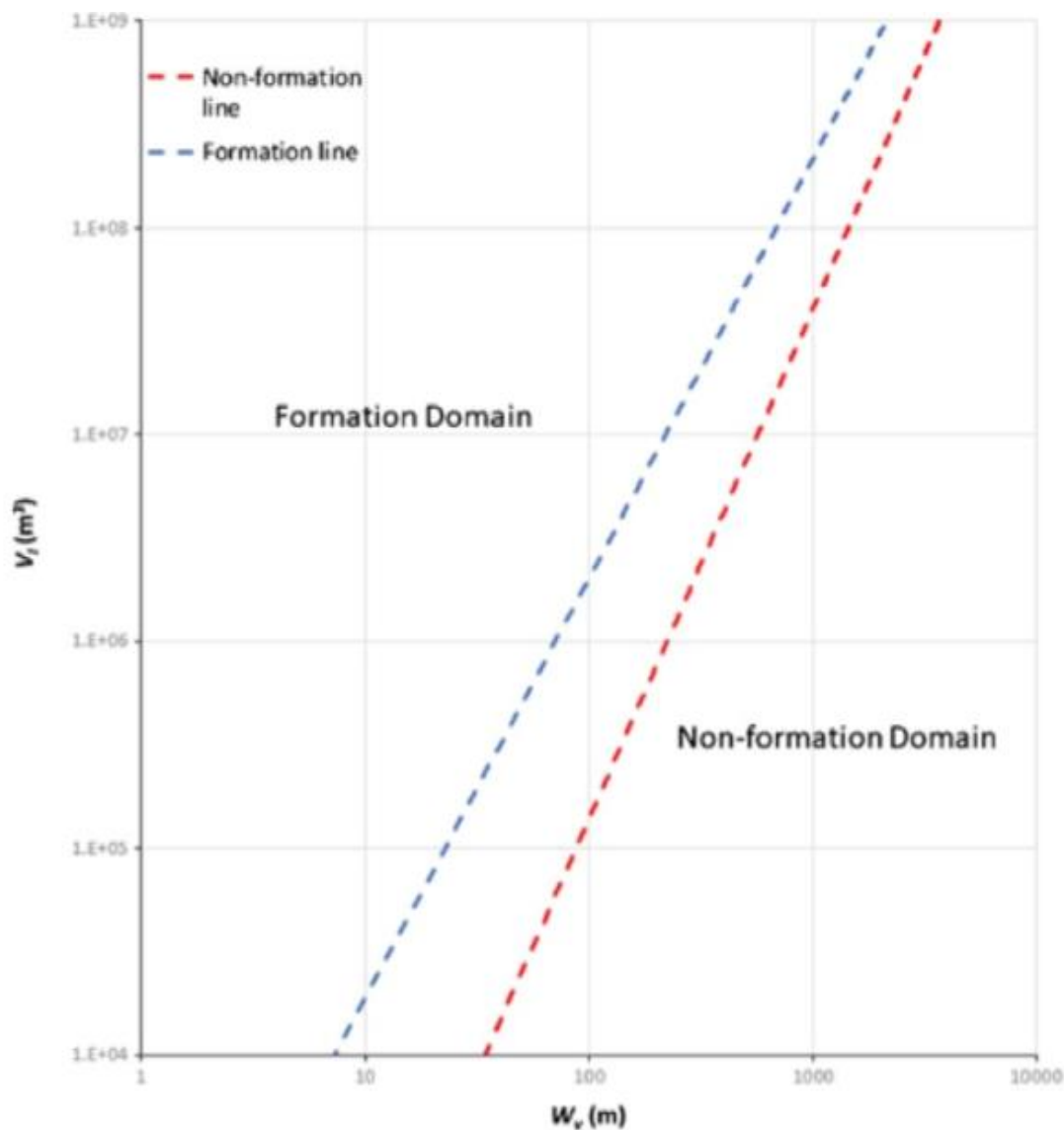


Figure 10- Schematic plot of the Morphological Obstruction Index showing the non-formation line and the formation line. Landslide volume is on the y axis and valley width on the x axis (Tacconi Stefanelli et al., 2020).

### 2.2.2 Outburst flood modelling

There are many studies that model dam (either natural or constructed) failure and their breaching parameters (Butt et al., 2012; Crosta et al., 2004; Peng & Zhang, 2011; Perrin & Hancox, 1992). Depending on the size of the dam, this includes a combination of computational hydraulic modelling software with inputs from aerial photography and ground based remote sensing (New Zealand Dam Safety Guidelines, 2015). In New Zealand, outburst flood modelling has been undertaken for several landslide dams triggered by the Kaikōura earthquake (Dellow et al., 2017a; Massey et al., 2018). Further, the construction of engineered dams requires an assessment of hypothetical dam break outburst flooding and identifying exposure to the downstream community (New Zealand Dam Safety Guidelines, 2015). As well as landslide and constructed dams, a variety of modelling approaches have been identified for modelling outburst floods from glacial lakes (Klimeš et al., 2014; Westoby et al., 2014). Consequently, there is a wealth of outburst flood modelling approaches available.

The most common approaches are to use the software packages such as RAMMS or HEC-RAS, which use a digital elevation model (DEM) to model flow downslope (Westoby et al., 2014). RAMMS simulates a variety of flow-type hazards, from dam break floods to debris flows, considering environmental influences such as landcover (WSL, 2022). The benefit of RAMMS is the ability to integrate debris into a flood, providing more realistic and accurate flood models, especially for dambreak floods, which typically include substantial debris (WSL, 2022). For instance, modelling of glacial lake outburst floods (GLOFs) in the Mt Cook region of New Zealand using RAMMS effectively established outburst flow path dynamics in the region (Allen et al., 2009). RAMMS was also used to model flow heights from rapid failure of the Hapuku landslide dam after the Kaikōura earthquake in New Zealand (Dellow et al., 2017a). However, due to its complexity, highly parameterised and high resolution outputs, RAMMS is typically suited to specific, local-scale case studies where the desire is often to understand the effect of the numerous input variables, or to replicate a previous outburst flood and identify the corresponding values of the different input variables (WSL, 2022).

The open source HEC-RAS software can also be used for outburst flood modelling. HEC-RAS performs one- and two-dimensional hydraulic calculations for both natural and constructed

channels (Hydraulic Engineering Centre, 2022). Butt et al. (2013) successfully used HEC-RAS to model landslide dam outburst flooding in the Hunza River in Pakistan after a landslide formed a large lake that threatened downstream villages. In the Chucchun River in Peru, HEC-RAS was used to determine maximum and minimum flood levels, lake displacement height and flood extent from an historic GLOF (Klimeš et al., 2014). In the Bolivian Andes in the Cordillera Apolobamba, HEC-RAS has been used to model GLOF to six villages from three potential lake sites, and found to reproduce realistic flood depths and inundation (Kougkoulos et al., 2018). Compared to RAMMS, HEC-RAS is a relatively simple software package to operate that is compatible with GIS systems and can accurately determine flow paths from a DEM. However, although it can incorporate sediment transport in its computations, it doesn't integrate debris into flow calculations, instead representing only 'clear water floods', and thus may not be fully representative of debris-laden landslide dam outburst floods (Hydraulic Engineering Centre, 2022).

## 2.3 Global Landslide Dams and Outburst floods

### 2.3.1 Distribution and global hotspots

Research on landslide dam locations globally has shown that landslide dams are most common in countries that are tectonically active (Fan et al., 2020; Wu et al., 2022; Zheng et al., 2021). Mountainous regions with steep valleys, high rainfall and that are prone to earthquakes are especially susceptible to landslide dams (Costa & Schuster, 1988; Korup, 2002). Consequently, regions such as New Zealand, Italy, the Himalaya, Central Asia, and Japan are notable landslide dam hotspots (Figure 11). However, there is bias in the reporting as these regions have been extensively researched in comparison to locations such as the African rift valley and the Andes (Fan et al., 2020), suggesting these locations may be over-represented in the data.

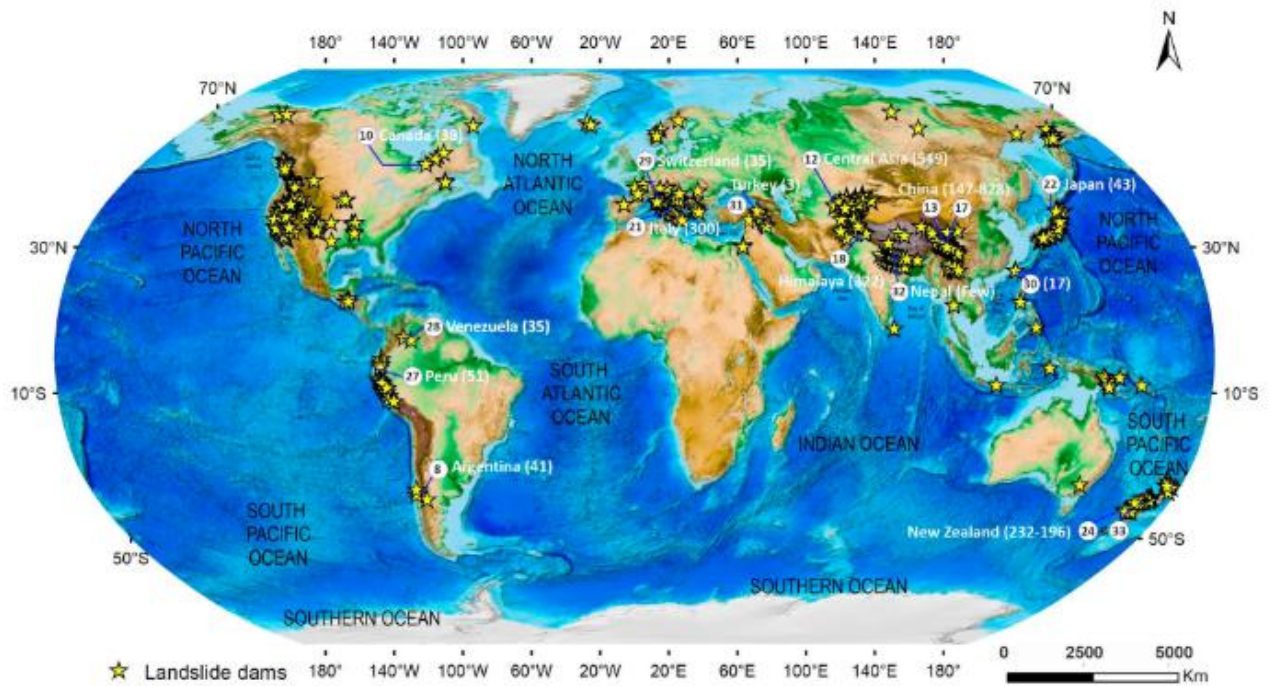


Figure 11- Worldwide distributions of existing landslide inventories and recent large landslide dams in different regions. The yellow stars are landslide dam locations, the circles relate to countries, and the numbers inside the brackets are the total number of landslide dams (Fan et al., 2020).

### 2.3.2 International Case Studies

Hazards and risk related to landslide dams are documented in many historical accounts of catastrophic floods from natural dam failures (Fan et al., 2020). Three major case studies of landslide dam research include the Dadu River in China in 1786, the Wenchuan earthquake-induced landslides in China in 2008, and the Val Pola landslide dam in Italy in 1987. Each of these catastrophic events was caused by landslide dam outburst flooding, resulting in loss of life and extreme damage to infrastructure and lifelines.

#### 2.3.2.1 Dadu River, SW China, 1786

In June 1786 a M7.75 earthquake in the Kangding-Luding area in Southwest China formed a significant landslide which blocked the Dadu River (Dai et al., 2005; Lee & Dai, 2011). This formed a large landslide dam with a height of 70 m, and a lake with volume of  $50 \times 10^6 \text{ m}^3$  and area of  $1.7 \text{ km}^2$  (Dai et al., 2005). Ten days later, the landslide dam breached due to an aftershock and resulted in catastrophic flooding, particularly in the downstream city of Leshan (Dai et al., 2005; Lee & Dai, 2011). The landslide dam caused damage both due to downstream



flooding, which inundated river levees, agricultural land, and swept away houses on the Dadu River, and also by upstream flooding submerging farmland (Dai et al., 2005). It is estimated 100,000 people died as a result of the outburst flood and it is considered the most disastrous landslide dam failure ever recorded (Dai et al., 2005; Lee & Dai, 2011; Liu et al., 2019).

#### 2.3.2.2 *Wenchuan Earthquake*

In May 2008, the M7.9 Wenchuan earthquake in China triggered an unprecedented number of landslides (>60,000) and 828 landslide dams along the fault rupture zone and river channels, of which 501 completely dammed the rivers (Fan et al., 2014; Fan et al., 2013). Landslide dam failure and outburst flooding was common as the dams largely consisted of unstable and loosely consolidated material, with most failures occurring soon after the earthquake (Cui et al., 2009). Of the landslide dams created in the Wenchuan earthquake, 25% failed within a week, and 60% within one month, giving very little time for hazard assessment (Fan et al., 2014). Out of the landslide lakes, 32 presented a substantial outburst flooding hazard (Cui et al., 2009; Xu et al., 2009). In total, these lakes threatened the lives and properties of ~130 million people downstream (Cui et al., 2009).

The most dangerous landslide dam was the Tangjiashan landslide dam (Figure 12), which had over 1.2 million people living immediately downstream in Mianyang (Cui et al., 2009; Xu et al., 2009; Zhu et al., 2021). The Tangjiashan landslide dam was considered particularly hazardous due to its size and location, with a mass of 20.4 million m<sup>3</sup>, a dam height of 82 m and a lake volume of 247 million m<sup>3</sup> (Cui et al., 2009; Peng & Zhang, 2012a; Xu et al., 2009). The landslide lake submerged land 23 km upstream and the incoming rainy season increased the risk of an outburst flood (Cui et al., 2009). In addition, there was concern the breaching of the Tangjiashan landslide dam would trigger outburst flooding from seven other smaller landslide dams downstream, increasing the flood wave intensity (Xu et al., 2009; Zhu et al., 2021). To reduce the risk of the dam failing, the Chinese government lowered the water level of the lake and excavated a diversion channel, lowering the crest elevation and reducing lake capacity (Peng & Zhang, 2012b). The diversion channel reduced the lake volume significantly, although a large, hazardous lake of 86 million m<sup>3</sup> still remained (Peng & Zhang, 2012a). Nevertheless, the dam breached on 10<sup>th</sup> June, flooding Beichuan town and Mianyang City (Cui et al., 2012; Peng & Zhang, 2012a). Fortunately, 250,000 people had been evacuated 10 days

before due to the risk of outburst flooding and no lives were lost (Cui et al., 2012; Peng & Zhang, 2012a).



Figure 12: Helicopter view of the Tangjiashan landslide dam and scarp (Xu et al., 2009).

### 2.3.2.3 Val Pola Landslide, Italy 1987

In July 1987, the central European Alps in Italy experienced extremely heavy rainfall resulting in a significant rock avalanche in the Val Pola region (Costa, 1991b; Crosta et al., 2006; Crosta et al., 2004). Severe flooding and hundreds of landslides occurred in the mountains during this time (Crosta et al., 2006). The Val Pola landslide was the largest and most destructive event, with a volume of 40 million m<sup>3</sup> that deposited into the Val Pola creek (Crosta et al., 2006). A lake began to form (Figure 13), reaching a volume of 50,000 m<sup>3</sup> and a depth of 1-5 m (Costa, 1991b; Crosta et al., 2006). Eventually, a fracture developed at the base of the landslide head scarp and reached a length of 900 m, which eventually detached from the slope to the valley bottom, displacing large amounts of water both upstream and downstream (Crosta et al., 2006; Crosta et al., 2004). Upstream flooding extending for 1 km while downstream flooding extended 1.5 km, causing significant geomorphic changes to the landscape (Crosta et al., 2004). The debris avalanche sent a 35 m mudflow 2.7 km upstream,

destroying buildings in the village of Aquilone and causing 27 fatalities (Crosta et al., 2006; Crosta et al., 2004). At the time, the Val Pola landslide dam was the most destructive and expensive disaster to affect Italy in since World War 2 (Costa, 1991a; Crosta et al., 2004).

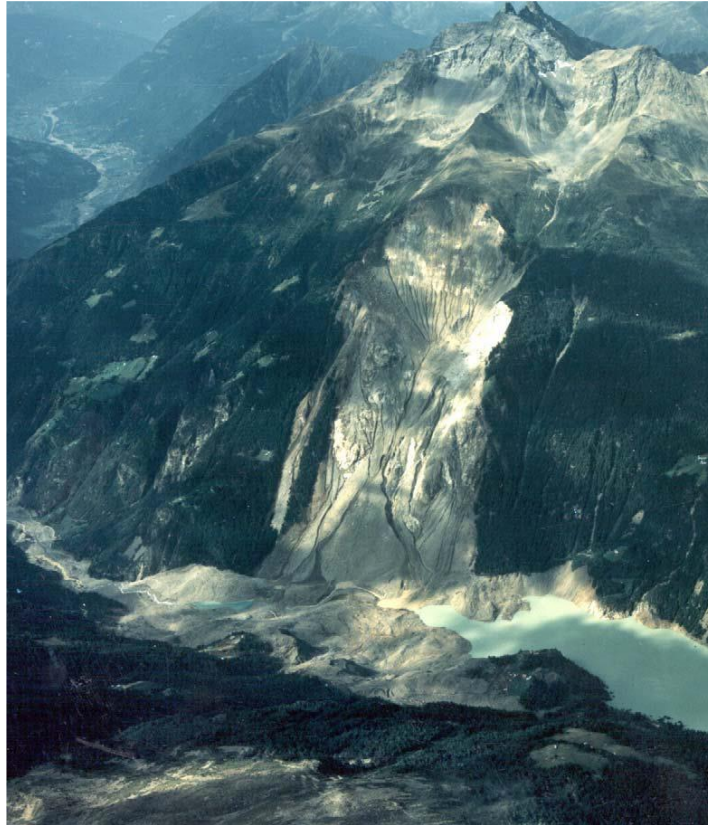


Figure 13- The 28 July 1987 Val Pola rock avalanche with the impounded lake, looking downstream (Crosta et al., 2004).

## 2.4 Landslide dams in New Zealand

### 2.4.1 2016 Kaikōura earthquake and landslide dams

On the 14<sup>th</sup> November 2016, an M7.8 earthquake in the North Canterbury region triggered >30,000 landslides and at least 196 landslide dams over an area of 10,000 km<sup>2</sup> (Dellow et al., 2017a; Morgenstern et al., 2020) as shown in Figure 14. Rapid aerial assessments (Dellow et al., 2017b) and modelling of landslide impacts (Robinson et al., 2018) found landslides were diverting rivers, blocking valleys, and disrupting road and rail networks, with landslide dams causing significant hazard to public safety. There was a concern that rapid failure of one or more of these landslide dams would result in a potentially damaging outburst flood wave, risking lives and damage to property (Dellow et al., 2017a; Massey et al., 2018; Robinson et al., 2018). An initial risk assessment of outburst flood modelling was subsequently undertaken

to understand the probable flow paths based on dam height, width, and potential discharge (Dellow et al., 2017a). For example, just 16 hours after the mainshock a large dam on the Clarence River that had been identified as at-risk of failure failed, sending a rapid flood wave downstream (Dellow et al., 2017a). This event highlights the potential short duration between dam formation and failure and the need for a rapid or pre-event hazard analysis.

Consequently, a rapid, empirical assessment tool, based on valley geometry and landslide size, was used to identify those landslide dams thought to have the highest likelihood of failure during a subsequent high rainfall event or aftershock (Massey et al., 2018). Landslide dams were then surveyed in detail in order of risk from this initial analysis, assessing the life safety of exposed occupied buildings and risks to road users (Dellow et al., 2017a). Seven dams were identified as potentially causing ongoing risks to downstream communities and properties (Dellow et al., 2017a). These included the Leader, Hapuku and Conway landslide dams (Figure 15-Figure 16). The most significant was the Hapuku landslide dam, where landslide debris blocked the Hapuku River and formed a >80 m high dam, with an upstream area above the dam of 8.8 km<sup>2</sup> (Massey et al., 2018; Wolter et al., 2022). Fortunately, the large dam height and its location high in the catchment meant the lake was slow to fill, and it only overtopped after Cyclone Cook in April 2017, >6 months after forming (Massey et al., 2018).

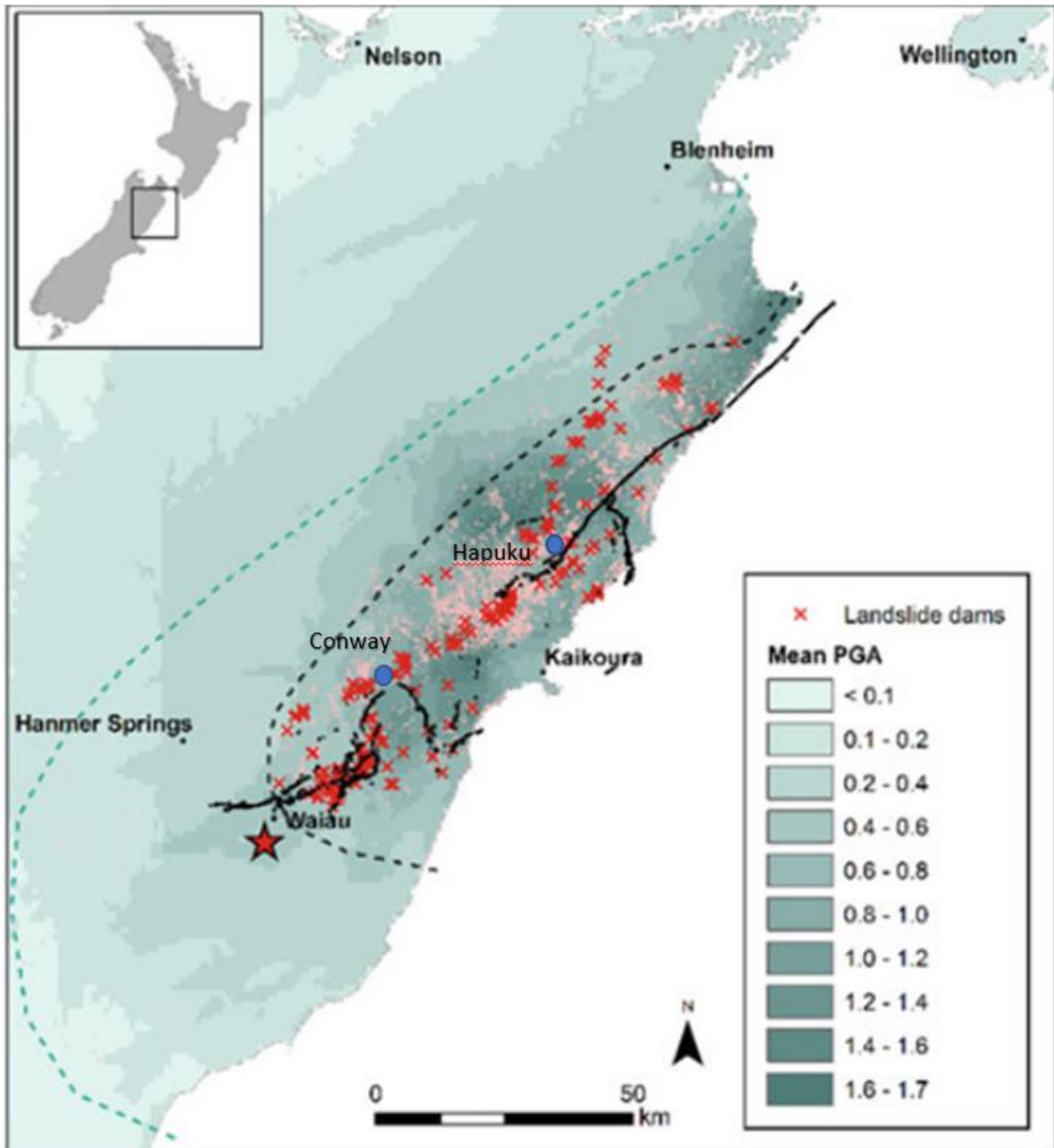


Figure 14- The location of significant landslides (pink polygons) and landslide dams (red crosses) generated during the 2016 Kaikōura Earthquake (epicentre shown by red star), overlain onto the mean Peak Ground Acceleration (PGA) experienced in the region. Areas with light to moderate (green dash) and severe (black dash) landslide damage are shown. Surface fault ruptures are shown by solid black lines (Morgenstern et al., 2020).



Figure 15 - Landslide dam on the Leader River. The landslide is a slump/block slide in a siltstone unit. The landslide dam overtopped and partially breached on the 15<sup>th</sup> of November 2016 within 24 hours after the earthquake, with the full breach occurring on the 13<sup>th</sup> – 14<sup>th</sup> of February 2017 (Dellow et al., 2017a).

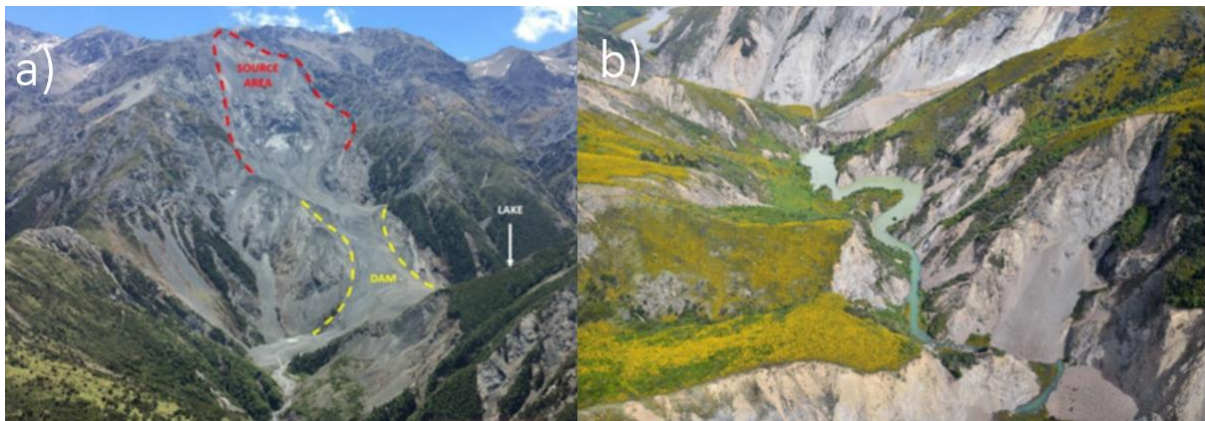


Figure 16 - a) Hapuku River Landslide dam showing source area, landslide dam and valley downstream of dam. This is a greywacke dam with internal flows apparent as water is flowing through the dam (Dellow et al., 2017a). b) Greywacke Landslide dams visible in the Conway River. Neither of these overtopped, however developed flow through the permeable rock (Dellow et al., 2017a).

## 2.5 West Coast Region

Research into former landslide dams in New Zealand (Hancox et al., 2005; Korup, 2004; Morgenstern et al., 2020) demonstrates that landslide dams occur throughout the North to South. However due to the topography and mountainous regions the vast majority of known landslide dams not triggered by the Kaikōura earthquake sequence are located in the Southern Alps and Fiordland, particularly in the West Coast Region (Figure 17). However, there is bias in the reporting as these regions have been extensively researched compared to other parts of the country (Korup, 2002). The West Coast Region of the South Island of New Zealand is particularly susceptible to landslides and landslide dams given the steep valleys, high rainfall and proximity to the Alpine Fault (Becker et al., 2007; Korup, 2002, 2005). Due to the climatic and tectonic setting in New Zealand, landslide dams triggered by rainfall and earthquake events are common (Korup, 2004; Morgenstern et al., 2020). A major earthquake on the Alpine Fault will likely cause significant numbers of landslides in the West Coast Region, and thus potentially landslide dams, however the precise locations and number of dams has not been investigated (Robinson et al., 2016).

Historically, there have been 2 major historic landslide dams researched in the West Coast Region in the last century: on the Poerua River in 1999 (Becker et al., 2007; Hancox et al., 2005) and at Ram Creek in 1968 (Nash et al., 2008). In terms of potential future landslide dams, extensive site specific research has shown the Callery River to be a site of particular concern, primarily due to the presence of the popular tourist town of Franz Josef downstream (Davies & Scott, 1997; Davies, 2002; Dunant et al., 2021; Howarth et al., 2021). Prior to the 2016 Kaikōura earthquake, most case studies investigating landslide dam risk in New Zealand were over 15 years old, highlighting the need for further research. The majority of previous research has been site specific, focusing on the geomorphic impacts of past events such as the Poerua landslide dam, or anticipated future events such as the hazard from the Callery River (Becker et al., 2007; Davies & Scott, 1997; Davies, 2002; Hancox et al., 2005; Korup, 2005). Korup, (2005) undertook a geomorphic hazard assessment using four case studies in the West Coast Region to estimate potential dam height, volume and infill times. However, currently, no previous regional-scale studies in New Zealand have attempted to assess the future potential for landslide dam formation.

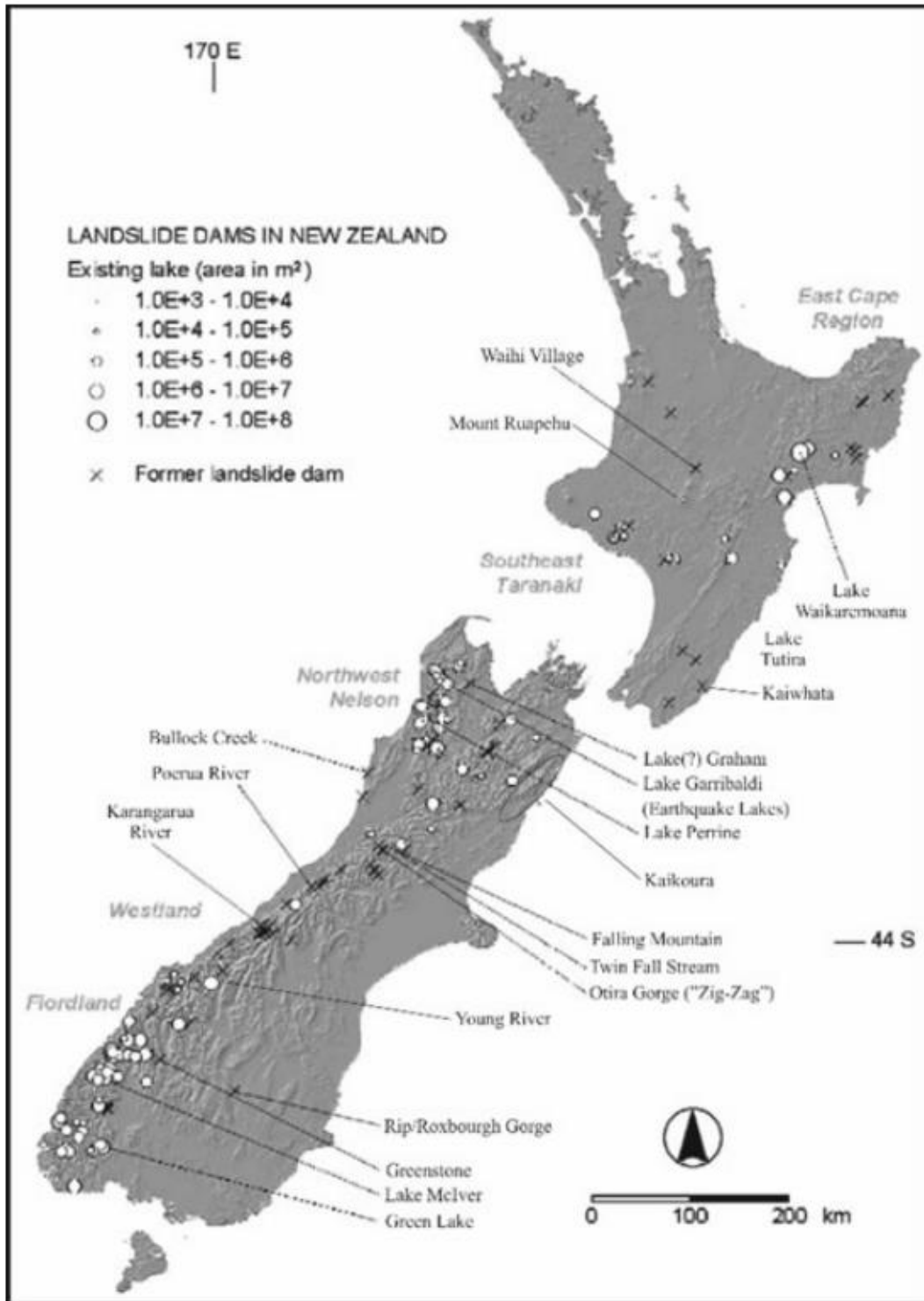


Figure 17- The location of landslide dammed lakes and former landslide dams in New Zealand updated from (Korup, 2004), (Morgenstern et al., 2020).



### 2.5.1 Poerua River Landslide Dam

On the 6<sup>th</sup> of October 1999, a large (c. 7 Mm<sup>3</sup>) rock avalanche from Mt Adams blocked the Poerua River (Figure 18), creating a landslide dam 11 km upstream of the State Highway (SH) 6 road bridge (Hancox et al., 2005). The Poerua dam impounded a lake that filled to a maximum depth of 120 m and a maximum length of 700 m and held 5-7 million m<sup>3</sup> of water (Becker et al., 2007; Hancox et al., 2005). There is no evidence to show that the rock avalanche was initiated by rainfall or earthquake, and was most likely due to significant weathering, stress release, weakening of the steep mountain slope and fluvial erosion from a previous landslide in 1997 (Hancox et al., 2005). This highlights that landslide dams can form in the West Coast Region at any time. The location on the Poerua River where the landslide dam formed was particularly susceptible to blockage, with a valley width of just 105 m, surrounding local relief of 541 m and upstream area ~71,500 m<sup>2</sup>.

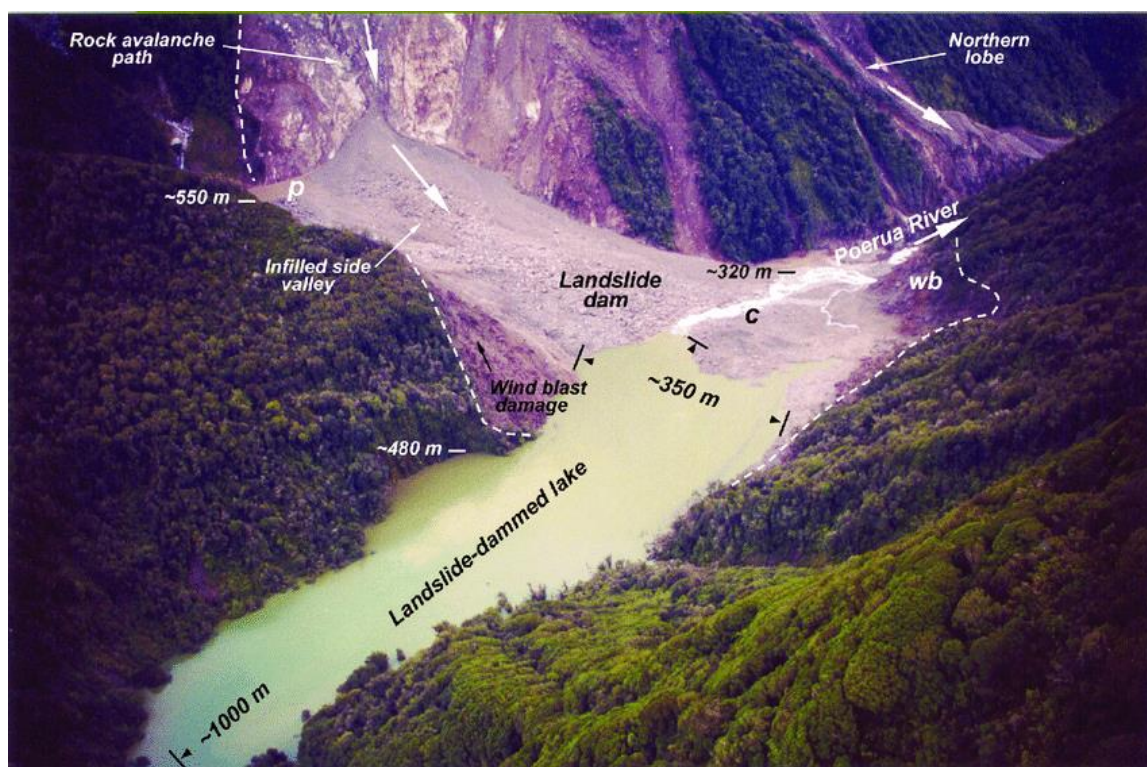


Figure 18 Aerial view of the Poerua landslide dam and lake on the 8th of October 1999, the day after overtopping (Hancox et al., 2005).

A heavy rain event occurred 6 days after formation, when 81 mm of rain was recorded at the Kowhitirangi weather station 50 km north-east of the dam (Hancox et al., 2005). Sometime

before 8 AM that day the landslide dam breached catastrophically as a result of overtopping, indicated by swiftly rising river levels along the river flats and farmland downstream (Becker et al., 2007). This resulted in a Civil Defence Emergency being declared and evacuation of the downstream areas, including holiday homes at the Poerua river mouth (Becker et al., 2007). The breach eroded a 300 m long, 50 m deep breach channel at the site of the lake outlet, repositioning boulders and removing trees (Hancox et al., 2005). The failing of the dam caused significant deposition of debris downstream on the alluvial fan below the Poerua Gorge and inundated farmland on the floodplain (Hancox et al., 2005). Fortunately, the short-term impacts of the outburst flood were confined to farmland and there was no loss of life. However, the long-term impacts had a significant influence on the geomorphic environment, as considerable sediment deposition, aggradation and erosion caused the river to avulse, and damage large swathes of productive farmland on the true right of the river immediately downstream of the gorge (Hancox et al., 2005) (Figure 19-Figure 20). By 2005 stopbanks had been constructed to prevent erosion of farmland in the Poerua valley and remedial works to the SH6 bridge were required to prevent sediment accumulation and future flooding risk (Hancox et al., 2005).

The formation and breaching of the Poerua landslide dam highlighted the vulnerability of the West Coast Region to dam break flood hazards (Becker et al., 2007). In particular, the Poerua event emphasised the risk to downstream communities of a dam break occurring during an extreme rainfall event, which are common in the region (Macara, 2016).



Figure 19- Oblique aerial photos of the Poerua River fan showing the effects of the dam break flood. October 1999, 2 days after the dam breach (Hancox et al., 2005).



Figure 20- Oblique aerial photos of the Poerua River fan showing the effects of the dam break flood. August 2001, after 22 months of sediment aggradation and erosion (Hancox et al., 2005).

### 2.5.2 Ram Creek Landslide Dam

In May 1968, the M7.2 Inangahua earthquake caused a landslide dam to form in the headwaters of Ram Creek, a tributary of Dee Creek (Nash et al., 2008). The Ram Creek landslide dam was located 7 km east of Inangahua Junction at the bottom of the Brunner Range (Nash et al., 2008). The landslide had an estimated volume of  $4.4 \times 10^6 \text{ m}^3$  and completely blocked Ram Creek, impounding a lake that was 500 m long, 425 m wide and an estimated 40 m deep, giving a total estimated lake volume of  $8.5 \times 10^6 \text{ m}^3$  (Nash et al., 2008). As in the Poerua River case, the location where the landslide dam formed was particularly susceptible, with a valley width of 73 m, surrounding local relief of 161 m and an upstream area of  $\sim 8000 \text{ m}^2$ .

Unusually, this dam survived for 13 years, when in April 1981, a high rainfall event eventually triggered subsequent catastrophic dam failure. While there were no reported casualties, the river at the SH6 bridge was in flood for several hours (Nash et al., 2008). The Ram Creek catchment is short and steep, resulting in a significant flash flood with large surges of debris flows (Nash et al., 2008). Landslide dam failure after such a long period of stability is rare (Costa and Shuster, 1989) and if not for the high precipitation event, it has been suggested the lake may have remained intact for considerably longer (Nash et al., 2008). The theoretical models available to assess stability of landslide dams at the time did not take into account the impact of intense and long rainfall events (Nash et al., 2008). The Ram Creek event demonstrates the risk of landslide dam failure after a significant period of time and highlights the complexity of failure modes and timing.

### 2.5.3 Callery River, Westland

The Callery River is one of the best studied and most well-known potential landslide dam sites in New Zealand. Research by Davies & Scott (1997) and Davies (2002) highlighted the significant dam break flood risk from the Callery River, a tributary of the Waiho River directly south of the township of Franz Josef (Figure 21). The Callery River consists of a deep, narrow and steep-sided gorge, which is particularly susceptible to landslide events from earthquakes or significant rainfall (Davies & Scott, 1997). Modelling has demonstrated a landslide dam break flood in the proximity of the SH6 bridge at Franz Josef would threaten the township and cause significant risk to human life (Davies, 2002). The impact of a landslide dam break flood on the Franz Josef township could be catastrophic, as there would be insufficient time for any warning system to be effective (Davies & Scott, 1997). This is one of the few case studies in New Zealand that identifies the potential hazard from landslide dams through investigating order-of-magnitude estimates for a major dam break flood (Korup, 2005). The annual probability of a landslide dam event at the Callery River was estimated to be between 1% and 2% (Davies, 2002), comparable to the time dependent annual probability of an Alpine Fault earthquake (Howarth et al., 2021).

These studies highlight the consequences of both earthquake- and high rainfall-induced dam break flood hazards in general and in New Zealand in particular. Highlighting that heavy rainfall would cause breaching of landslide dams rapidly without adequate time for evacuations, while earthquake induced landslide dams may provide longer warning times to communities (Davies, 2002). More recent research by Tonkin & Taylor (2017) identified Franz Josef as a significantly exposed area due to proximity to the Alpine Fault and additional flooding hazards in the Callery and Waiho rivers.

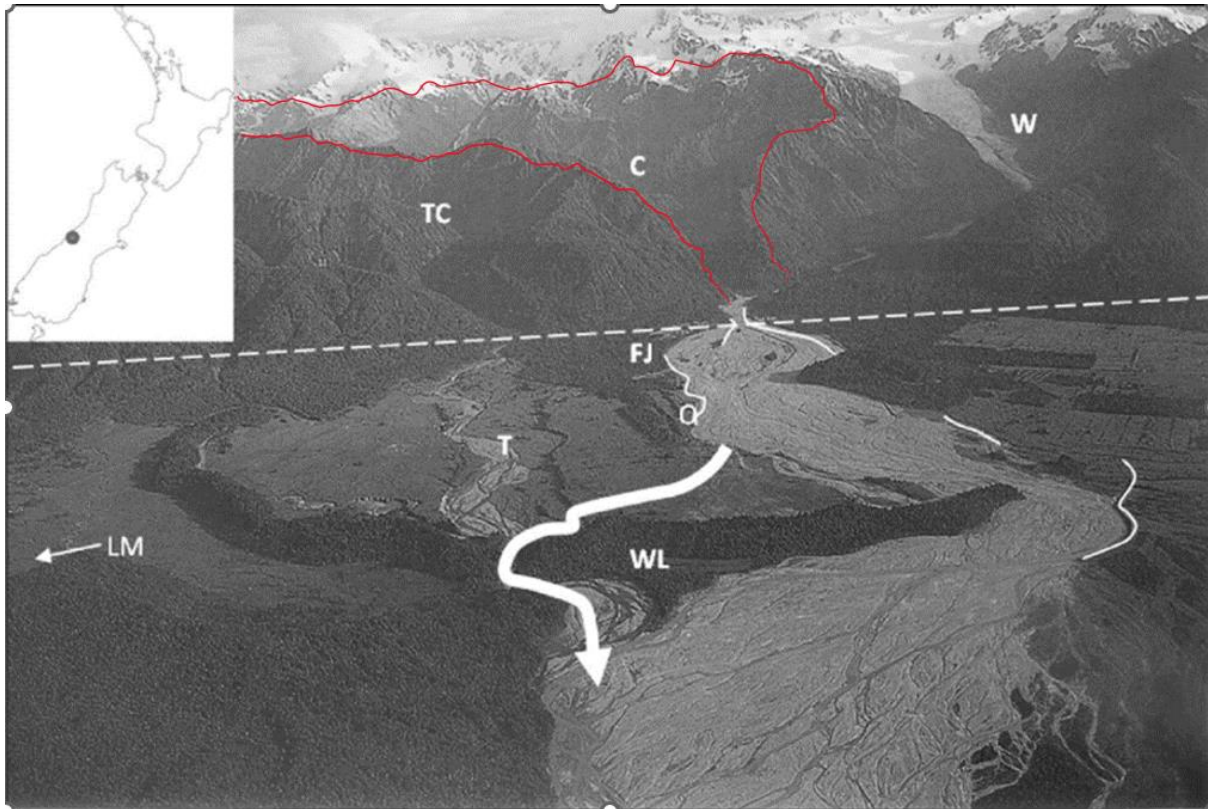


Figure 21 Waiho river flowing from the Southern Alps and looking south. C and Red Lines = Callery catchment; W = Waiho catchment; T = Tatare river; TC = Tatare catchment; WL = Waiho Loop; FJ = Franz Josef township; O = oxidation ponds; LM = Lake Mapourika. Dashed line = Alpine fault. Franz Josef glacier at top right. White lines = stopbanks. Arrow = anticipated course of future avulsion. Inset – location map (Davies et al., 2013).

## 3 Methods

### 3.1 Conceptual Overview

The objective of this study is to identify the most likely locations for landslide dams to form in the West Coast Region and quantify the exposure to potential landslide dam outburst flooding scenarios. Whilst other landslide dam hazard metrics (e.g. DBI) attempt to quantify both landslide dam potential and subsequent dam stability, this study focusses solely on dam formation potential. To identify where hazardous landslide dams could form, a series of simple topographic variables that relate to landslide dam hazard were assessed: valley width, local relief, and upstream area (Figure 22). First, a method for calculating valley width on a regional scale was developed using GIS. This method identified valley bottoms by measuring valley width and established valley width points along the river network for every catchment in the West Coast Region. From these points, surrounding local relief was calculated to identify the steepness of the surrounding topography within a given search radius. Upstream area was also calculated for each valley point to determine locations where large lakes could form.

These metrics were initially calculated for the region affected by the 2016 Kaikōura earthquake to establish a threshold relationship between local relief and local valley width for known landslide dams from the event. The resulting threshold relationship was then applied to the West Coast Region to identify locations with potential landslide dam hazard, with upstream area used to distinguish potential locations that could cost large, dangerous lakes. Importantly, this approach does not consider the subsequent stability of landslide dams, as there are already various methods available for analysing landslide dam stability (Dong et al., 2011; Fan et al., 2021; Shan et al., 2020; Zhong et al., 2021), instead focussing solely on the potential for dam formation. Finally, four high-hazard sites suitable for simple outburst flood modelling and evaluation of exposure were selected. At each of these sites, outburst flood modelling scenarios of 10 m and 50 m dam heights were undertaken.

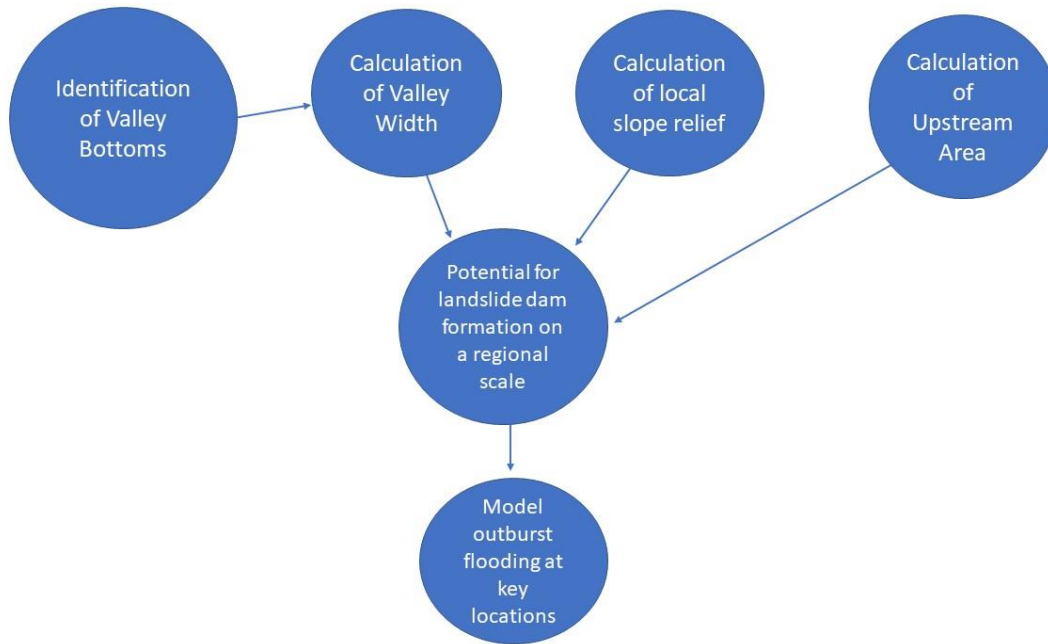


Figure 22- Flow Chart of method for identifying the hazard and exposure of the West Coast Region to landslide dam outburst flooding.

### 3.2 Valley width

Hazardous landslide dams require three components:

- 1) a narrow valley width;
- 2) sufficient relief to generate a large landslide; and
- 3) a large upstream area to form a dangerous lake.

The narrowest parts of river valleys are typically located in the headwaters where there is often sufficient local relief to generate a suitable landslide volume to block the narrow valley, yet insufficient upstream area to form a large enough lake to pose a substantial hazard. Furthermore, these locations can be significant distances from downstream populations and infrastructure, meaning outburst floods may have attenuated substantially by the time they reach them. Larger more hazardous lakes can form as upstream area increases down-catchment and the potential attenuation of any flood wave decreases. However, valley width also typically increases downstream, requiring larger landslide volumes to cause a blockage, while local relief also decreases, making such landslide volumes less likely. Thus, for a hazardous landslide dam to form, there needs to be a 'sweet spot' in the river catchment, where valley width remains low, but local relief is still high and the upstream area is large



enough to form a sizeable lake. Combining these three easily measurable topographic factors (valley width, local relief, and upstream area) may allow for the identification of such landslide dam 'sweet spots' (Figure 23).

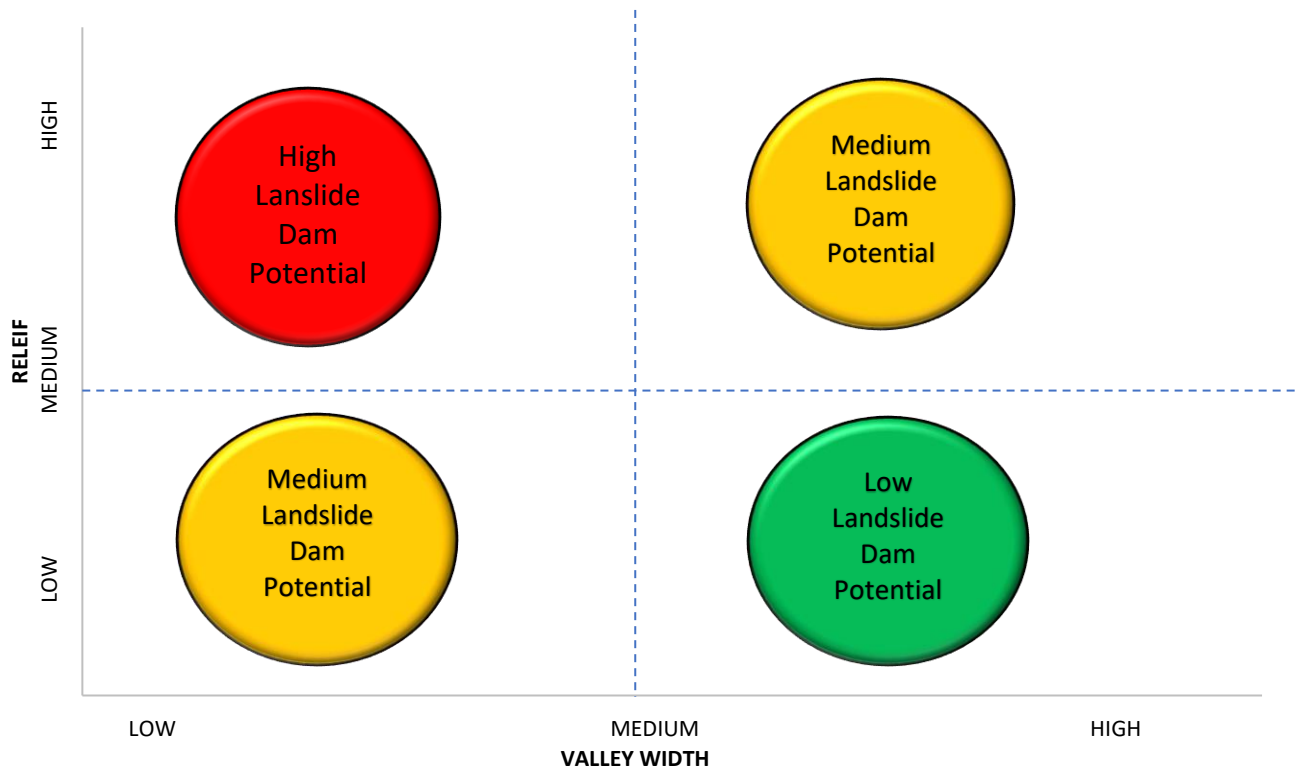


Figure 23- Conceptual graph of relief vs valley width. Red areas have the highest landslide hazard potential, with narrow valleys and high relief, while orange areas still have landslide dam potential, however due to low relief or wide valleys is not as significant. Green areas are unlikely to be a landslide dam hazard.

A key first step is identifying the spatial extent of valley bottoms. Several studies to define valleys and measure their width exist. The majority of these studies require direct field measurements (Lancaster, 2008; Lifton et al., 2009) or manually-mapped valley floor widths (Brocard & Van der Beek, 2006; Clubb et al., 2022). While these methods provide accurate representations of valley width, they are time intensive and limited over large spatial scales (Clubb et al., 2022). There are relatively few semi-automated approaches for estimating valley width over large scales, which is required to understand landslide dam risk on a regional scale.

Here, two methods to identify valley bottoms and two further methods to measure valley widths were compared for the Whataroa River catchment in the West Coast Region. The methods used to identify valley bottoms were from Jones (2022) and an approach using the Topographic Position Index (TPI). The two methods used to measure valley width were from

Clubb et al., (2022) and an approach developed as part of this study using semi-automated transects. The Whataroa River catchment was selected as a test region due to its widely varying topography, including narrow gorges and wide floodplains, and its relative accessibility providing the opportunity for ground truthing.

### 3.2.1 Identification of valley bottoms

In order to evaluate potential landslide dam locations, first valley bottoms need to be defined and identified. Valley bottoms are generally the flattest parts of mountain environments where river flow concentrates, and can be defined as the region containing the active river channel and its surrounding floodplain. Importantly, in these locations there is no alternative route for the river to flow if completely blocked. Whilst conceptually simple, demarcating the location and spatial extent of valley bottoms at regional-scales is difficult. Most approaches to constrain valley bottoms use either field measurements (Lancaster, 2008), or manual mapping on topographic maps (Brocard & Van der Beek, 2006) or DEMs (Langston & Temme, 2019), which is time consuming over large-scales. More recently, automated methods to extract valley floors from DEMs (Clubb et al., 2022) have made larger-scale studies possible, however as yet, no single approach has been widely adopted.

The first method to calculate valley bottoms in this study used an approach by Jones (2022) and involves delineating the fluvial network and river valley using a DEM. The fluvial network is delineated by combining flow direction and flow accumulation layers and setting a flow accumulation threshold to represent channel initiation. The flow accumulation raster is the count of the upstream cells which flow into each cell. Therefore, thresholds for a 25 m DEM would be 1 = 625 m<sup>2</sup>, 2 = 1250 m<sup>2</sup>, etc., and for an 8 m DEM, 1 = 64 m<sup>2</sup>, 2 = 128 m<sup>2</sup>, etc. River valleys were defined by thresholding a slope map so all locations below a certain slope angle were considered valleys. For this analysis, all values below 10 degrees were considered valleys, and these values were intersected with stream polylines to form valley polygons (Figure 24a).

The second method to calculate valley bottom width was developed as part of this study and used the TPI (Jenness et al., 2013; Weiss, 2001) to qualitatively classify a DEM into both

topographic position (e.g. ridge top, valley bottom, mid slope) and landform category (e.g. steep narrow canyons, gentle valleys, plains, open slopes). TPI achieves this by comparing the elevation of each pixel to the mean elevation of all pixels in a user defined neighbourhood around each pixel, whilst using the central pixel slope angle to distinguish between steep and gentle slopes. Positive TPI values therefore represent locations higher than their surroundings (i.e. ridges), while negative TPI values represent locations lower than their surroundings (i.e. valleys). For this analysis, the TPI Category 6 tool was used with a circular neighbourhood with radius = 5 pixels, to classify the DEM into 6 unique classes: (i) Valleys ( $TPI \leq -1$ ), (ii) Lower Slopes ( $-1 \leq TPI \leq -0.5$ ), (iii) Gentle Slopes ( $-0.5 \leq TPI \leq 0.5$  and slope  $< 5^\circ$ ), (iv) Steep Slopes ( $-0.5 \leq TPI \leq 0.5$  and slope  $> 5^\circ$ ), (v) Upper Slopes ( $0.5 \leq TPI \leq 1$ ), and (vi) Ridges ( $TPI > 1$ ). Valley bottoms were then derived from the combination of valleys, lower slopes and gentle slopes, with steep slopes, upper slopes and ridges removed from the analysis. The combined valleys, lower slopes and gentle slopes were converted into individual polygon layers and overlaid on the river network to identify outliers not intersecting with rivers, which were manually removed. Finally, the polygon outlines were smoothed and combined into one single polygon for analysis (Figure 24b).

Both methods were applied to the national 25 m DEM across the Whataroa River catchment. Notably, the Jones (2022) method performed well in wide floodplains and larger river sections, but struggled to correctly identify smaller and narrower valley sections (Figure 24a) where landslide dams are considered most likely to form. Visual comparisons of the outputs suggested the TPI method provided the most accurate representation of the distribution of valley bottoms, and importantly was able to identify smaller order 1, 2 and 3 streams (Figure 24b). Therefore, the TPI method was selected for further analysis of valley widths.

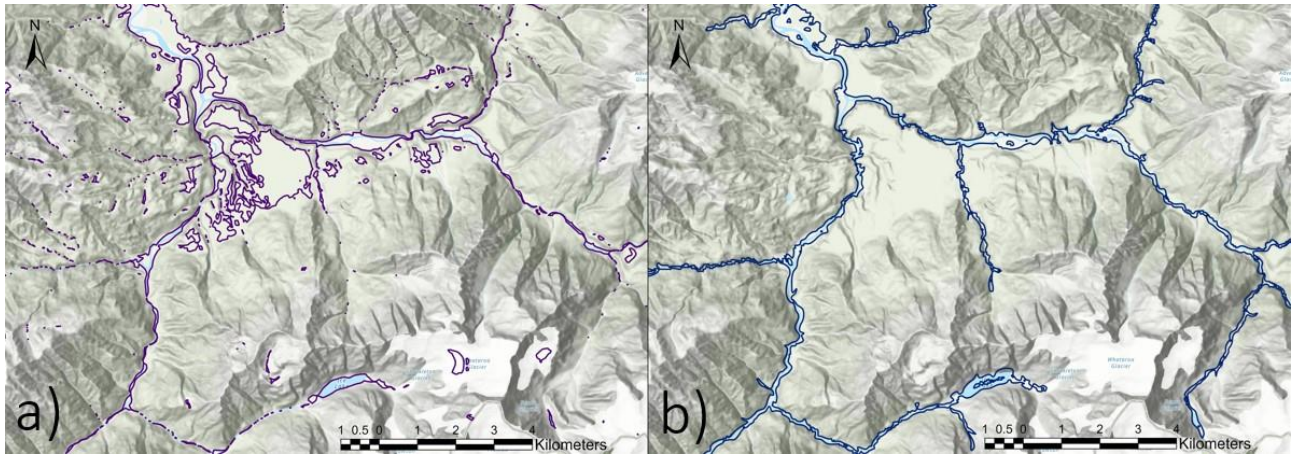


Figure 24 Comparison of the two measuring valley bottom approaches a) Jones Method b) TPI method. The TPI method is more accurate as it takes into account the smaller order 1, 2 and 3 streams and visually matches river valleys.

### 3.2.2 Measuring Valley Bottom Width

The first method to calculate valley width was adapted from Clubb et al. (2022) and identifies valley floors from a DEM based on thresholds of slope and elevation compared to the modern-day channel. Valley centrelines are then extracted from the resulting valley bottom polygons and the width of the polygon is subsequently measured at intervals corresponding to the DEM pixel size to generate a semi-continuous point measurement of valley width (Clubb et al., 2022).

The transect method was developed as part of this study and involved using semi-automated transects in GIS to extract the width of the identified valley bottoms. Transects were generated along and perpendicular to the river network intersecting with the TPI-derived valley bottom layer. Transects were taken every 200 m along the river network to provide a balance between model resolution and computational efforts, however this spacing is user defined, allowing for larger or smaller spacing as required. The NIWA River Environment Classification (REC) layer was used as the most complete and accurate national river database for New Zealand (NIWA, 2022). Transects were taken only for order 2 and above streams as including order 1 streams doubled the number of transects to be evaluated, adding considerable computing requirements. Further, order 1 streams were considered to represent a low landslide dam hazard due to the typically low upstream area available. Valley bottom widths were extracted up to a maximum of 500 m as values greater than this require

landslide volumes  $>10^8 \text{ m}^3$  (Tacconi Stefanelli et al., 2020; 2016), of which few exist globally, making their likelihood and corresponding hazard low.

The Clubb et al (2022) method provided an acceptable representation of valley widths, however multiple sections of river were missing from the output, and the method did not adequately identify smaller valleys, such as order 1, 2 and 3 streams. In addition, the output was only the final point data containing valley widths; the method does not output a polygon or polyline of valley bottoms to provide further analysis, making field-based verification difficult. By comparison, the transect method provided an acceptable representation of valley widths in smaller valleys in the order 1, 2 and 3 streams (Figure 25). In addition, it can be calculated as both point and polyline datasets enabling a wide range of analysis. Therefore, the transect method was considered a more appropriate method for calculation of valley bottom widths in this study.

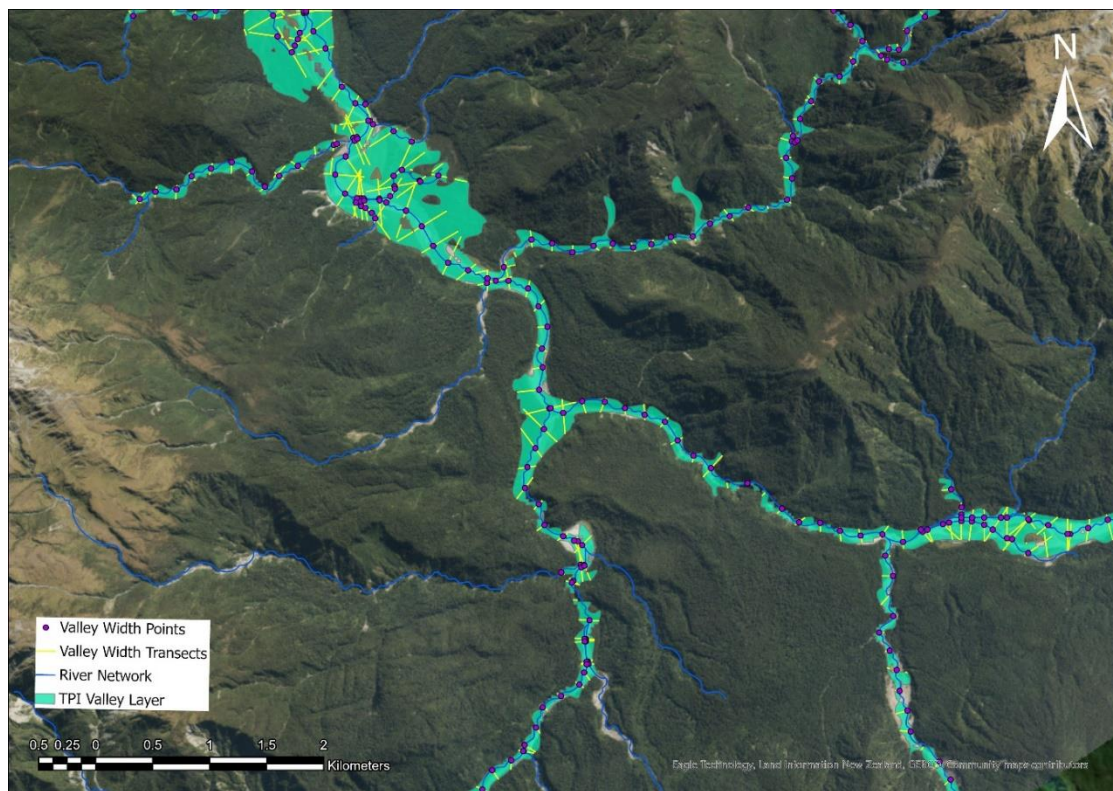


Figure 25- Valley width mapping using GIS for the Whataroa River catchment showing valley width points, transects, river network and the TPI Valley layer.

### 3.2.3 Valley Width Validation

To validate the outputs from the combined TPI and transect models, manual valley widths were measured within the Whataroa catchment (Figure 26). Sites were selected from the lower and mid reaches of the catchment as well as the nearby Little Man River sub-catchment in order to evaluate model performance across morphologically-varied river sections. A laser telemeter was used to measure valley width in the field. Laser telemeters are typically used in forestry and work by converting time to distance by measuring the time taken for a laser fired from the telemeter to reach its target and bounce back to the recorder (Figure 27). As such, these tools can provide highly accurate distance measures over large (up to kilometres) distances.



Figure 26: Fieldwork locations a) Mid Whataroa (Mid Catchment) b) Lower Whataroa (Lower Catchment) c) Little Man River (Upper Catchment).

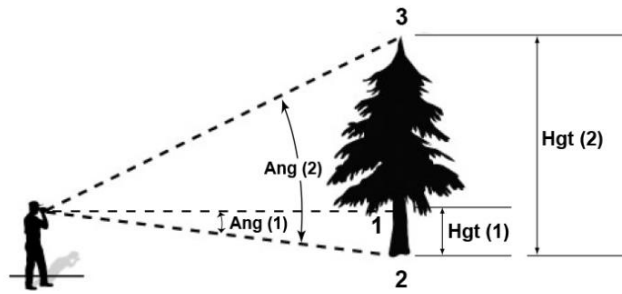


Figure 27: Laser Telemeter in use for measuring distance and height (Nikon, 2011).

Field measurements were taken at 38 sites in total, with 15 in the Lower Whataroa, 10 in the Mid-Whataroa, and 13 in the Little Man River catchment (Figure 28). Site selection required the user to be able to identify and access one edge of the river valley and have a direct line of sight to the opposing valley wall that was perpendicular to the valley trend. Valley edges were identified as locations with notable changes in slope, where shallower lower slopes transitioned to steeper 'upper' slopes, however valley edges, as with many landforms, are difficult parameters to identify, particularly in heavily vegetated terrain (Tacconi Stefanelli et al., 2020). To maintain consistency, all measurements were taken at eye-level (approximately 1.5 m above ground level) and care was taken to ensure the telemeter maintained a horizontal level during the measurement. Three unique measurements were taken at each site and an average of the recordings was taken to validate the model.

This confirmed the model performed well in the upper and mid portion of the catchment but was less accurate in the wider, lower valleys (Figure 29). In total, 63% of measurements gave widths within 100 m of the automated model. In the Little Man River catchment, this rose to 83% of measurements within 100 m, while 66% of measurements were within 20 m of the model with all but 3 of the measurements within measurement error. Importantly, in most instances, the model produces lower widths than were recorded in the field, suggesting it provides a conservative estimate of valley width and therefore in terms of landslide dam potential, however no sensitivity testing was undertaken. Together, this suggests the model performs well in the upper portions of catchments, where the landslide dam formation potential is expected to be highest. The model performs more poorly at river confluences where rivers typically widen and river meanders mean the river course is no longer parallel to

valley direction, resulting in the transects overlapping, as can be seen in Figure 25. However, river confluences tend to be locations of increased valley width, suggesting such locations have lower landslide dam formation potential.

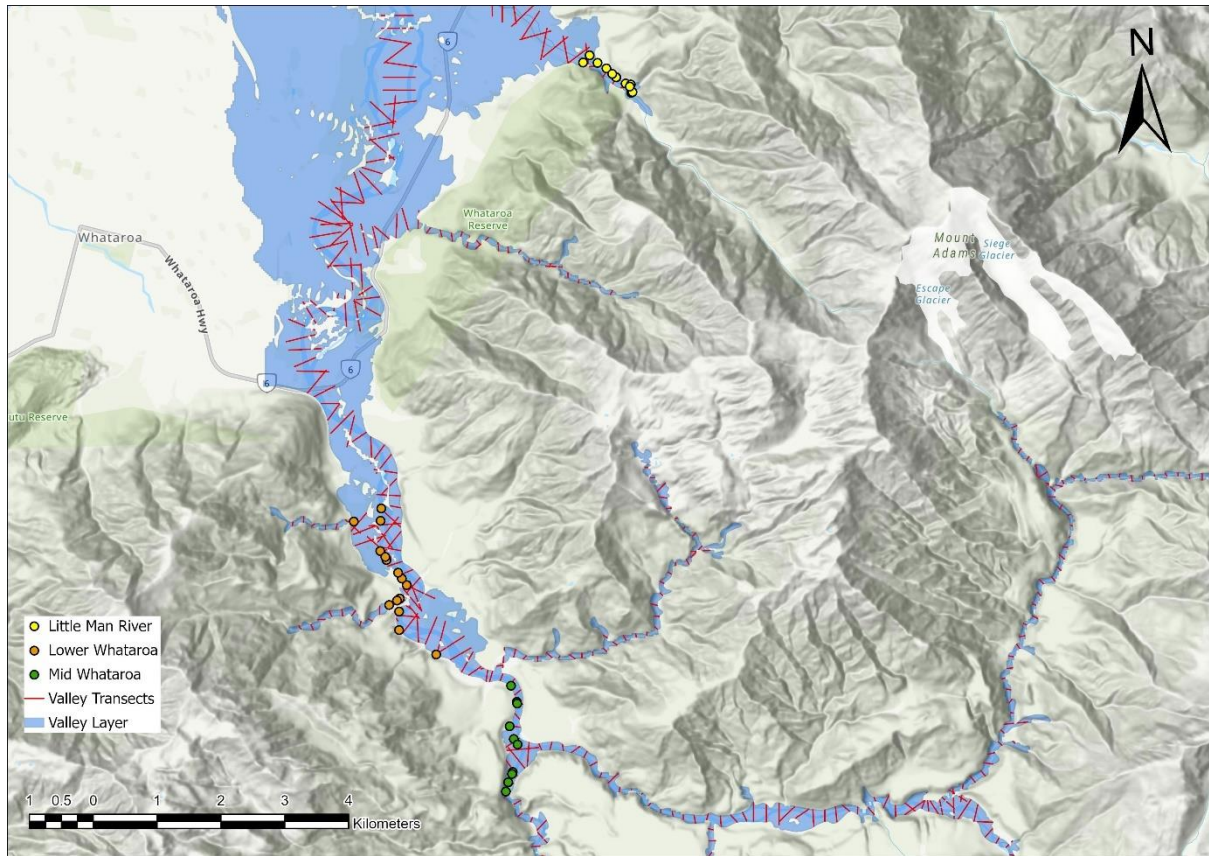


Figure 28: Fieldwork locations in the Whataroa catchment, Little Man River= Yellow, Lower Whataroa= Blue and Mid Whataroa = Green.



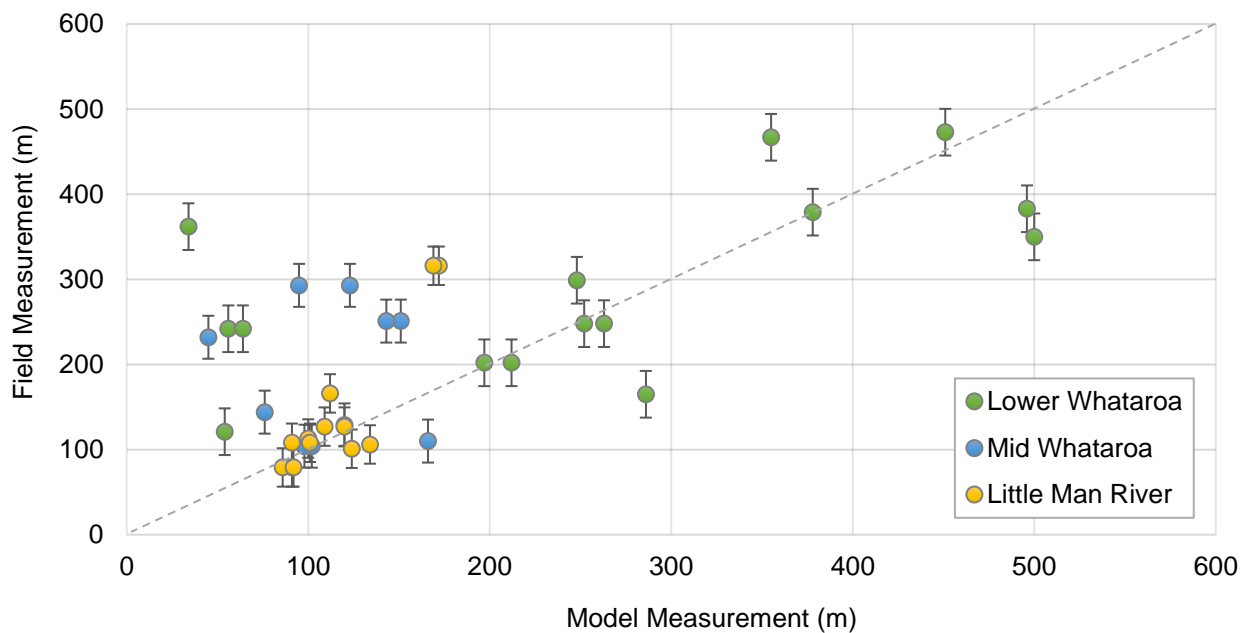


Figure 29: Field Measurements vs valley width model in the Whataroa catchment with vertical uncertainty bars.

### 3.2.4 Landslide volume proxy – local relief

Valley width is just one factor influencing whether a landslide results in a river blockage. It is important to understand whether sufficient material exists above the valley bottom to produce a large enough landslide to block the corresponding section of river. Potential landslide volume is difficult to estimate prior to a failure, particularly at regional scale. However, local relief provides a simple proxy for potential volume by estimating the change in elevation over a given region (i.e. how much material sits above the valley bottom). Conceptually, landslide dams should primarily occur in locations with narrow valley bottoms and high surrounding relief, whilst being virtually absent in locations with wide valley bottoms and low surrounding relief; locations with wide valleys and high relief, or narrow valleys and low relief may experience blockages, but only in extreme circumstances.

To confirm this theory, the combined TPI and valley width model was applied to the Kaikōura Region. The Kaikōura Region post-2016 has been mapped more extensively for landslide dams than any other region in the country based on high-resolution data and therefore includes many smaller dams (Wolter, 2022). Valley width was calculated every 200 m for order 2 rivers and above. Local relief was calculated as the elevation difference in a circle with a 500 m

radius surrounding each valley width point. Locations of all mapped historic landslide dams (Morgenstern et al., in. prep) were then identified and matched to within 100 m of measured valley width points (Figure 30). The historic landslide dam database is the most comprehensive database of pre-historic and historic landslide dams in New Zealand and includes large and small dams with comprehensive attributes (Morgenstern et al., in. prep). The relationship between relief and width was evaluated for all dam and non-dam locations to identify any defining thresholds. Using the results from the Kaikōura Region, the same analysis can be applied to the West Coast Region using the identified threshold to identify potential landslide dam locations.

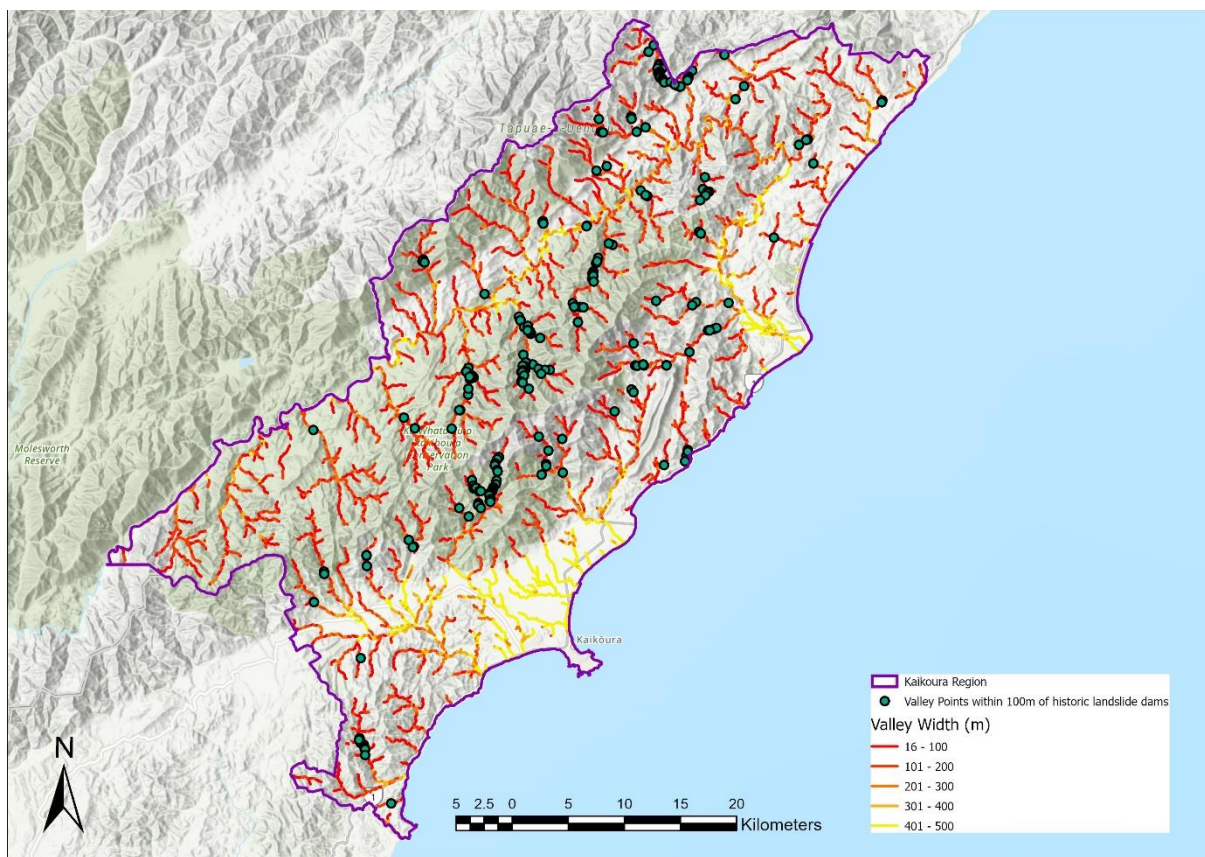


Figure 30- Kaikōura Region with valley width measurements overlaid with valley points (green) located within 100m of a historic landslide dam (Morgenstern et al., in prep).

### 3.2.5 Aggregated Landslide Dam Hazard

To further understand the hazard of landside dams, upstream area was calculated for each point to use as a proxy for the size of a potential landslide dam lake. The larger the upstream area, the greater potential for a bigger lake. Upstream area was calculated using a flow accumulation raster and focal statistics for each valley point.

The combination of narrow valley width, high relief, and large upstream area demonstrate locations where there is potential for landslide dams that could impound dangerous lakes. Combined with downstream infrastructure exposure, these factors were used to select high landslide dam hazard locations to undertake outburst flood modelling. Eight major catchments on the West Coast were selected for potential outburst flooding sites based on downstream exposure. These were the Buller, Grey, Haast, Hokitika, Taramakau, Waiho, Whataroa and Whanganui catchments. From these catchments sites with arbitrarily defined short valley widths (<150m), high relief (>350m) and large upstream area (>20,000m<sup>2</sup>) were selected as potential outburst flood modelling sites. These values were selected as they formed where clusters occurred above the reference line and were visually accurate for analysing spatial data. The downstream exposure of communities, State Highways, bridges, lifelines and farmland was evaluated and four sites with the greatest exposure were selected for outburst modelling. In addition these points were evaluated in terms of previous research. For example, valley points in the Waiho catchment in the Callery river demonstrated high landslide dam potential, however, were not selected for outburst flooding analysis as the hazard within the Callery River in particular has already been extensively researched (Davies & Scott, 1997; Davies, 2002; Ollett, 2001). From this analysis, four locations with high potential for landslide dam formation were selected for detailed outburst flood modelling.

### 3.3 Outburst Flood Hazard

Outburst flood modelling was undertaken using HECRAS in 2D at the four selected locations. In HECRAS the “storage area” was identified as the potential landslide dammed lake and was calculated from elevation contours at the relevant dam heights. HECRAS then calculated lake volume from the corresponding elevation and lake size. Two potential dam heights were considered: 10 m and 50 m. These values were selected based on analysis of dam heights from the 2016 Kaikōura earthquake, with 10 m considered a ‘typical’ average dam height, and 50 m is a reasonable upper estimate (Wolter et al., 2022). Landslide dams of 100 m or higher have occurred historically, but in general are comparatively rare (Liu et al., 2019; Shan et al., 2020).

In the HECRAS breach plan, the transect calculated valley width was selected as the final bottom width and the trigger failure was breaching by overtopping, as the most common style of failure (Costa and Shuster, 1988). In the lateral flow hydrograph, slope was calculated from the elevation of the DEM at the dam location. Unsteady data analysis was used for running the simulation, as this incorporates a non-uniform flow. The simulations ran over 66 hours, with peak discharge set to occur at 12 minutes after the initial breach, based on observations of the breach of the Hapuku River dam in Kaikōura (Wolter et al., 2022). For a 10 m dam, the maximum discharge was set at 100 m<sup>3</sup> and for a 50 m dam, the maximum discharge was 500 m<sup>3</sup>. These values were taken from the partial breach of the Hapuku River dam, where maximum recorded discharge during a partial failure was 90 m<sup>3</sup> over 30-40 minutes (Wolter et al., 2022). For the final unsteady flow analysis the computation interval was set at 5 minutes, with the mapping output, hydrograph output interval and detailed output interval set at 30 minutes. Exposure of communities and lifelines to outburst flooding was then undertaken through simple map overlays and assessment of bulk statistics.

#### 3.3.1 Exposure

To determine exposure from the 10 m and 50 m dam heights, the total area affected by the outburst flooding was considered. New Zealand roads (including State Highway 6) were selected from the LINZ database. Farmland was evaluated using the New Zealand land cover database with high producing exotic grassland and short rotation crop considered to

represent typical West Coast Region farmland. Finally, building footprints were taken from the LINZ database, and population data were taken from Statistics NZ and the 2018 Census. To estimate population exposure to outburst flooding, the total population per catchment was divided by the number of buildings to generate an average per building per catchment inhabitancy rate, which was then combined with the total number of exposed buildings to give total exposed population. This likely represents a conservative estimate of population exposure since not all buildings in the dataset are residential or inhabited, with barns, milking sheds, and other non-residential building types present in exposed areas.

## 4 Results

### 4.1 Kaikōura Region Analysis

A total of 6026 river points were evaluated across the Kaikōura Region using the Morgenstern et al., (in prep) dataset (Figure 31). Of these, 228 (3.8%) were within 100 m of a known landslide dam location (Figure 30). As expected (Figure 31), the majority of these points cluster in locations with narrow valley widths (<~150 m) and high local relief (>~350 m), with 98% forming in locations where local relief exceeded local valley width. This suggests that locations where local relief exceeds valley width may provide the necessary (but not sufficient) conditions for landslide dam formation. The reference line, or line with a slope of 1 (Figure 31), therefore provides a useful threshold above which landslide dams may form. A total of 1484 km (72.5%) of evaluated river in the Kaikōura Region lies above this threshold, corresponding to a rate of 1 dam per 6.6 km of river above the threshold. By comparison, just two landslide dams from the Kaikōura earthquake are found below the reference line from a total of 563 km of river, corresponding to a rate of 1 dam per 281.5 km of river below the threshold.

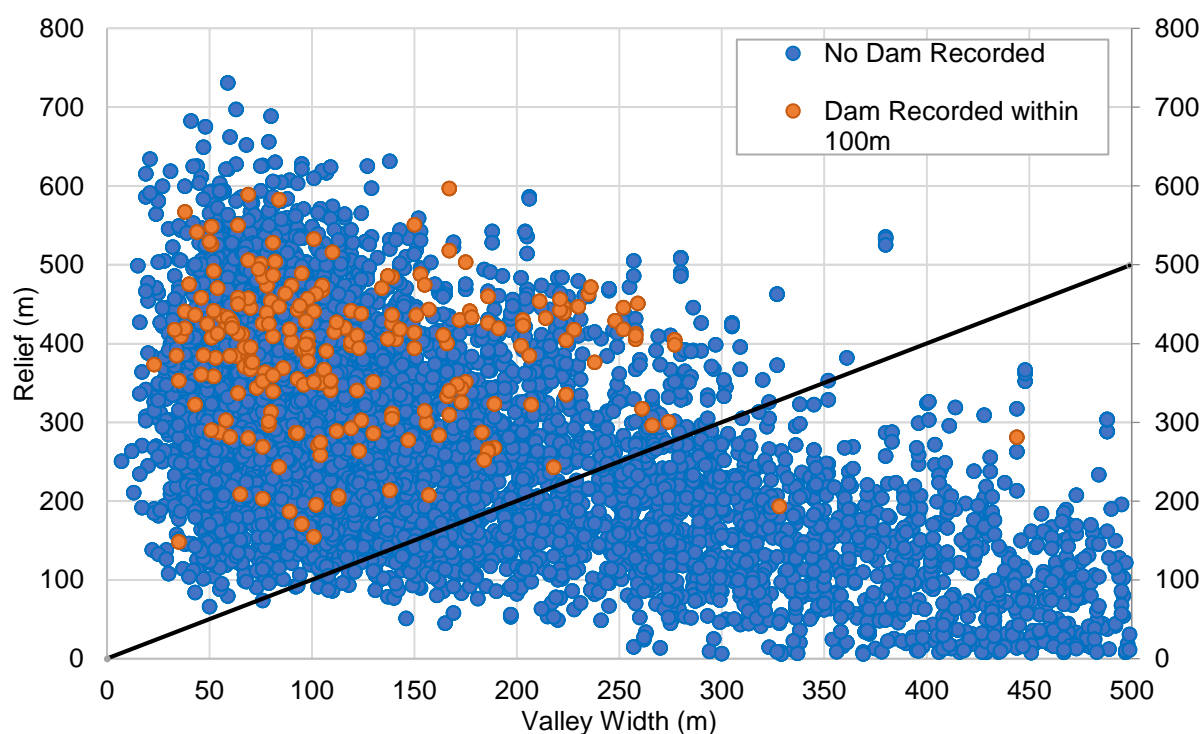


Figure 31- Kaikōura valley points, with orange points representing historical dams from the Morgenstern et al. (in prep) dataset.

## 4.2 Comparison between West Coast and Kaikōura Regions

With an area of 23,318 km<sup>2</sup>, the West Coast Region is significantly larger than the Kaikōura Region, which has an area of 2,047km<sup>2</sup>. Figure 32 shows the spatial difference between the two regions, highlighting that the Kaikōura Region appears to have a denser river network compared to the West Coast Region. The Whataroa catchment highlights the method on a local scale (Figure 33). Despite this, the comparative distributions of valley widths across the two regions indicate there is a broadly similar pattern for both regions. Valley widths in both regions peak in the 75-99 m category, before rapidly decreasing (Figure 34). Notably, the West Coast Region has a significantly higher proportion of large (>300 m) valley widths, approximately double the rate in the Kaikōura Region, highlighting the larger average catchment areas and higher frequency of large floodplains, particular west of the Alpine Fault.

A total of 48,344 valley points were evaluated across the West Coast Region (Figure 35), of which 123 (0.25%) occurred within locations of known landslide dams from Morgenstern et al (in prep). Of these historic and prehistoric landslide dam points, 106 (86%) occurred above the 1:1 reference line. This is a notably smaller percentage than identified in Kaikōura and suggests that some previous landslide dams on the West Coast appear to have occurred in regions with relatively wide valleys and low surrounding relief. Of the evaluated river sections, 10,582 km (45.4%) of order 2 or greater streams sit above this 1:1 threshold and therefore may have the potential for landslide dams to form. Applying the conversion rate of 1 dam per 6.6 km of river above the threshold from the Kaikōura earthquake translates to 1603 potential dam locations in the West Coast Region, assuming the entire region experiences sufficient shaking to trigger landsliding in a large-scale event.

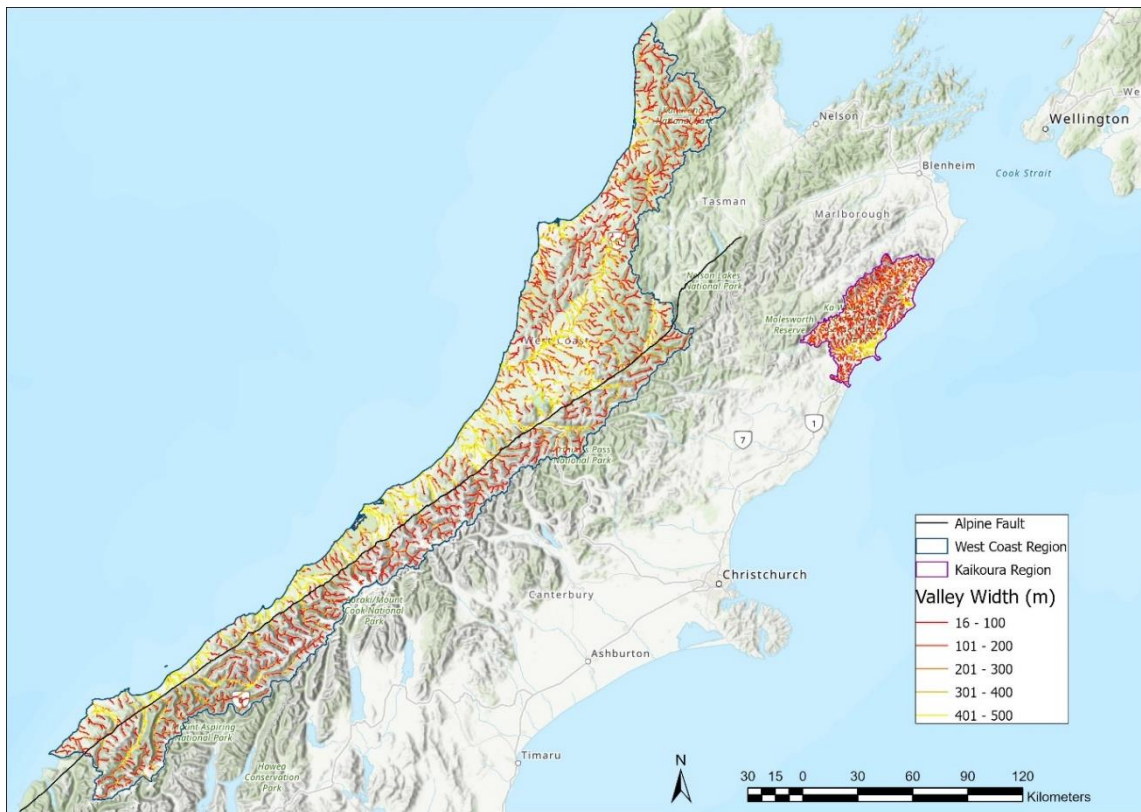


Figure 32- Valley width method applied to the West Coast Region and Kaikōura Region. This highlights the spatial variation as the West Coast Region is significantly larger than the Kaikōura Region. The West Coast Region also has a higher percentage of large valley widths (yellow lines) primarily due to the broad alluvial plains west of the Alpine fault.

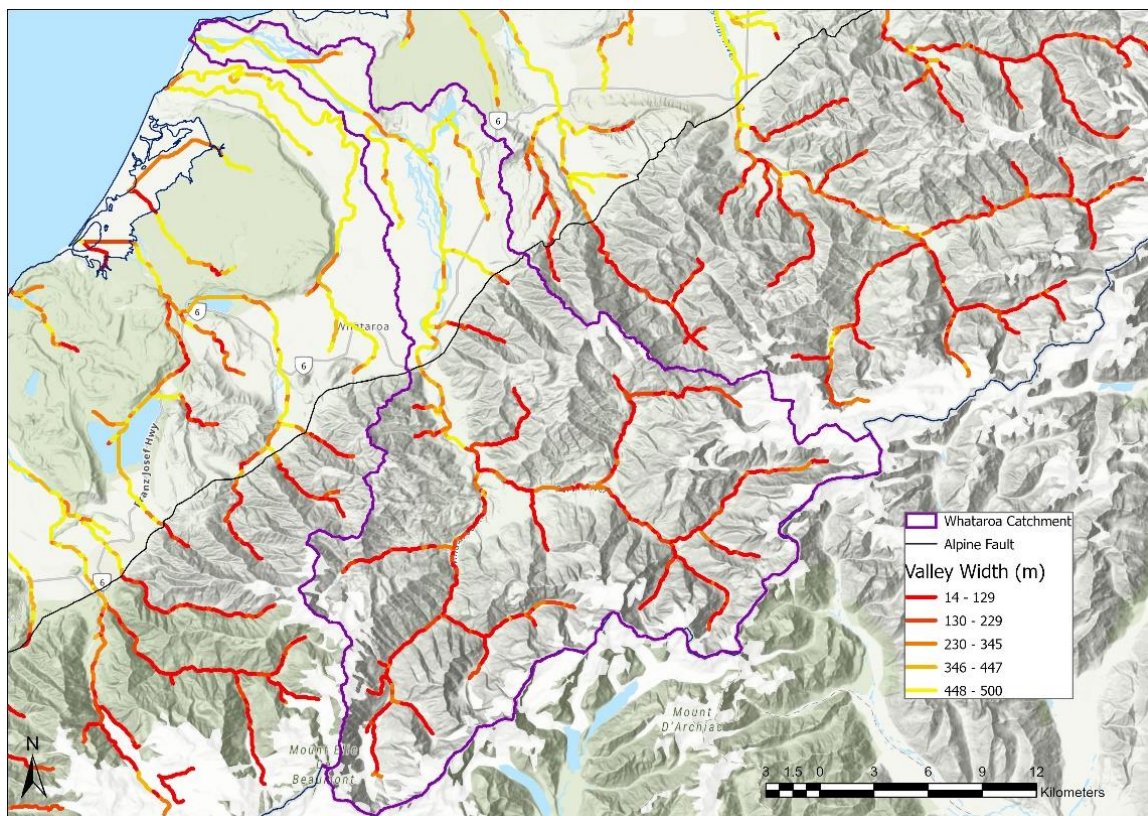


Figure 33- Modelled valley widths in the region surrounding the Whataroa catchment highlighting the typically narrow valley widths east of the Alpine Fault compared to the much wider valley widths west of the Alpine Fault.



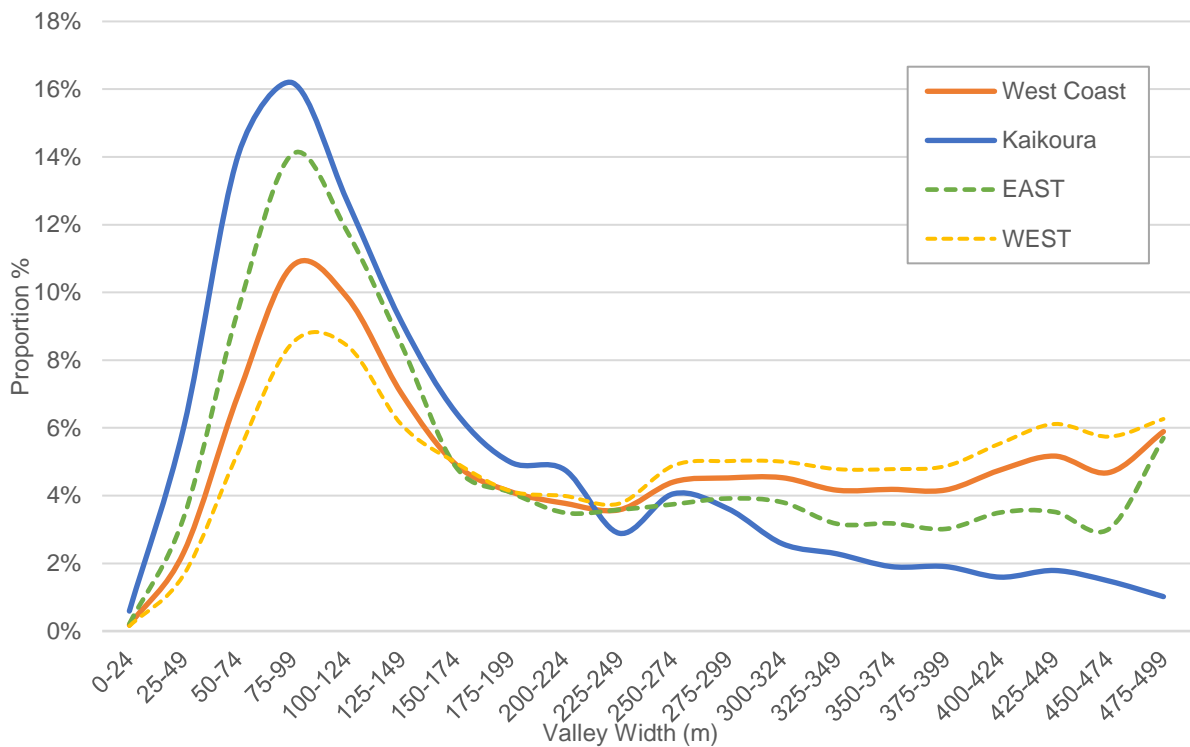


Figure 34- Valley width frequency for the West Coast Region vs Kaikōura Region. For both regions valley widths increase until 75-99 m, then rapidly decrease, forming a similar bell curve. The longer tail for the West Coast Region indicates the larger catchment area and high frequency of floodplains. Valley width frequency on the East of the Alpine Fault follows a similar bell curve to Kaikōura, while West of the Alpine Fault appears more bi-modal, with a much higher frequency of wide (>300 m) valleys.

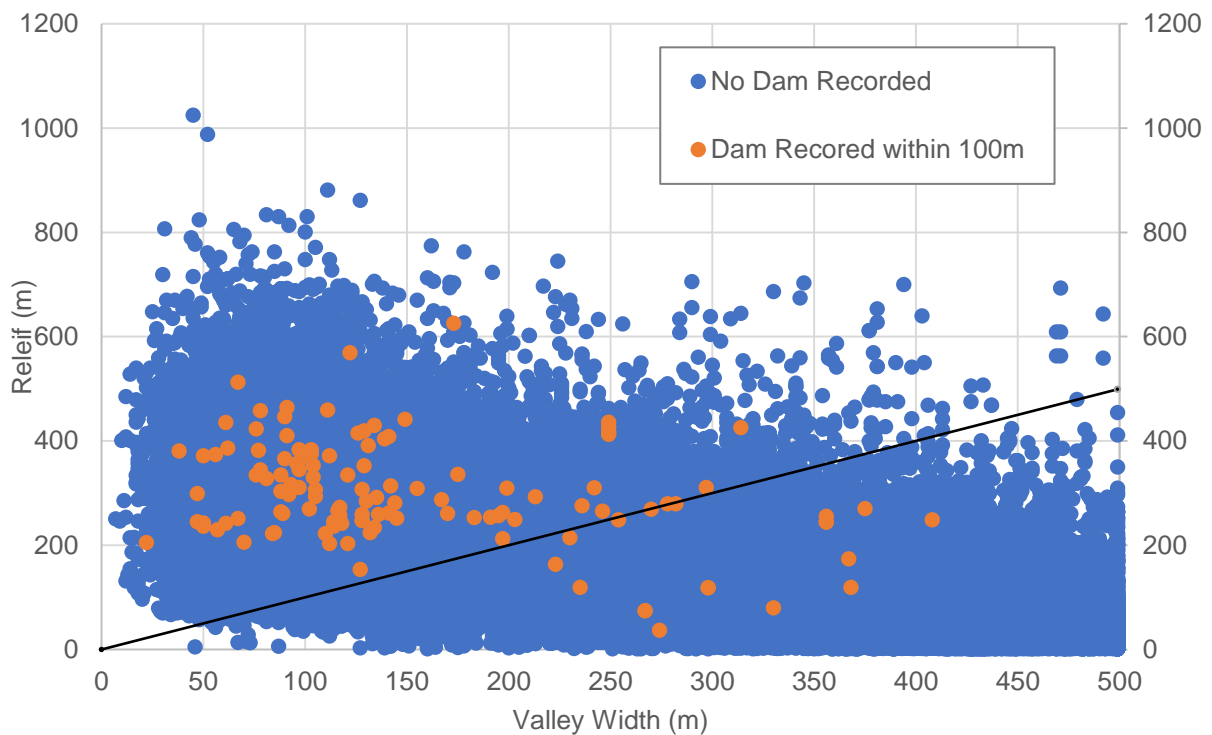


Figure 35- West Coast Region Valley Points with orange points representing known dam sites from the Morgenstern et al. (in prep) dataset. The reference line shows locations where local relief equals local valley width. 86% of known landslide dams occur above this threshold, notably lower than observed in Kaikōura Region (Figure 31).

### 4.3 Catchment Scale Analysis

Within the West Coast Region, eight of the major catchments (Figure 36) were selected for detailed analysis based on the downstream presence of communities and critical lifelines. These catchments were the Buller, Grey, Haast, Hokitika, Taramakau, Waiho, Whanganui and Whataroa. Mean valley width across all eight catchments was similar, while median values showed a greater degree of variation (Table 1). All catchments demonstrate a similar distribution of valley widths, again each peaking in the 75-99 m class, before rapidly decreasing (Figure 37). Notably, the Grey River is the only catchment that shows a bi-modal distribution with peaks in the 75-99 m and 425-449 m categories, highlighting the wide valley floodplains between Reefton and Greymouth. All other catchments show a unimodal distribution peaking in the 75-99 m category.

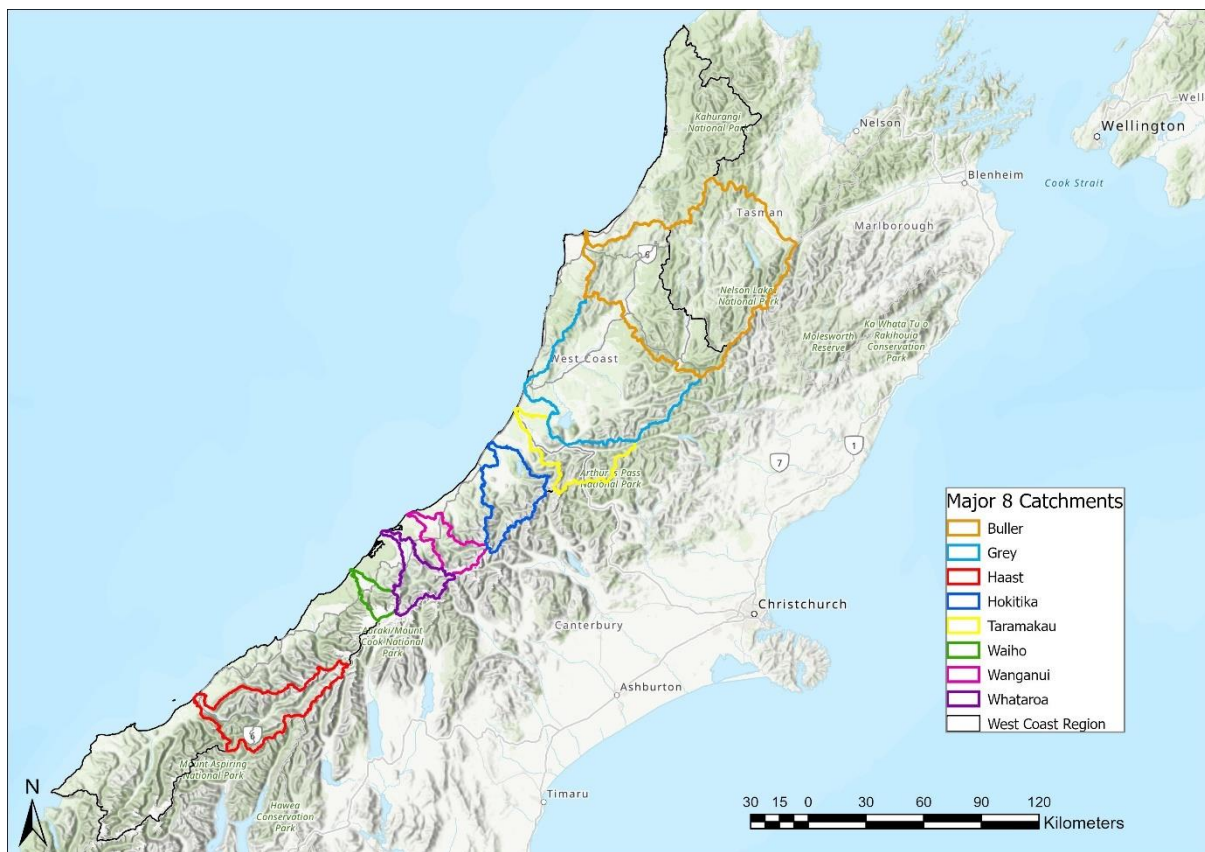


Figure 36- Location and extent of the eight major catchments evaluated within the West Coast Region. Note that part of the Buller catchment extends into Tasman Region, which was not included in this study. Values quoted throughout correspond to only the catchment area within the West Coast Region.

Table 1- Valley width statistics for the 8 major catchments in the West Coast Region.

Catchment	Buller	Grey	Haast	Hokitika	Taramakau	Waiho	Whanganui	Whataroa
Mean Valley Width (m)	221	278	232	232	258	244	217	202
Median Valley Width (m)	186	289	200	199	266	207	177	141
Standard Deviation	133	135	138	143	141	150	136	136
Catchment Area (km <sup>2</sup> )	2658	3949	1356	1068	1005	292	524	593

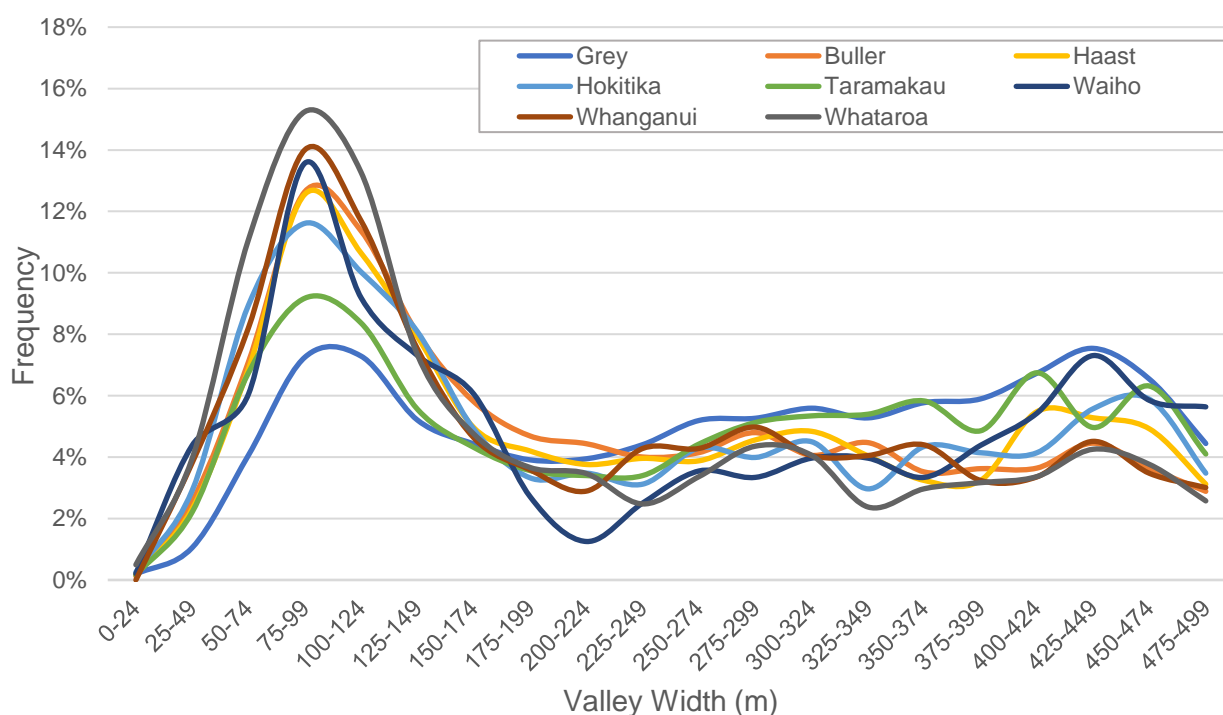


Figure 37- Frequency of valley points for the eight major catchments in the West Coast Region, demonstrating a similar bell curve for each catchment, where valley widths increase to 75-99 m, then rapidly decrease. The Whataroa catchment has the highest frequency curve, with the Grey catchment having the lowest frequency curve and a long tail, with a bi-modal distribution.

For the eight major catchments (Table 2) the number of points above the reference line can be calculated for each catchment, and from the Kaikōura Region-based conversion rate, the

total number of potential dam sites estimated. Especially hazardous locations can further be determined from locations that have large upstream areas (i.e. greater than 20,000 m<sup>2</sup>). An upstream area of 20,000 m<sup>2</sup> was considered as it is the median upstream area for the West Coast Region. As expected, the largest catchments have the highest number of potential dam locations. However, in contrast, smaller catchments such as the Whataroa have a greater density of potential dam sites, which represents a better measure of impact than total number. Overall, the Haast, Hokitika, Wanganui and Whataroa catchments have the highest density of potential dam sites (>1 per km<sup>2</sup>) as well as a large percentage of potential landslide dam sites with large upstream areas, suggesting considerable landslide dam hazard (Table 2). The Haast catchment was considered the most hazardous, as in all calculations it had high values, with 118 potential landslide dams sites in total and one third of all points above the 1:1 line with large upstream area (Table 2). This suggests the Haast catchment is one of the highest hazard locations in the West Coast Region for landslide dam formation. The Whataroa catchment also has a high density of potential landslide dam sites, with 40% of potential locations also having large upstream area, however this would result in considerably fewer landslide dams (59) due to the much smaller catchment size. In contrast, although the Buller and Grey catchments have the highest number of potential dam sites, they have the lowest percentage of dam points with large upstream area (Table 2). The Grey catchment also has a lower density of potential landslide dam sites in relation to the large catchment area and total valley points. Given the area of the Buller catchment analysed was only 41% of the total catchment, the high density of potential dam sites is anomalous. The section of the Buller catchment in the Tasman Region has lower relief and wider valleys that would result in a low density of potential dam sites when combined with the section in the West Coast Region.

Table 2- Catchment data for the 8 major catchments showing catchment area, points above the 1:1 line, high upstream area and potential dam sites (UA- Upstream Area, AF- Alpine Fault).

<b>Catchment</b>	<b>Catchment Area (km<sup>2</sup>)</b>	<b>Number of points above 1:1 line</b>	<b>Points and Percentages above 1:1 line with high UA</b>	<b>Potential number of dams at 1 dam per 6.6km of river above the reference line</b>	<b>Density (Potential Dam sites per km<sup>2</sup>)</b>
<b>Haast</b>	1356	1,503	812 (31%)	118	1.11
<b>Grey</b>	3949	2,368	675 (8%)	161	0.60
<b>Buller</b>	2658	2,996	274 (4%)	207	1.13
<b>Hokitika</b>	1068	1,075	842 (41%)	84	1.01
<b>Taramakau</b>	1005	815	528 (27%)	63	0.81
<b>Waiho</b>	292	247	204 (41%)	22	0.85
<b>Whanganui</b>	524	529	326 (37%)	47	1.01
<b>Whataroa</b>	593	690	419 (40%)	59	1.16

The individual catchment analysis highlights those valley points occurring above the 1:1 reference line in the 'sweet spot' areas of low valley width and high relief, as well as the upstream area are the corresponding location (Figure 38 a-h). Particularly in the Haast, Hokitika, Waiho, Whanganui and Whataroa catchments there are clear clusters of potential landslide dam sites occurring above the reference line to the east of the Alpine Fault with notably large upstream areas. Due to the location in the north of the West Coast Region, the Grey and Buller catchments have significantly more valley measurements west of the Alpine Fault, and these catchments typically have lower relief, with most evaluated points below 400 m relief. Notably the Whanganui catchment has two valley points occurring in areas of extremely high relief (>1000 m) and low valley width (<60 m), although upstream area measurements at these locations are small, suggesting these points are high in the catchment where any impounded lake is likely to be small, regardless of the dam height.

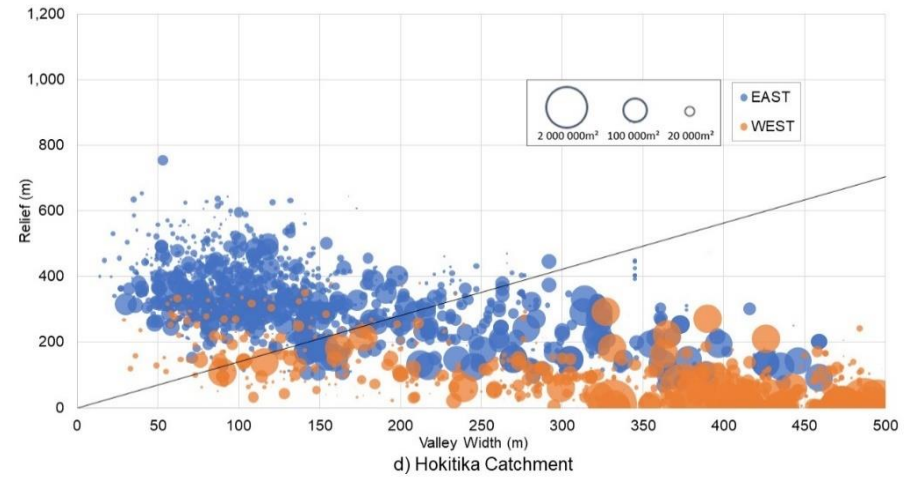
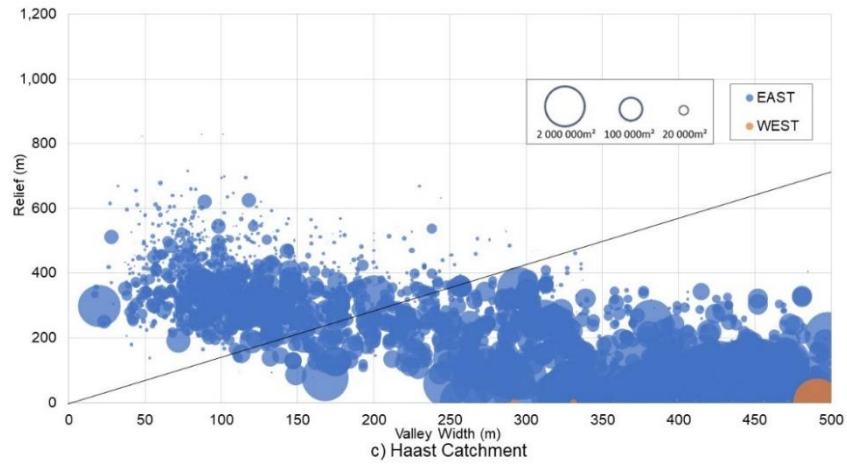
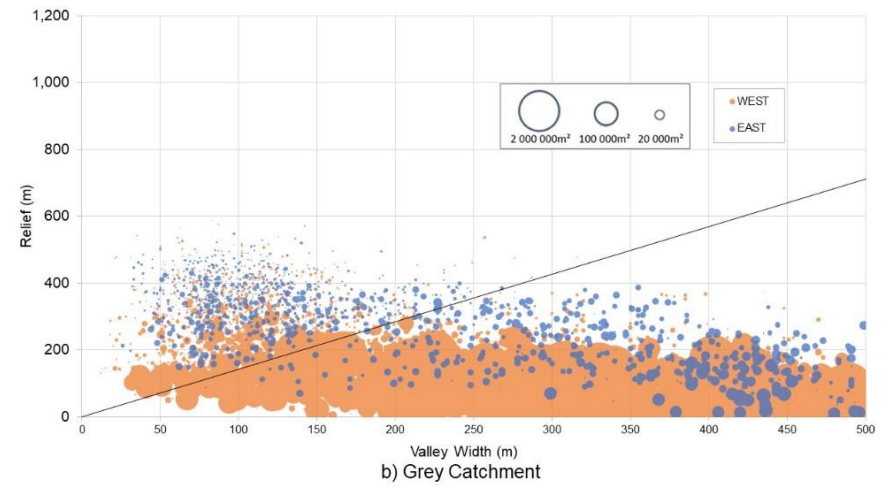
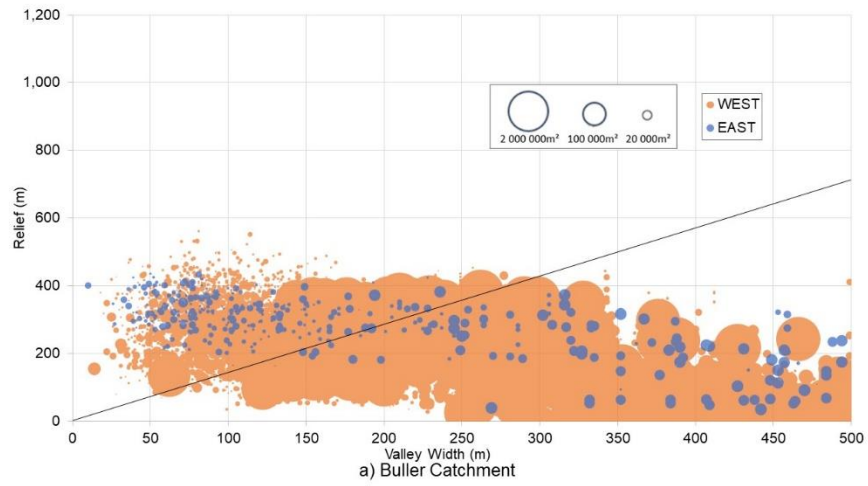


Figure 38- Bubble plots of the major eight catchments in the West Coast Region.  
 a) Buller, b) Grey, c) Haast, d) Hokitika

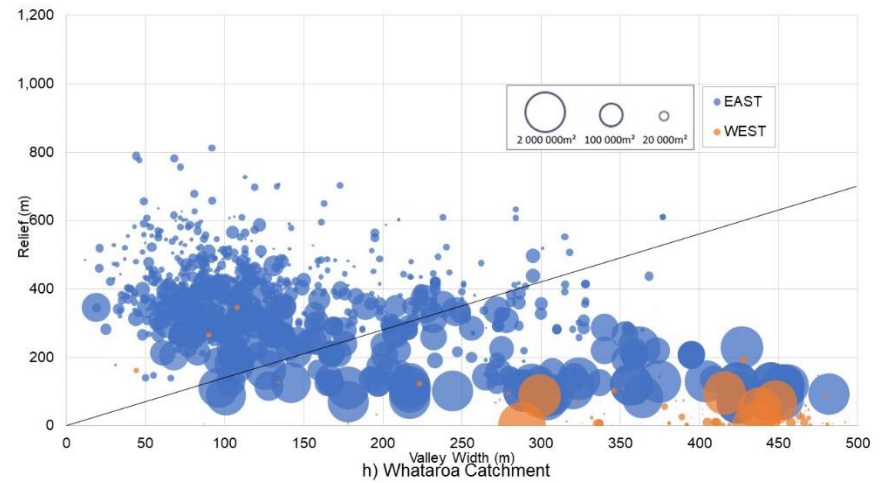
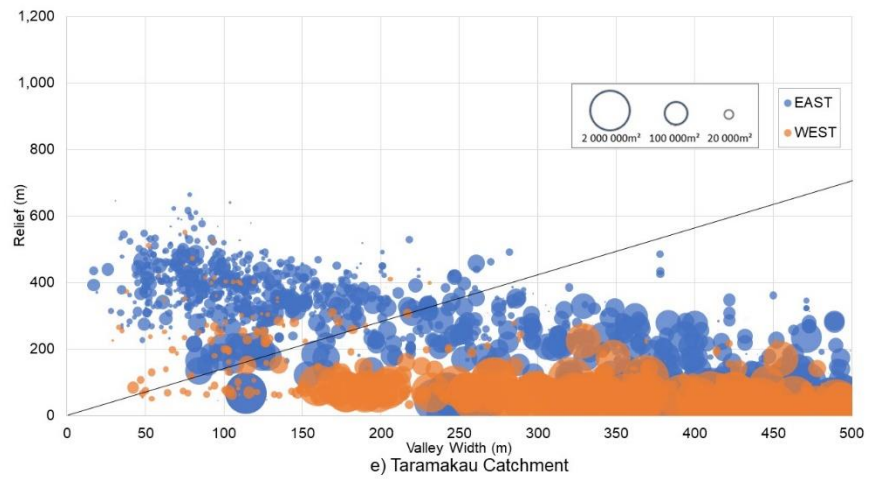
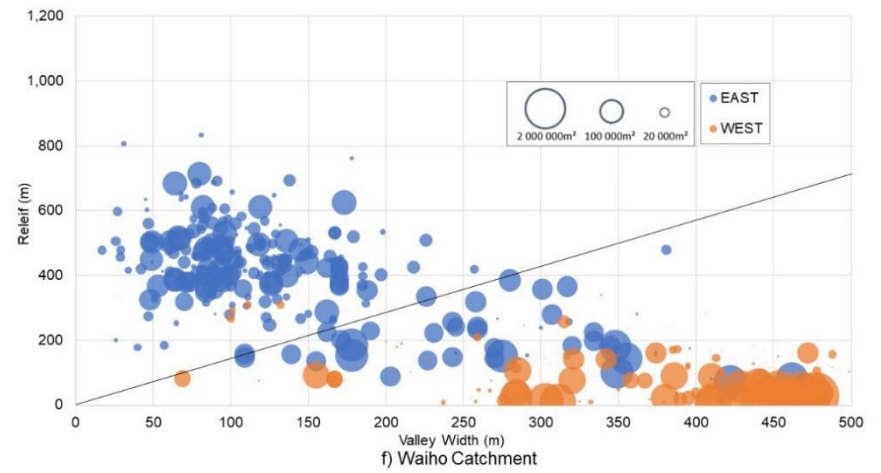
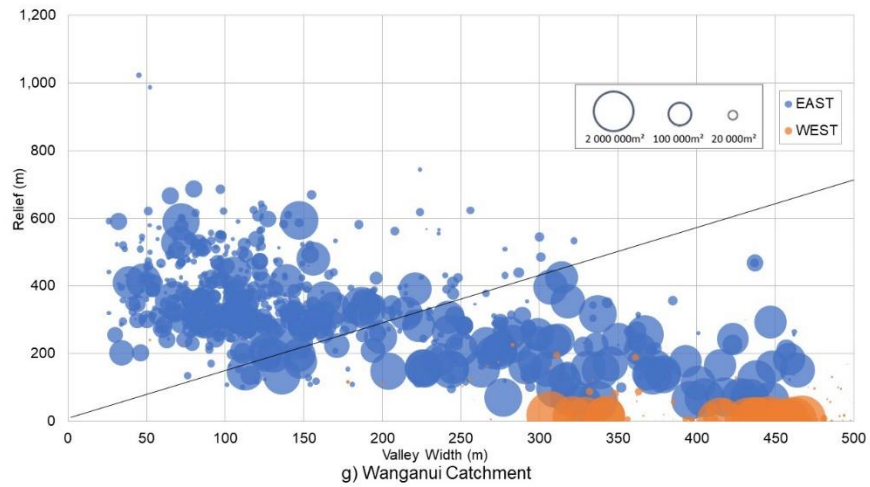


Figure 38 continued- Bubble Plots of the major eight catchments in the West Coast Region.  
e) Taramakau, f) Waiho, g) Wanganui, h) Whataroa

#### 4.4 Selection of outburst flooding locations

The spatial distribution of valley 'sweet spots' with low valley width, high relief and large upstream area is shown in Figure 39-Figure 41. This is a relative landslide dam hazard map that can be used to estimate landslide dam hazard on regional scale, showing both the locations where landslide dams are most likely to form (narrow valleys with high surrounding relief) and which sites have potential to form large, hazardous lakes (large upstream area). Over the entire West Coast Region there were 2481 points with narrow width ( $\leq 150$  m), high relief ( $\geq 350$  m) and large upstream area ( $\geq 20,000$  m<sup>2</sup>). Of these values, 1243 (50%) were located in the eight major catchments. The Whataroa and Hokitika had the largest proportion (24% and 22% respectively) despite being substantially smaller than the Grey and Buller catchments, while the Taramakau and Waiho had the least (11% and 12% respectively). The biggest upstream areas were located in the Buller and Grey catchments, however these are typically at proportionally wide valley points ( $>150$  m) where landslide dam formation is less likely. Of those sites with narrow valley width and high relief, there are 21 that have an upstream area  $>200,000$  m<sup>2</sup>, all of which are located in the Haast, Hokitika and Whataroa catchments. Consequently, the Haast, Hokitika and Whataroa catchments were considered the most hazardous locations for landslide dam formation and were therefore selected for outburst flood modelling.

Two sites were selected within the Haast catchment (Gates of Haast and the Landsborough River), and one each in the Hokitika catchment and Whataroa catchment (on the Perth River) for outburst flood modelling (Table 3 and Figure 42). Using the individual catchment analysis, these points can be viewed in relation to the other valley points within the corresponding catchment (Figure 43-Figure 45).



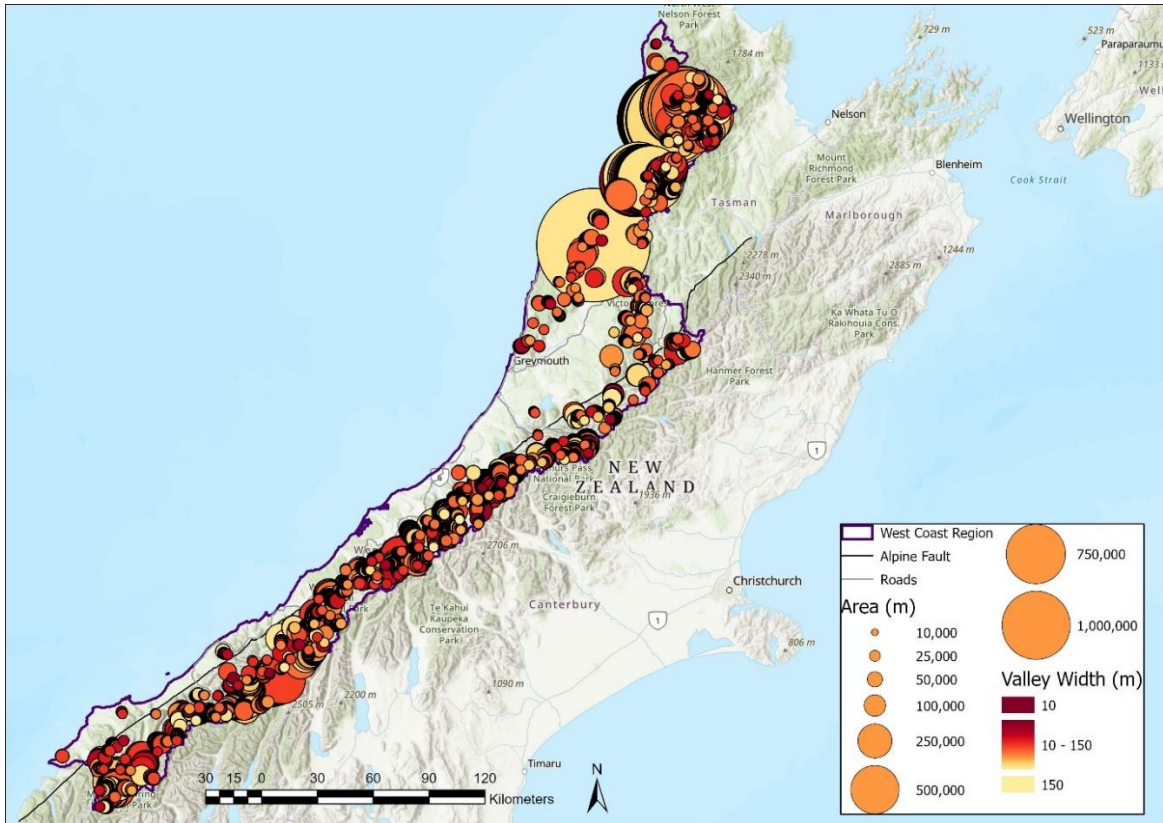


Figure 39- Relative Landslide Dam Hazard Map. This graph shows locations where local slope relief is  $>350$  m, valley width is  $<150$  m and upstream area is  $>20,000$  m. The colours represent valley width, with darker red representing short valley widths. Upstream area, or the size of a potential lake is represented by bubble size, with the largest upstream areas having the largest bubbles. Therefore, the greatest landslide dam hazard locations are where large red bubbles are located.

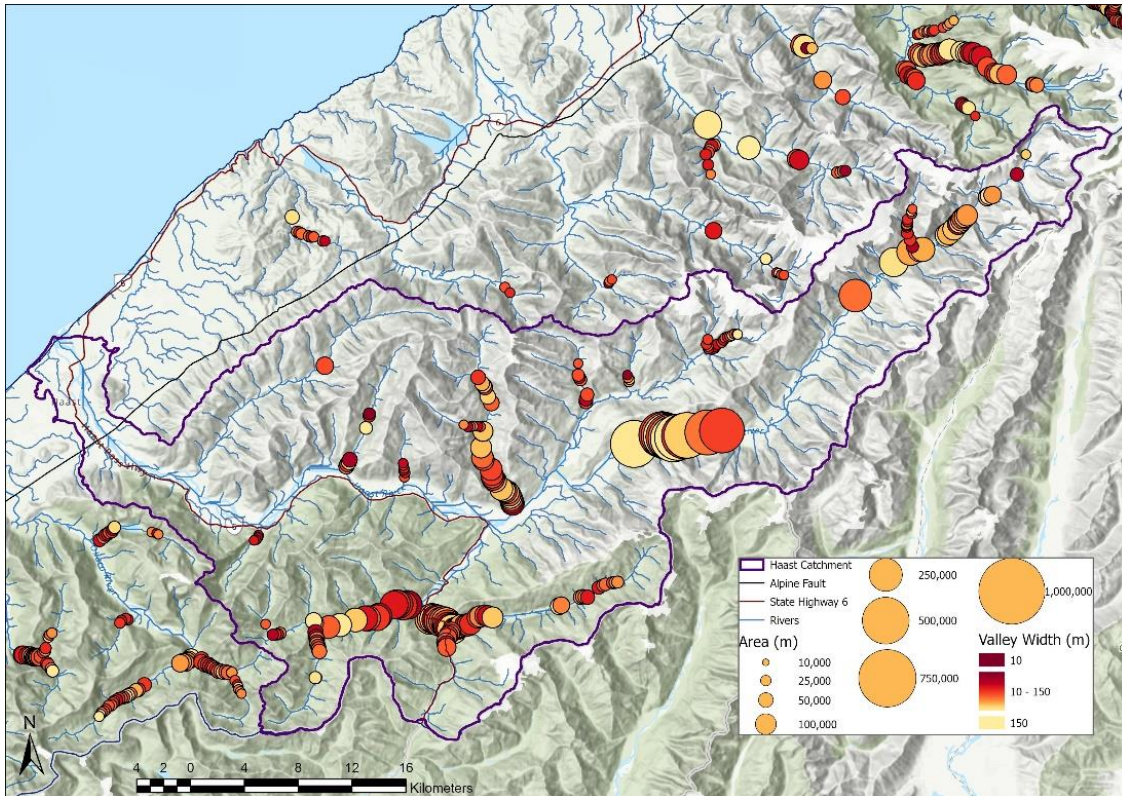


Figure 40- Relative Landslide Dam Hazard Map of the Haast Region, indicating where the most hazardous landslide dam locations occur. The larger red bubbles occur in the Landsborough river and the Gates of Haast.

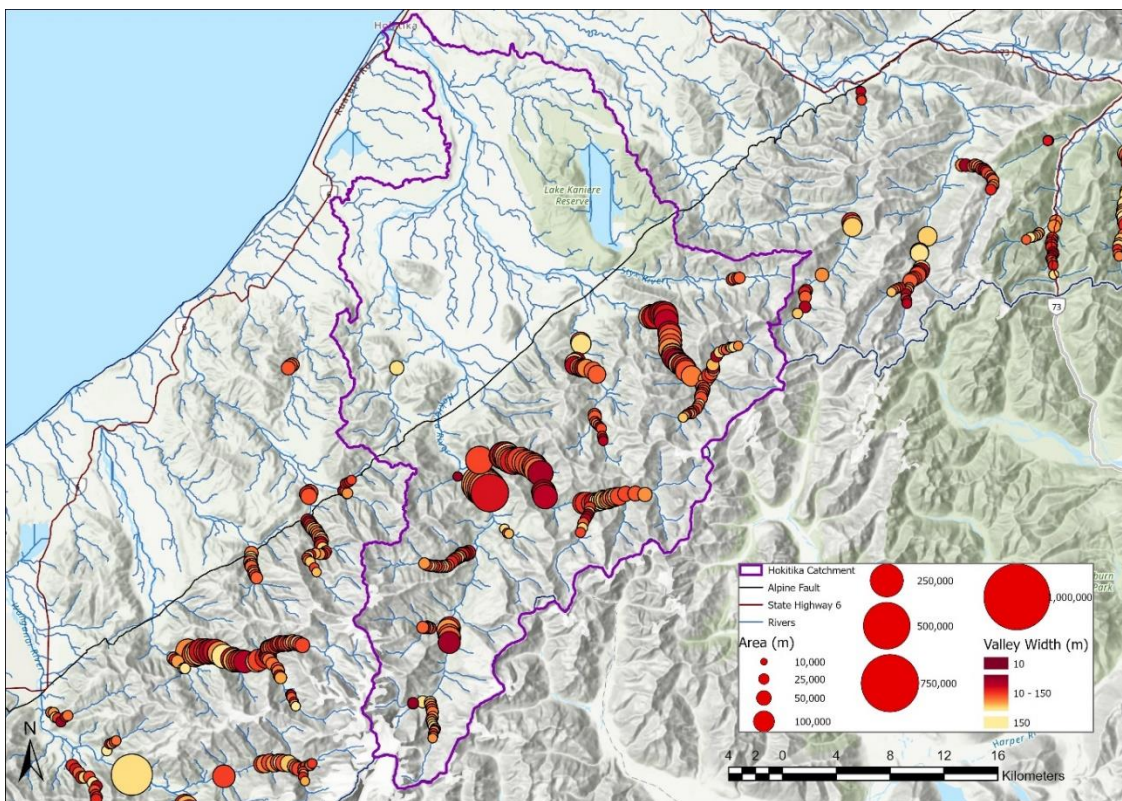


Figure 41- Relative Landslide dam hazard map of the Hokitika region, indicating where the most hazardous locations occur. The largest red bubbles occur in the Hokitika River.

Table 3- Parameters of locations selected for outburst flood modelling in the West Coast Region.

Catchment	Valley Width	Relief	Upstream Area	Downstream Exposure
Gates of Haast	98 m	545 m	200 200 m <sup>2</sup>	SH6, farmland Haast Township
Haast-Landsborough	85 m	375 m	484 962 m <sup>2</sup>	SH6, farmland Haast Township
Hokitika	118 m	499 m	327 175 m <sup>2</sup>	Road networks, SH6, farmland, Hokitika Township
Whataroa	75 m	359 m	337 305 m <sup>2</sup>	SH6, farmland, Whataroa township,

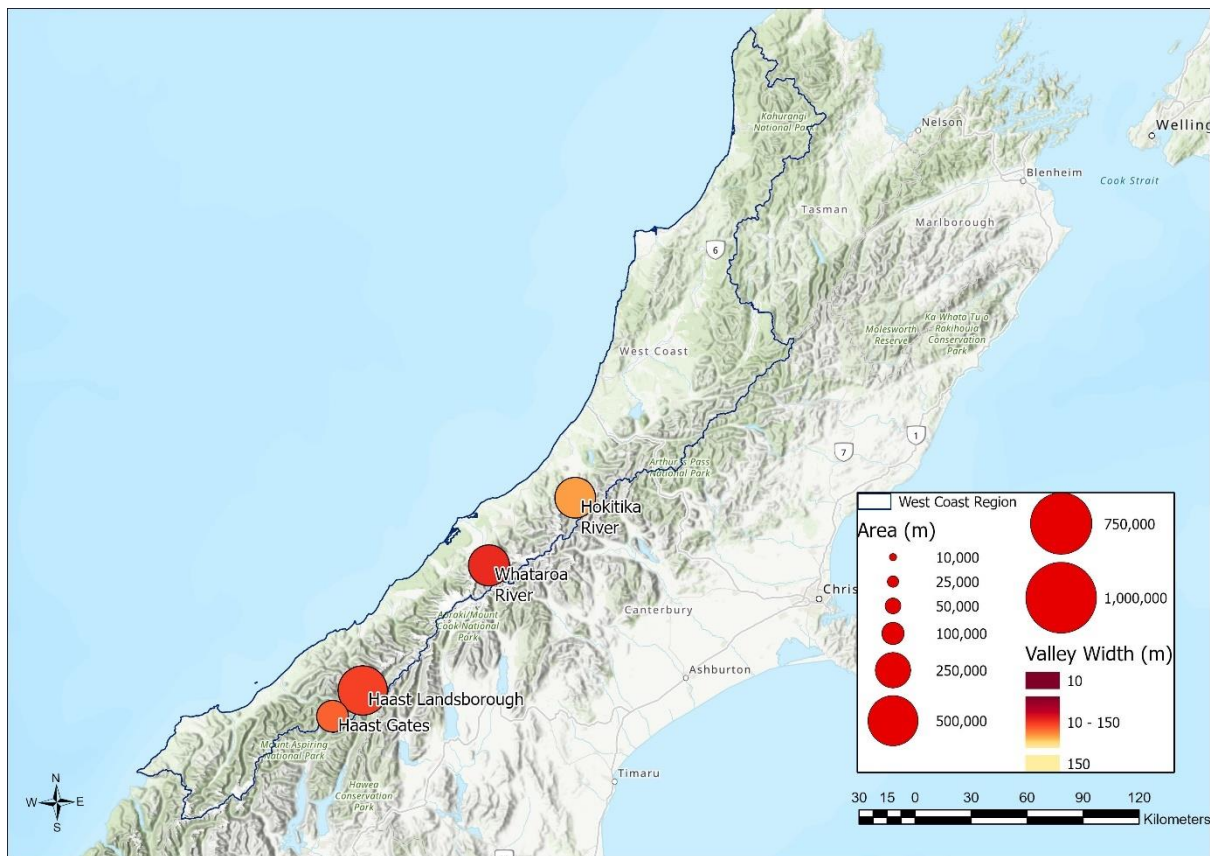


Figure 42- Sites selected for Outburst Flood modelling in the West Coast Region from the relative landslide dam hazard map.

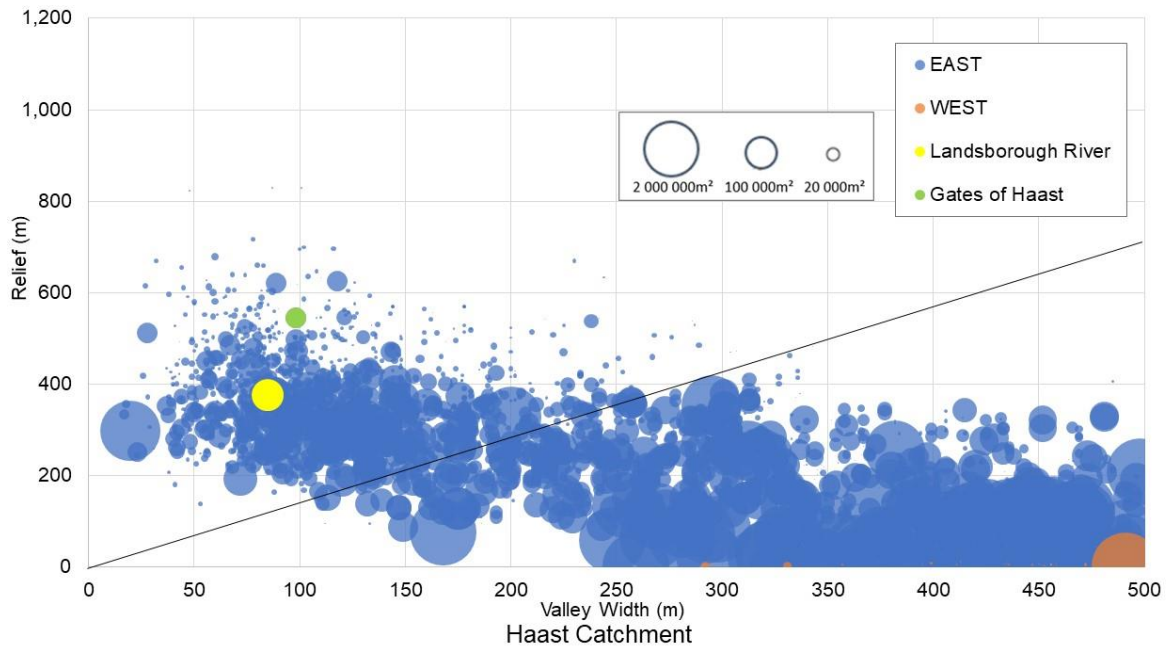


Figure 43- Bubble graph for the Haast Catchment showing locations of Landsborough River and Gates of Haast locations selected for outburst flood modelling.

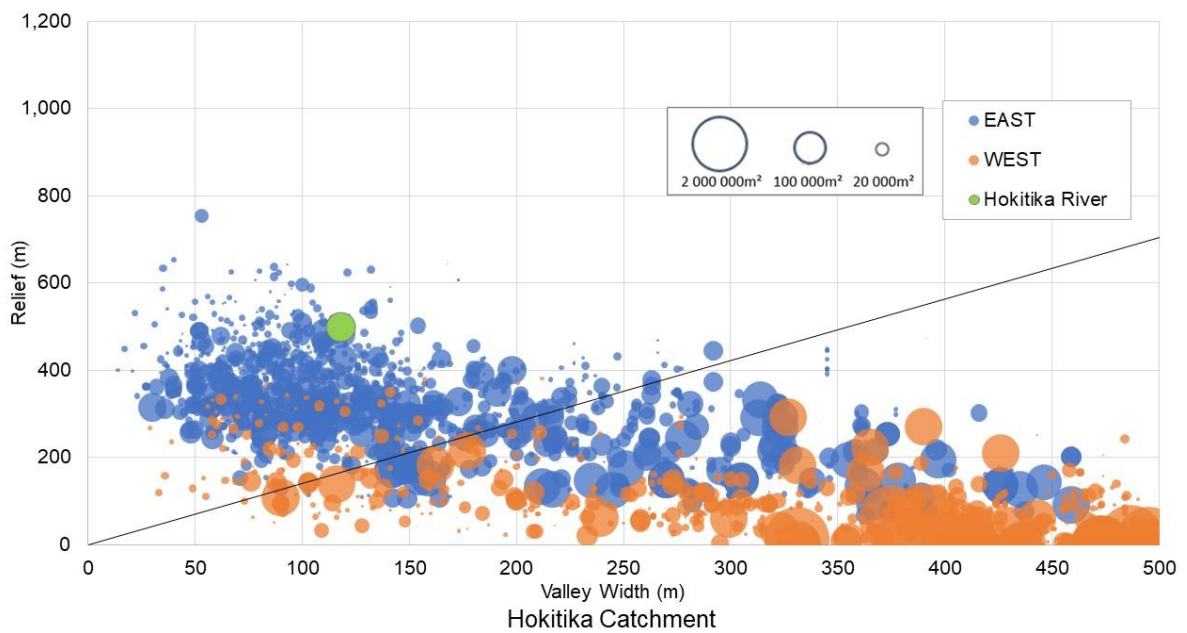


Figure 44- Bubble graph for the Hokitika catchment showing locations of the Hokitika river selected for outburst flood modelling.

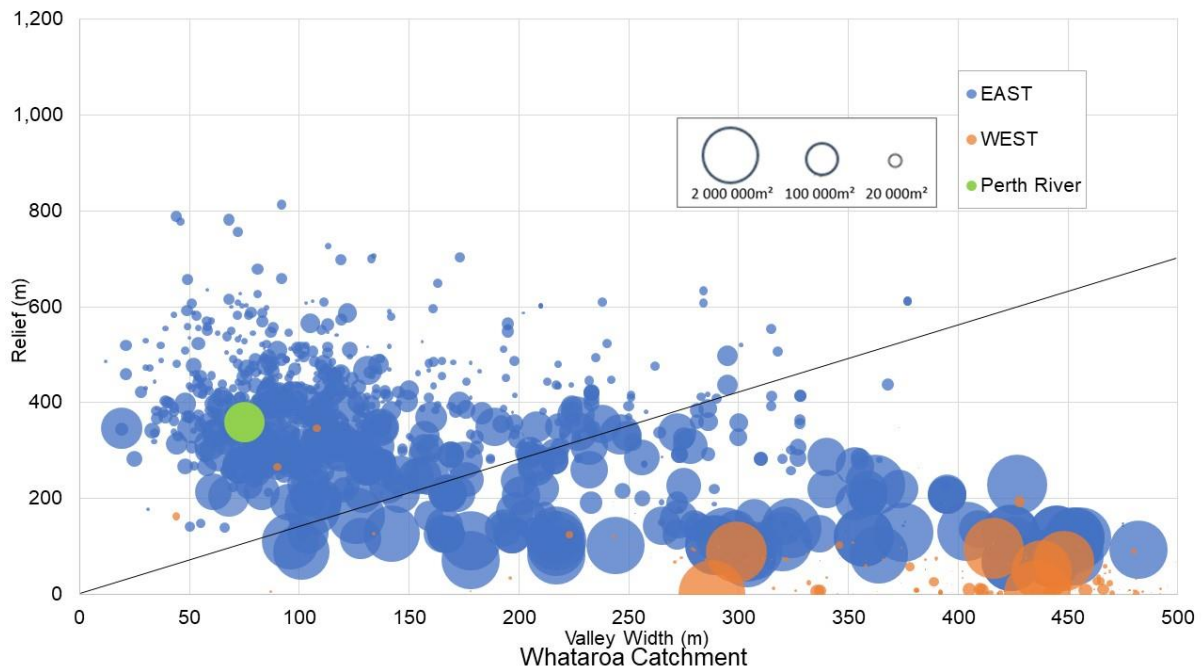


Figure 45- Bubble graph for the Whataroa catchment showing location of the Perth river selected for outburst flood modelling.

## 4.5 Outburst flooding

Outburst flood modelling was undertaken at each location for dam heights of 10 m and 50 m (Table 4). The outburst flood inundation models for each location demonstrated extensive potential flooding downstream to roads, farmland and buildings (Table 5). Comparing floods from 10 m and 50 m dams in each location, the 50 m outburst flood more than doubled the total inundated area from each location. Due to the nature of the catchments downstream of the selected sites, flooding at the Gates of Haast and Haast-Landsborough sites (Figures 46-47) remain confined almost all the way to the coast, while the Hokitika and Whataroa outburst floods are able to spread over a wider area of floodplains once they cross the Alpine Fault (Figure 48-Figure 49,). Overall, the Hokitika catchment has the largest amount of roads, farmland and buildings exposed, however the Haast catchment has the highest total percentage of roads, farmland and buildings exposed within the catchment. For example, in Haast, a 50 m outburst flood event would expose 96% of all buildings, however this is only 5% of the total buildings within the Hokitika catchment. A 50 m outburst flood in the Whataroa catchment would affect over half the catchment, exposing 53% of total buildings and 59% of farmland. The highest percentage of farmland exposed occurs from the Haast-Landsborough

site, followed by the Whataroa site. Combining the maximum exposed area over 50 m floods in the three catchments, there is 51.8 km of SH6, 142,708 km<sup>2</sup> of farmland and 2173 buildings potentially exposed to landslide dam outburst flooding. Combined across the 3 catchments, there are 2,340 people who are permanently located in these regions who would be exposed to outburst flooding. Hokitika exposes the largest amount of people, however the Haast catchment exposes the largest percentages of the total population. The Haast-Landsborough and Gates of Haast sites account for 92% of the total exposure to SH6, covering a length of 45 km, although in an outburst flood event these locations will overlap since both locations drain similar river sections. All locations indicate significant exposure to critical infrastructure and communities downstream with both scenarios.

*Table 4 – Outburst flooding for 10m and 50m dam heights at the four selected locations.*

<b>Location</b>	<b>10m Outburst Flood Area</b>	<b>50m Outburst Flood Area</b>	<b>Figure</b>
<b>Gates of Haast</b>	32 km <sup>2</sup>	67 km <sup>2</sup>	Figure 46
<b>Haast- Landsborough</b>	33 km <sup>2</sup>	73 km <sup>2</sup>	Figure 47
<b>Hokitika</b>	50 km <sup>2</sup>	117 km <sup>2</sup>	Figure 48
<b>Whataroa</b>	44 km <sup>2</sup>	111 km <sup>2</sup>	Figure 49

Table 5- Outburst flooding exposure to roads, farmland and buildings with population statistics (Data obtained from LINZ - NZ road network, LandCover database, NZ buildings database and Statistics New Zealand- 2018 Census population data).

Location	Dam Height	Length of Road Exposed	Area of Farmland Exposed	Buildings Exposed	Exposed Permanent Population
<b>Gates of Haast</b>	10 m	11.5 km (10.747 km on SH6) 15% of total road length	3,990.6 km <sup>2</sup> 21% of total farmland	38 buildings 15% of total buildings	39 People 15% of total people
	50 m	51.2 km (45.419 km on SH6) 67% of total road length	10,644.5 km <sup>2</sup> 57% of total farmland	244 buildings 96% of total buildings	248 People 96% of total people
<b>Haast-Landsborough</b>	10 m	6.5 km (5.74 km on SH6) 9% of total road length	4,752 km <sup>2</sup> 26% of total farmland	36 buildings 14% of total buildings	37 People 14% of total people
	50 m	38.5 km (32.857 km on SH6) 51% of total road length	12,760.1 km <sup>2</sup> 68% of total farmland	244 buildings 96% of total buildings	248 People 96% of total people
<b>Hokitika</b>	10 m	29.2 km 13% of total road length	35,207.4 km <sup>2</sup> 24% of total farmland	304 buildings 6% of total buildings	92 People 6% of total people
	50 m	79.4 km (0.9 km on SH6) 35% of total road length	74,625.8 km <sup>2</sup> 52% of total farmland	1522 buildings 32% of total buildings	459 People 32% of total people
<b>Whataroa</b>	10 m	9.6 km (1.3 km on SH6) 12% of total road length	15,925.5 km <sup>2</sup> 17% of total farmland	59 buildings 8% of total buildings	50 People 8% of total people
	50 m	48.1 km (5.5km on SH6) 58% of total road length	55,322.2 km <sup>2</sup> 59% of total farmland	407 buildings 53% of total buildings	342 People 53% of total people



Figure 46- Outburst flood inundation map for the Gates of Haast at 10m and 50m landslide dam heights showing downstream exposure.





Figure 47- Outburst flood inundation map for the Haast Landsborough catchment at 10 m and 50 m landslide dam heights showing downstream exposure.

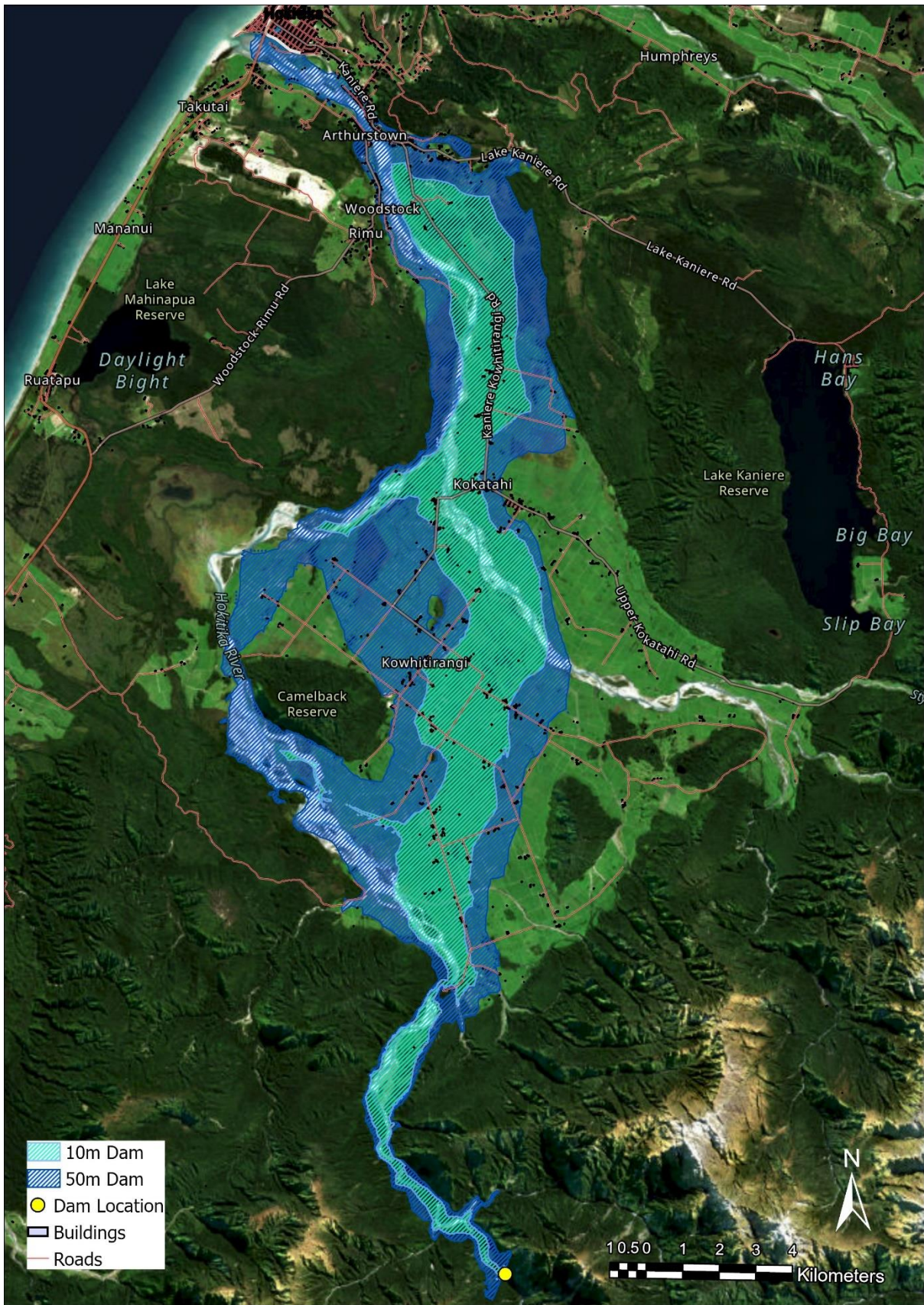


Figure 48- Outburst flood inundation map for Hokitika for 10m and 50m landslide dam heights showing downstream exposure.

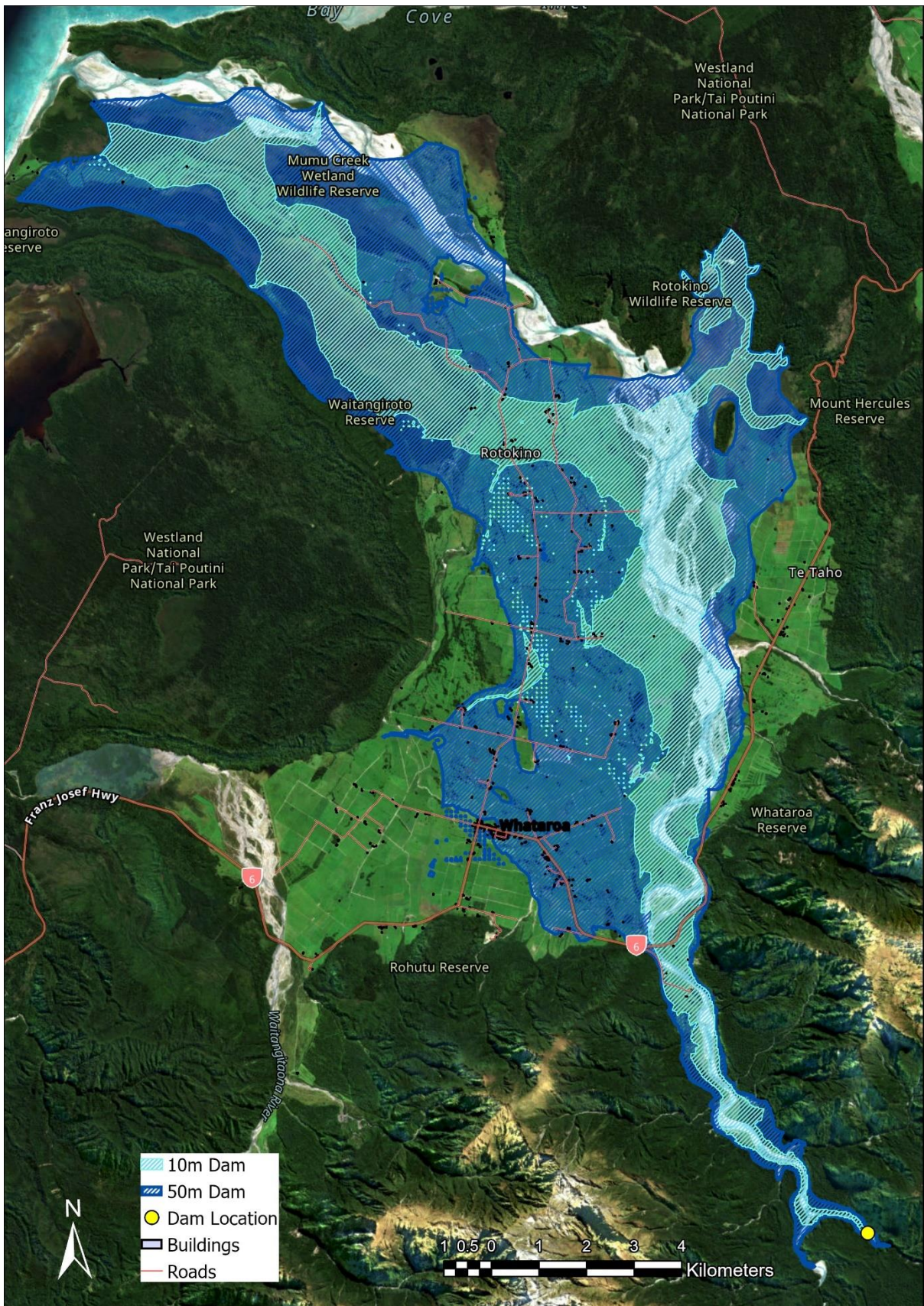


Figure 49 - Outburst flood inundation map for Whataroa at 10m and 50m landslide dam heights showing downstream exposure.

## 4.6 Summary of key findings

To summarise the key findings, there is a high hazard of landslide dams forming on the West Coast Region of New Zealand. Landslide dam potential in the West Coast Region is comparable to that witnessed during the Kaikōura earthquake and in the event of an Alpine Fault earthquake, seems likely to result in significantly higher numbers of landslide dams forming due to the larger total area. Comparisons of the eight major catchments showed the most hazardous locations were in locations above the 1:1 line, with short valley width, high relief and the highest percentages of upstream area per catchment. The Haast catchment was found to be particularly hazardous across all statistics, with a high density of potential dam sites and up to 812 potentially high hazard landslide dam sites. The relative landslide dam hazard map provides a spatial output to identify these locations on a regional scale. The Haast, Hokitika and Whataroa catchments had the highest combination of high relief, short valley widths, and significant upstream area and were selected for outburst flood modelling. Outburst flood modelling for 10 m and 50 m high dam sites at each of these locations identified potential significant exposure to roads, farmland and buildings in these catchments, with the Hokitika catchment having particularly high absolute levels of exposure, but the Haast catchment having the largest percentage of infrastructure exposed.

## 5 Discussion

This study aimed to model landslide dam hazard at a regional scale and undertake outburst flood scenario modelling to evaluate downstream exposure of population and critical infrastructure at high hazard sites. The analysis suggests that landslide dam potential in the West Coast Region is comparable to that observed in the Kaikōura Region following the 2016 Kaikōura earthquake, with a large Alpine Fault earthquake potentially triggering significantly more landslide dams across a significantly larger area. The most hazardous locations appear to be the Haast, Hokitika and Whataroa catchments, where the potential for landslide dams is highest, with the potential for 1 dam per km<sup>2</sup>. Comparatively, the much larger Buller and Grey catchments may have potential for a larger number of total landslide dams, but at lower densities. Outburst flood modelling from high hazard sites in the Haast, Hokitika, and Whataroa catchments suggests there is large exposure in each catchment. The Haast catchment was identified as significantly hazardous due to high values across all calculations. Combining landslide dam formation hazard, exposure to outburst flooding and the vulnerability of the West Coast Region suggests there is a high risk from landslide dams across the entire region.

### 5.1 How does landslide dam potential in the West Coast region compare globally?

Data from Morgernstern et al (In Press) identified 171 mapped landslide dams across the West Coast Region. This study identified 123 valley points in the West Coast Region within 100 m of a historic landslide dam. The remaining 48 dams were in locations with smaller order 1 streams that were not analysed. Based on the analysis in this study, this number appears small given the number of potential dam sites, suggesting that evidence for many previous landslide dams has been erased, likely as a combined result of the short survival time of most dams (Costa and Shuster, 1989) and rapid erosion rates in the Southern Alps (Korup, 2005). The large number of landslide dams in the database that are located in comparatively wide valleys with relatively low relief (Figure 35) supports this, suggesting the database is bias towards larger and/or more stable dams that still have evidence visible in the landscape. This

is particularly evident when compared to the Kaikōura earthquake landslide dam dataset (Figure 31), where just two landslide dams occurred in locations with local relief < valley width. Therefore, given the remoteness of the West Coast Region and frequent strong earthquakes and heavy rainfall, it is likely that many ancient smaller landslide dams and/or dams that failed quickly are missing from the database. Consequently, the rate of known landslide dams in the West Coast Region above the 1:1 reference line (Figure 35) is considered an underestimate.

Earthquakes are one of the primary triggers for landslide dam formation (Costa & Schuster, 1988; Fan et al., 2020). The West Coast region experiences  $M \sim 8$  earthquakes every 300 years, with the most recent event in  $\sim 1717$  (Orchiston et al., 2016). Such an event would cause widespread landslides, and therefore formation of landslide dams on a large scale across the entire West Coast Region is expected (Robinson et al., 2016). Assuming a conversion rate similar to the Kaikōura earthquake, this could result in  $\sim 1600$  landslide dams across the West Coast Region, assuming the entire region receives sufficiently strong shaking. This is significantly larger than witnessed in the comparably sized Kaikōura and Wenchuan earthquakes. The Kaikōura earthquake resulted in  $>200$  landslide dams (Dellow et al., 2017a) while the Wenchuan earthquake, one of the most significant landslide dam forming events in recent history, generated 828 landslide dams (Fan et al., 2013; Xu et al., 2009). This suggests landslide dam hazard following an Alpine Fault earthquake is likely to exceed that witnessed in the Kaikōura earthquake and may even exceed that of the Wenchuan earthquake. Given the significance and considerable disruption the Kaikōura earthquake sequence and Wenchuan earthquake caused, this further validates that a similar sized earthquake on the Alpine Fault could be catastrophic. At the time of writing, the 2008 Wenchuan earthquake had the highest number of landslides witnessed globally (Xu et al., 2016). Given the Wenchuan earthquake was the most considerable and destructive movement in China over 100 years and displaced millions of people (Cui et al., 2009; Fan et al., 2013; Xu et al., 2009), something of this scale in New Zealand could have disastrous effects on critical infrastructure and communities.

## 5.2 How can we determine where the most high hazard locations are in the West Coast Region?

Observed landslide dams in the Kaikōura earthquake and West Coast Region have been shown to occur in locations where relief exceeds valley width. This provides a simple way to assess landslide dam potential on any section of river in New Zealand. If the local relief does not exceed the valley width, that particular location may be considered unlikely (however not impossible) to form a landslide dam. If the relief does exceed the valley width then there is higher potential for landslide dams to form. However, not all sites that meet this criteria will experience landslide dams, it simply suggests a higher potential for landslide dam formation. Based on this analysis for the West Coast Region, the Haast, Hokitika and Whataroa catchments have the highest potential for landslide dam formation and hence the highest hazard.

However, high hazard potential can change depending on the slope of the reference line (Figure 50). The current 1:1 threshold line captures 90% of known landslide dams from both the Kaikōura and West Coast datasets, however includes 26,139 sites with no previously recorded landslide dam. By comparison, a relief/width ratio of 3 would capture the most hazardous locations and have fewer total locations above the threshold, however would miss lower hazard possible dam sites. Interestingly, a relief/width ratio of 3 would still capture a majority of landslide dams from the Kaikōura earthquake (61%) but only a minority of known landslide dams from the West Coast Region (35%). When selecting the most appropriate threshold for forward modelling, there may therefore be a trade-off between identifying the maximum number of potential dam sites (true positives) whilst reducing the total number of points above the threshold (false positives). The cumulative distribution graph highlights the distributive functions for different slope thresholds (Figure 51). The current slope threshold captures 90% of dams over both regions, while a slope threshold of 2.3 would capture 65% of dams. The most appropriate threshold will vary by end-user and thus this study has focussed on maximising the number of potential dam sites identified as an initial assessment.

There is a clear correlation between where most valley measurements are taken and where mapped landslide dams are located (Figure 52-Figure 53). That is, one of the possible factors influencing the locations of landslide dams in relief vs. width space is simply the number of

valley locations with those dimensions. However, for the West Coast Region, the densest assemblage of valley measurements are those from wide, low relief locations, and there are relatively few historic landslide dams in these locations. This suggests that landslide dam location is not solely a function of this underlying bias. Future work could actually utilise these relationships (Figures 50-53) to determine the relative hazard of all possible dam locations: given all available valley measurements above a desired threshold, what percentage are occupied by mapped dams? As a first-order estimate, dividing the mapped dam density by the valley measurement densities (possible dam locations) would be informative. In this case, the highest ratios (where many dams are observed relative to valley measurements) would indicate the highest hazard, but such analysis lies outside the scope of this thesis.

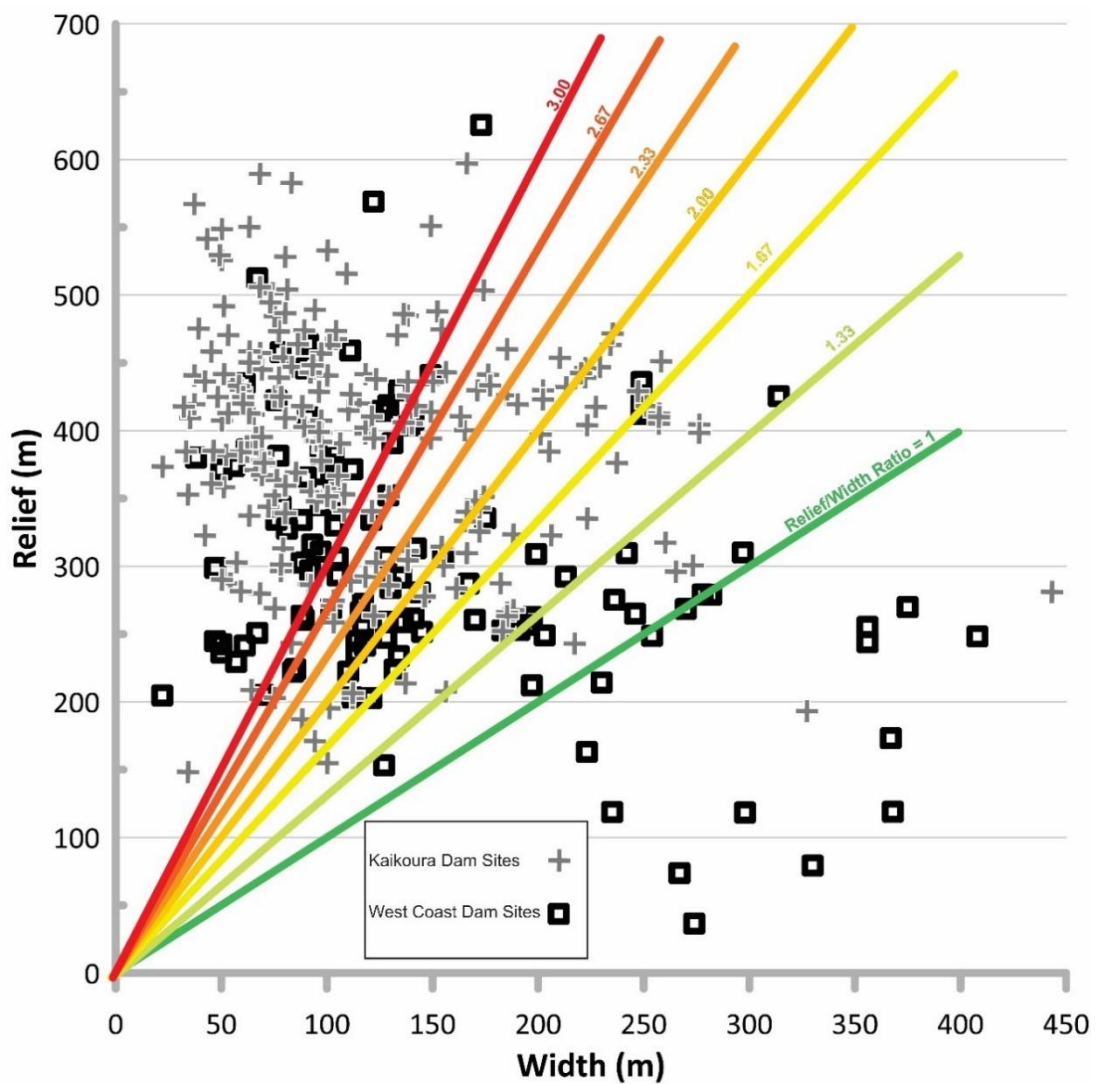


Figure 50- Threshold plot for relative landslide dam hazard indicating the different reference lines and how they relate to historic landslide dam locations from the Morgenstern et al (in prep) dataset.



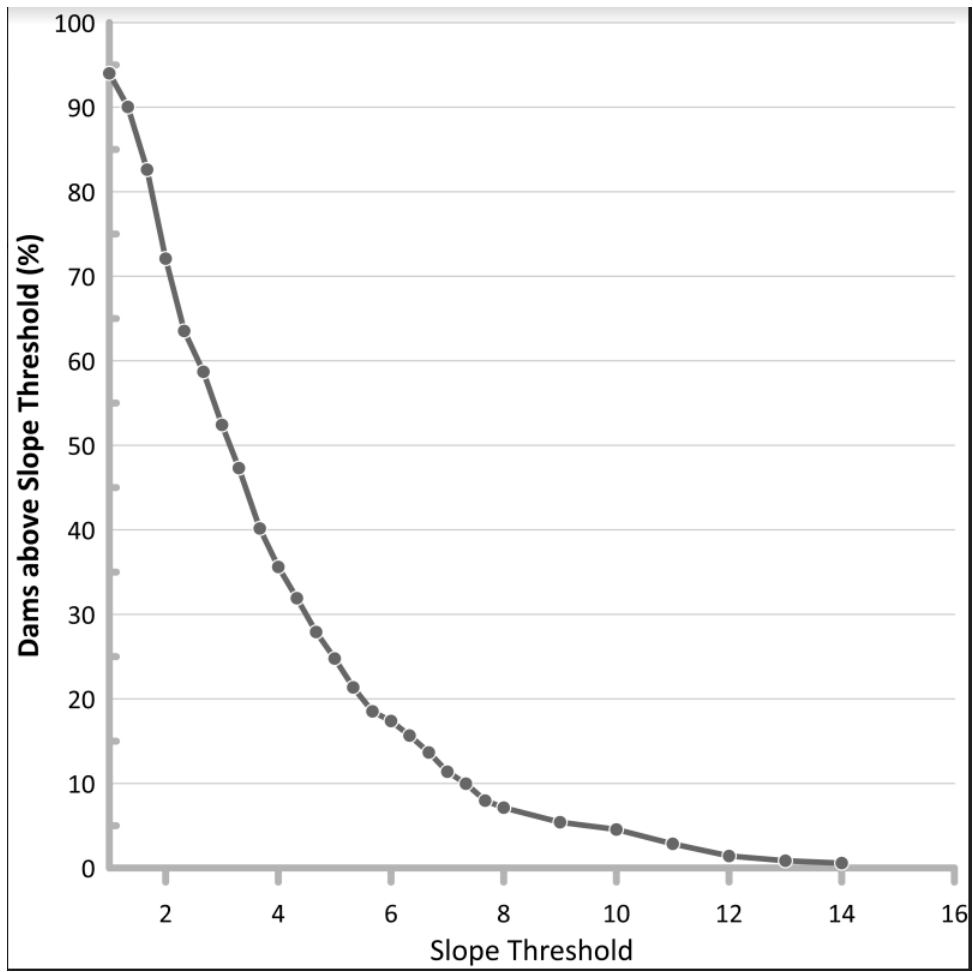


Figure 51- Cumulative Distribution Figure for dam locations with the West Coast Region and Kaikōura Region combined.

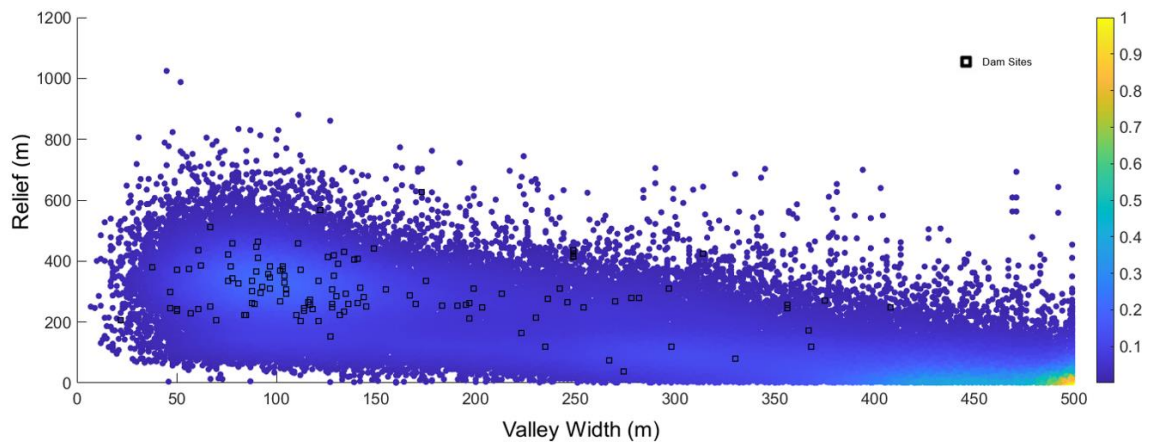


Figure 52- Density Plot for the West Coast region indicating a clear correlation between where valley measurements are taken and where mapped landslide dams are located.

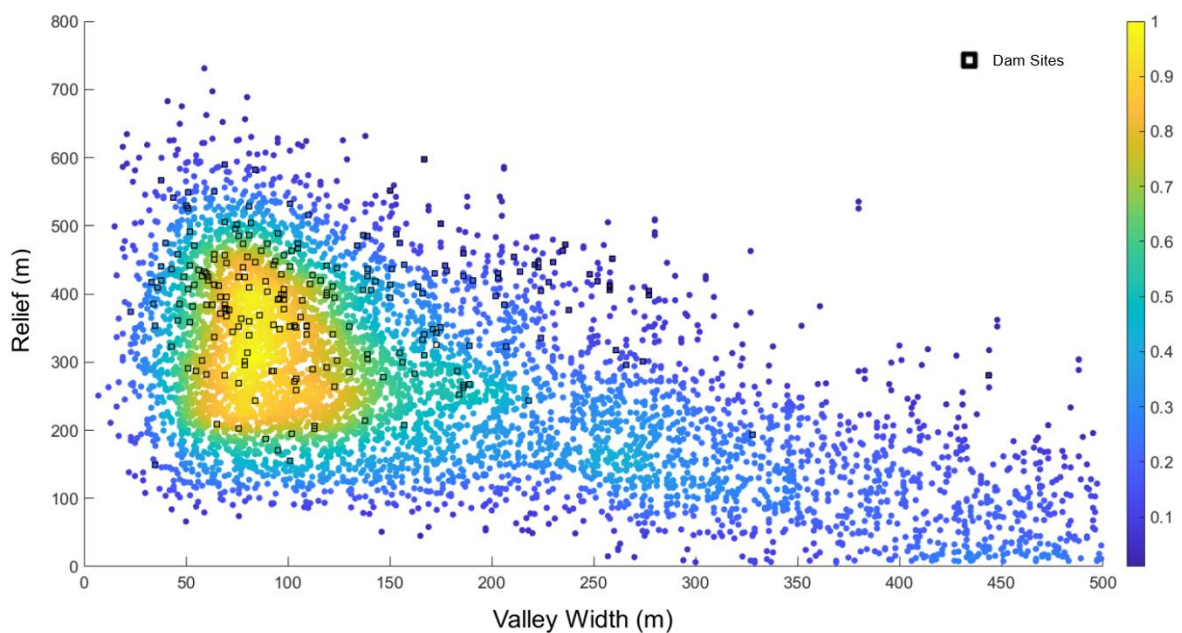


Figure 53- Density Plot for the Kaikōura Region indicating a clear correlation between where valley measurements are taken and where mapped landslide dams are located.

Landslide dam outburst flood hazard is different than landslide dam hazard. For outburst flooding, the highest dam hazard locations have an additional criterion of having large upstream contributing area, which is where enough water will be impounded to cause lake build-up. The most hazardous catchments then are those with highest upstream contributing area and highest percentage of points above the relief vs width reference line. From this, it

became clear the Haast, Hokitika, Waiho, Wanganui and Whataroa catchments had the highest hazard (Table 2). Increasing the upstream area threshold further confirmed the highest hazard locations occurred in the Haast, Hokitika and Whataroa catchments. This study used arbitrary thresholds for upstream area based on a median value for the West Coast region. However, there is further sensitivity analysis that could be conducted to test the influence of upstream area on relative outburst hazard. Future research could consider a set value to separate large hazardous lake sites from less hazardous lake sites. This would also likely be a factor of proximity to downstream infrastructure in order to account for flood wave attenuation.

The Buller and Grey catchments are large, therefore have the highest potential dam sites and biggest upstream areas. However, proportionally, they have a lower percentage of sites in hazardous locations compared to the other catchments (Table 2). Therefore, they are not considered as hazardous as the Haast, Hokitika and Whataroa catchments. To compare, Hokitika had 1075 potential landslide dam sites, of which 41% had a large (>20,000 km<sup>2</sup>) upstream area. In contrast the Buller catchment had significantly high numbers of potential dam sites at 2996, however only 5% had a large upstream area. This suggests that landslide dams that form in the Hokitika Region will be in steep mountain areas with greater sediment relative to discharge, and therefore more likely to cause large destructive outburst floods. In contrast, the Buller catchment could have higher numbers of landslide dams in gentle slopes and greater amounts of sediment to move, however a higher discharge, therefore outburst flooding may be less intense. Therefore, large catchment area and large number of valley points above the reference line does not necessarily indicate the most hazardous locations.

Of all sites considered, points in the Haast catchment appear to be the most hazardous, because they have a large upstream area, large number of potential dam sites, high percentages of hazardous valley points and high density of dams per km<sup>2</sup>. Interestingly, the Haast catchment has significant dune systems at the river mouth that have been used to date Alpine Fault earthquakes (Nobes et al., 2016; Wells & Goff, 2007). Coastal dunes provide a record of sediment movement from seismic activity on the Alpine Fault (Wells & Goff, 2007). This project supports this research by suggesting landslide dam hazard is high throughout the Haast catchment and, following remobilisation of the landslide debris, could have eventuated in coastal sediment deposits. As a result two locations on the Haast catchment were selected

for outburst flooding. However, the Waiho catchment also had a high landslide dam potential, primarily from sites along the Callery River, which has been extensively studied (Davies & Scott, 1997; Davies, 2002; Ollett, 2001). However, the Haast, Hokitika, Wanganui and Whataroa catchments produced similar percentages for valley points above the reference line with high upstream area and higher densities of potential landslide dams by area (Table 2). These catchments have not been as extensively researched as the hazard from the Callery river. This suggests research has understandably focused on the hazard to Franz Josef in the Waiho catchment, however there are other locations in the West Coast Region that are just as hazardous, and possibly more hazardous to landslide dams such as the Haast catchment. Therefore, future research should consider locations in the West Coast Region outside of the Callery River and Franz Josef area for further detailed analysis.

### 5.3 What critical infrastructure is exposed to outburst flood hazard from landslide dams?

All four of the modelled outburst locations indicate substantial flooding impacts to roads, farmland and buildings that would impact downstream communities. Whilst on a different scale, this is reminiscent of the Tangjiashan landslide dam event following the Wenchuan earthquake where people and critical infrastructure were exposed to the possibility of an uncontrolled release (Cui et al., 2009). Due to the steep geography, in the Haast catchment flooding is more spatially contained than in the Hokitika and Whataroa catchments. Therefore, as the flood is limited to a narrow valley the area impacted won't be as large, however flood depth could potentially be higher. In the Hokitika and Whataroa catchments that are much wider, particularly on the floodplains west of the Alpine Fault, flooding could spread out over large areas of farmland and attenuate. As a result, the depth and peak flow is likely to be lower, however the affected area could be considerably larger.

There are some interesting patterns within the exposure models, as the results highlight the differences between amount of critical infrastructure exposed and the percentages of critical infrastructure exposed. To quantify this, the Hokitika catchment exposes at least double the length of roads, area of farmland and number of buildings compared to the other catchments

(Table 5). For the 10 m dam heights, the amount of buildings exposed in the Hokitika catchment accounts for 70% of the total buildings exposed over all 4 locations. This is due to the comparatively high population living in the Hokitika catchment, with five times the population of the Haast catchment and twice the population of the Whataroa catchment. This indicates that outburst flooding in Hokitika would impact more people and critical infrastructure than outburst flooding in the Haast and Whataroa catchments combined. However, Hokitika has the lowest percentages of flood exposure to roads, farmland and buildings within the catchment. Therefore, although outburst flooding in the Hokitika catchment could affect more people and infrastructure in total, outburst flooding could be proportionally more devastating to local communities with higher percentage exposure, as in the Haast catchment.

Again, the results indicate the high hazard and exposure to the Haast catchment in particular. Both considered sites in the Haast catchment produce high exposure statistics from all critical infrastructure evaluated, with 50 m high dam models impacting 96% of total buildings and up to 45 km of State Highway 6. This further confirms that the Haast catchment is particularly exposed to landslide dam outburst flooding impacts. Although the exposed area in the Hokitika catchment covers the highest amount of roads, these are mostly local roads with little wider regional benefit, while the exposed regions in the Haast and Whataroa catchments cover State Highway 6, the major Alpine Highway that links the West Coast Region to the rest of the South Island. The 50 m high dam outburst floods would expose 45 km of SH6 from the Gates of Haast site and 5 km in the Whataroa catchment site. This could result in SH6 being inaccessible to the South, resulting in long detours through Arthurs and Lewis Pass, which themselves are likely to be closed if the dam(s) were triggered by an Alpine Fault earthquake.

There are long term consequences of landslide dam outburst flooding on communities and critical infrastructure. For several years after the 1999 Poerua landslide dam and outburst flood, river fluctuations and transport of dam sediment caused changes to the landscape (Robinson & Davies, 2013). Sediment deposition caused severe damages to farmland and properties downstream. This had implications with the local farming community, as river erosion was not recognised as an insurance claim (Hancox et al., 2005). As a result, many farmers constructed stopbanks to prevent more flooding and erosion to their properties (Hancox & Perrin, 2009). In addition the bridge on SH6 was damaged and required remedial

works to prevent ongoing gravel deposition from future flooding (Hancox & Perrin, 2009). These events have long term mental and financial impacts on communities and cause huge disruption to everyday life. Whilst the Haast catchment appears to be the most exposed, these longer-term consequences are likely to be particularly important for the Hokitika catchment, where at least a quarter of the total farmland could be inundated and thus potentially lost to aggradation, potentially for several decades. The short- and long-term consequences of the Poerua event indicates potential consequences should outburst flooding occur in the Haast, Hokitika and Whataroa catchments. All of these regions are farming communities who rely on the land and critical road networks for their livelihoods. Thus, there are huge implications for the people in these communities if a landslide dam and outburst flood were to damage major roads, farmland and infrastructure.

#### 5.4 What is the risk from landslide dams on the West Coast of New Zealand?

Other natural hazard events in the West Coast region, such as the 2022 flooding in Westport caused considerable disruption that has proven costly and taken long periods of time to repair. These events have been difficult for local communities, having lasting impacts on wellbeing and requiring external aid and financial resources. If 50 km of State Highway 6 is damaged in the Haast and Whataroa catchments, there is no alternative access route from the south. It would take considerable time and resources to repair that may not be available after a major earthquake or other natural hazard event. The Nelson storm event in August 2022 resulted in large numbers of building damages due to flood inundation and landslides (Tasman District Council, 2022). In total, 89 houses were 'red stickered' due to flood damages and due to land stability issues were unable to be entered and more than 1200 people were evacuated from their homes (Nelson City Council, 2022). The February 2022 flood event in Westport in the West Coast region caused severe damage to farmland, destroying tracks, diverting streams and silting up paddocks so they were no longer productive (Burke, 2022). Just one of the landslide dam scenarios outlined here would likely be comparable to these events in terms of the considerable disruption inflicted based on the outburst flood modelling. Multiple events at once would be devastating for West Coast communities and would take considerable time and resources to recover.

The impacts of climate change further increases the hazard of landslide dams in the West Coast region. Climate change is expected to result in increased heavy rainfall events and the West Coast Region already has the highest average rainfall statistics in New Zealand, with an average of 10,000 mm of rainfall annually in the high elevations (Macara, 2016). As rainfall is another known trigger for both landslide dam formation and failure (Costa & Schuster, 1988; Fan et al., 2021; Korup, 2005; Morgenstern et al., 2020), landslide dams and consequent outburst floods may become more common in West Coast Region.

A large Alpine Fault earthquake is expected to result in high numbers of landslide dams in the West Coast Region (Robinson & Davies, 2013), however no previous work had sought to understand the total scale and potential locations of such dams. This study has shown that locations with high relief, short valley widths and large upstream areas, particularly in the Haast, Hokitika and Whataroa catchments, have high potential for landslide dams to form, with several hundred potential locations in each catchment. Due to the high annual rainfall in the West Coast Region, it is expected that most landslide dams are likely to fail shortly after formation and result in large outburst floods affecting downstream communities and critical infrastructure. Roads, farmland and buildings would be vulnerable to damages from outburst floods, with impacts from even a moderate dam being comparable and potentially more devastating than the Kaikōura earthquake and the recent flood events experienced in Nelson and Westport in 2022. Therefore, the risk from landslide dams and outburst flooding in the West Coast region is considered high and has the potential for significant long-term implications, as seen following the 1999 Poerua outburst flood.

## 5.5 Recommendations for future work

Future work should undertake analysis to determine (i) relative landslide dam hazard (using results in Figures 50-53) and (ii) an appropriate threshold for what upstream area constitutes a high hazard, ideally setting a value that separates large hazardous lake sites from less hazardous lake sites. More detailed outburst flood modelling should be undertaken for exploring other dam geometries and heights, particularly if ground investigations determine that any of the high-hazard sites presented herein also host emerging slope failures. More sensitively analysis should be undertaken to determine potential peak discharges. Other critical infrastructure such as powerlines could be incorporated into the exposure analysis. It would be useful to run this model in locations with large earthquake landslide dam formation sequences such Nepal in 2015 and Wenchuan. Comparisons of the Kaikōura and West Coast datasets to similar international events would determine its relevance both in New Zealand and overseas.



## 6 Conclusions

This study developed a method to model landslide dam hazard at a regional scale and applied it to the West Coast region. A model for identifying valley bottoms and semi-automatically measuring valley width was combined with local relief and upstream area calculations to determine the relative landslide dam hazard for the entire West Coast region. This approach was applied to the Kaikōura Region and compared to the mapped landslide dam database for from the 2016 earthquake to identify a threshold relationship between local relief and valley width describing landslide dam potential. This showed 98% of identified landslide dams occurred in locations where local relief exceeded valley width, although when applied to a dataset of known landslide dams from West Coast Region this dropped to 83%. Using this threshold relationship and upstream area of 20,000 km<sup>2</sup> identified the most hazardous locations in the West Coast region as being the Haast, Hokitika and Whataroa catchments, which each have >700 potential landslide dam sites. Within these three catchments, four especially high hazard sites were selected for outburst flood modelling using HECRAS, considering a 10 m and 50 m high dam scenario for each site. This outburst flood modelling suggested exposure of downstream critical infrastructure was highest in the Hokitika catchment, but as a proportion of total infrastructure present was highest in the Haast catchment. Combined with the vulnerability of the West Coast region from previous events, this indicates the risk from landslide dams and outburst flooding in the region is high. These results are important as regional scale modelling of landslide dam formation and potential is a relatively new area of research, and the high likelihood of an Alpine Fault earthquake in the near future highlights the need for better understanding of secondary hazards. This information will provide a greater understanding of the hazard from and exposure to landslide dams in the West Coast region. Therefore, it can provide local councils and communities with essential information to integrate into resilience and land use planning both prior to and after an event occurs. This model can be used in other locations in New Zealand and internationally to determine landslide dam formation potential at a regional scale, identifying potential landslide dam sites and provide a simple first-order estimation of the potential number of landslide dams that a large earthquake or heavy rainstorm may trigger.

## References

- Allen, S., Schneider, D., & Owens, I. (2009). First approaches towards modelling glacial hazards in the Mount Cook region of New Zealand's Southern Alps. *Natural Hazards and Earth System Sciences*, 9(2), 481-499. <https://doi.org/10.5194/nhess-9-481-2009>
- Argentin, A.-L., Robl, J., Prasicek, G., Hergarten, S., Hölbling, D., Abad, L., & Dabiri, Z. (2021). Controls on the formation and size of potential landslide dams and dammed lakes in the Austrian Alps. *Natural Hazards and Earth System Sciences*, 21(5), 1615-1637. <https://doi.org/10.5194/nhess-21-1615-2021>
- Baker, V. (2002). High-energy megafloods: planetary settings and sedimentary dynamics. *Flood and megaflood processes and deposits: recent and ancient examples*, 1-15. <https://doi.org/10.1002/9781444304299.ch1>
- Becker, J., Johnston, D. M., Paton, D., Hancox, G., Davies, T., McSaveney, M., & Manville, V. (2007). Response to landslide dam failure emergencies: issues resulting from the October 1999 Mount Adams landslide and dam-break flood in the Poerua River, Westland, New Zealand. *Natural hazards review*, 8(2), 35-42. <https://www.wcrc.govt.nz/repository/libraries/id:2459ikxj617q9ser65rr/hierarchy/Documents/Publications/Natural%20Hazard%20Reports/West%20Coast/Response%20to%20Landslide%20Dam%20Failures%20J%20Becker%20and%20Others%202007.pdf>
- Brocard, G., & Van der Beek, P. (2006). Influence of incision rate, rock strength, and bedload supply on bedrock river gradients and valley-flat widths: Field-based evidence and calibrations from western Alpine rivers (southeast France). *S. D. Willett et al., Spec. Pap. Geol. Soc. Am*, 398, 101-126. [https://hal.archives-ouvertes.fr/file/index/docid/83659/filename/Brocard\\_vdBeek\\_2.pdf](https://hal.archives-ouvertes.fr/file/index/docid/83659/filename/Brocard_vdBeek_2.pdf)
- Burke, P. (2022) West Coast faces costly clean up. Dairy News <https://www.ruralnewsgroup.co.nz/dairy-news/dairy-general-news/west-coast-faces-costly-clean-up>
- Butt, M. J., Umar, M., & Qamar, R. (2012). Landslide dam and subsequent dam-break flood estimation using HEC-RAS model in Northern Pakistan. *Natural Hazards*, 65(1), 241-254. <https://doi.org/10.1007/s11069-012-0361-8>
- Clubb, F. J., Weir, E. F., & Mudd, S. M. (2022). Continuous measurements of valley floor width in mountainous landscapes. *Earth Surface Dynamics*, 10(3), 437-456. <https://doi.org/10.5194/esurf-10-437-2022>
- Costa, J. E. (1991a). Documented historical landslide dams from around the world. US. *Geological Survey Open-File Report*, 91(239), 1-486.
- Costa, J. E. (1991b). Nature, mechanics, and mitigation of the Val Pola landslide, Valtellina, Italy, 1987-1988. *Zeitschrift für Geomorphologie*, 15-38. DOI: [10.1127/zfg/35/1991/15](https://doi.org/10.1127/zfg/35/1991/15)
- Costa, J. E., & Schuster, R. L. (1988). The formation and failure of natural dams. *Geological society of America bulletin*, 100(7), 1054-1068. [https://doi.org/10.1130/0016-7606\(1988\)100%3C1054:TFAFON%3E2.3.CO;2](https://doi.org/10.1130/0016-7606(1988)100%3C1054:TFAFON%3E2.3.CO;2)
- Crosta, G., Frattini, P., Fusi, N., & Sosio, R. (2006). Formation, characterization and modelling of the 1987 Val Pola rock-avalanche dam (Italy). *Italian J. Eng. Geol. Envir., Special Issue I*, 145-150. [https://scholar.google.com/scholar?hl=en&as\\_sdt=0%2C5&q=Crosta%2C+G.%2C+Frattini%2C+P.%2C+Fusi%2C+N.%2C+%26+Sosio%2C+R.%2C+Formation%2C+characterization+and+modelling+of+the+1987+Val+Pola+rock-avalanche+dam+%28Italy%29.+Italian+J.+Eng.+Geol.+Envir.%2C+Special+Issue+I%2C+145-150.+&btnG=](https://scholar.google.com/scholar?hl=en&as_sdt=0%2C5&q=Crosta%2C+G.%2C+Frattini%2C+P.%2C+Fusi%2C+N.%2C+%26+Sosio%2C+R.%2C+Formation%2C+characterization+and+modelling+of+the+1987+Val+Pola+rock-avalanche+dam+%28Italy%29.+Italian+J.+Eng.+Geol.+Envir.%2C+Special+Issue+I%2C+145-150.+&btnG=)
- Crosta, G. B., Chen, H., & Lee, C. F. (2004). Replay of the 1987 Val Pola Landslide, Italian Alps. *Geomorphology*, 60(1-2), 127-146. <https://doi.org/10.1016/j.geomorph.2003.07.015>

- Cui, P., Dang, C., Zhuang, J.-q., You, Y., Chen, X.-q., & Scott, K. M. (2012). Landslide-dammed lake at Tangjiashan, Sichuan province, China (triggered by the Wenchuan Earthquake, May 12, 2008): risk assessment, mitigation strategy, and lessons learned. *Environmental Earth Sciences*, 65(4), 1055-1065. <https://doi.org/10.1007/s12665-010-0749-2>
- Cui, P., Zhu, Y.-y., Han, Y.-s., Chen, X.-q., & Zhuang, J.-q. (2009). The 12 May Wenchuan earthquake-induced landslide lakes: distribution and preliminary risk evaluation. *Landslides*, 6(3), 209-223. <https://doi.org/10.1007/s10346-009-0160-9>
- Dai, F. C., Lee, C. F., Deng, J. H., & Tham, L. G. (2005). The 1786 earthquake-triggered landslide dam and subsequent dam-break flood on the Dadu River, southwestern China. *Geomorphology*, 65(3-4), 205-221. <https://doi.org/10.1016/j.geomorph.2004.08.011>
- Dal Sasso, S. F., Sole, A., Pascale, S., Sdao, F., Bateman Pinzòn, A., & Medina, V. (2014). Assessment methodology for the prediction of landslide dam hazard. *Natural Hazards and Earth System Sciences*, 14(3), 557-567. <https://doi.org/10.5194/nhess-14-557-2014>
- Davies, T., & Scott, B. (1997). Dambreak flood hazard from the Callery River, Westland, New Zealand. *Journal of Hydrology (New Zealand)*, 1-13. <https://www.jstor.org/stable/43944780>
- Davies, T. R. (2002). Landslide-dambreak floods at Franz Josef Glacier township, Westland, New Zealand: A risk assessment [Article]. *Journal of Hydrology New Zealand*, 41(1), 1-17. <https://www.scopus.com/inward/record.uri?eid=2-s2.0-0036288311&partnerID=40&md5=6c9b9930b45864b5335fb1f8ef0e21b9>
- De Pascale, G., & Langridge, R. (2012). New on-fault evidence for a great earthquake in AD 1717, central Alpine fault, New Zealand. *Geology*, 40(9), 791-794. <https://doi.org/10.1130/G33363.1>
- Dellow, S., Massey, C., & Cox, S. (2017a). Response and initial risk management of landslide dams caused by the 14 November 2016 Kaikoura earthquake, South Island, New Zealand. Proceedings of the 20th NZGS Geotechnical Symposium, Napier, New Zealand [http://fl-nzgs-media.s3.amazonaws.com/uploads/2017/11/NZGS\\_Symposium\\_20\\_Dellow1.pdf](http://fl-nzgs-media.s3.amazonaws.com/uploads/2017/11/NZGS_Symposium_20_Dellow1.pdf)
- Dellow, S., Massey, C., Cox, S., Archibald, G., Begg, J., Bruce, Z., Carey, J., Davidson, J., Pasqua, F. D., Glassey, P., Hill, M., Jones, K., Lyndsell, B., Lukovic, B., McColl, S., Rattenbury, M., Read, S., Rosser, B., Singeisen, C., . . . Little, M. (2017b). Landslides caused by the Mw7.8 Kaikōura earthquake and the immediate response. *Bulletin of the New Zealand Society for Earthquake Engineering*, 50(2), 106-116. <https://doi.org/10.5459/bnzsee.50.2.106-116>
- Dong, J.-J., Tung, Y.-H., Chen, C.-C., Liao, J.-J., & Pan, Y.-W. (2011). Logistic regression model for predicting the failure probability of a landslide dam. *Engineering Geology*, 117(1-2), 52-61. <https://doi.org/10.1016/j.enggeo.2010.10.004>
- Dunant, A., Bebbington, M., & Davies, T. (2021). Probabilistic cascading multi-hazard risk assessment methodology using graph theory, a New Zealand trial. *International Journal of Disaster Risk Reduction*, 54, 102018. <https://doi.org/10.1016/j.ijdr.2020.102018>
- Ermini, L., & Casagli, N. (2003). Prediction of the behaviour of landslide dams using a geomorphological dimensionless index. *Earth Surface Processes and Landforms: The Journal of the British Geomorphological Research Group*, 28(1), 31-47. <https://doi.org/10.1002/esp.424>
- Fan, X., Dufresne, A., Siva Subramanian, S., Strom, A., Hermanns, R., Tacconi Stefanelli, C., Hewitt, K., Yunus, A. P., Dunning, S., Capra, L., Geertsema, M., Miller, B., Casagli, N., Jansen, J. D., & Xu, Q. (2020). The formation and impact of landslide dams – State of the art. *Earth-Science Reviews*, 203. <https://doi.org/10.1016/j.earscirev.2020.103116>
- Fan, X., Dufresne, A., Whiteley, J., Yunus, A. P., Subramanian, S. S., Okeke, C. A. U., Pánek, T., Hermanns, R. L., Ming, P., Strom, A., Havenith, H.-B., Dunning, S., Wang, G., & Tacconi Stefanelli, C. (2021). Recent technological and methodological advances for the investigation of landslide dams. *Earth-Science Reviews*, 218. <https://doi.org/10.1016/j.earscirev.2021.103646>

- Fan, X., Rossiter, D. G., van Westen, C. J., Xu, Q., & Görüm, T. (2014). Empirical prediction of coseismic landslide dam formation. *Earth Surface Processes and Landforms*, 39(14), 1913-1926. <https://doi.org/10.1002/esp.3585>
- Fan, X., Scaringi, G., Korup, O., West, A. J., van Westen, C. J., Tanyas, H., Hovius, N., Hales, T. C., Jibson, R. W., & Allstadt, K. E. (2019). Earthquake-induced chains of geologic hazards: Patterns, mechanisms, and impacts. *Reviews of geophysics*, 57(2), 421-503. <https://doi.org/10.1029/2018RG000626>
- Fan, X., van Westen, C. J., Xu, Q., Gorum, T., Dai, F., Wang, G., & Huang, R. (2013). Spatial Distribution of Landslide Dams Triggered by the 2008 Wenchuan Earthquake. In *Landslide Science and Practice* (pp. 279-285). [https://doi.org/10.1007/978-3-642-31427-8\\_36](https://doi.org/10.1007/978-3-642-31427-8_36)
- Hancox, G. T., McSaveney, M. J., Manville, V. R., & Davies, T. R. (2005). The October 1999 Mt Adams rock avalanche and subsequent landslide dam-break flood and effects in Poerua river, Westland, New Zealand. *New Zealand Journal of Geology and Geophysics*, 48(4), 683-705. <https://doi.org/10.1080/00288306.2005.9515141>
- Hermanns, R. L., Hewitt, K., Strom, A., Evans, S. G., Dunning, S. A., & Scarascia-Mugnozza, G. (2011). The classification of rockslide dams. In *Natural and artificial rockslide dams* (pp. 581-593). Springer. [https://doi.org/10.1007/978-3-642-04764-0\\_24](https://doi.org/10.1007/978-3-642-04764-0_24)
- Howarth, J. D., Barth, N. C., Fitzsimons, S. J., Richards-Dinger, K., Clark, K. J., Biasi, G. P., Cochran, U. A., Langridge, R. M., Berryman, K. R., & Sutherland, R. (2021). Spatiotemporal clustering of great earthquakes on a transform fault controlled by geometry. *Nature Geoscience*, 14(5), 314-320. <https://doi.org/10.1038/s41561-021-00721-4>
- Infometrics. (2021) Annual Economic Profile, West Coast Region. <https://ecoprofile.infometrics.co.nz/West%20Coast%20Region/PDFProfile>
- Jenness, J., Brost, B., & Beier, P. (2013). Land facet corridor designer. *USDA forest service rocky mountain research station*. [http://www.jennessent.com/downloads/Land\\_Facet\\_Tools.pdf](http://www.jennessent.com/downloads/Land_Facet_Tools.pdf)
- Jin, J., Chen, G., Meng, X., Zhang, Y., Shi, W., Li, Y., Yang, Y., & Jiang, W. (2022). Prediction of river damming susceptibility by landslides based on a logistic regression model and InSAR techniques: A case study of the Bailong River Basin, China. *Engineering Geology*, 299, 106562. <https://doi.org/10.1016/j.enggeo.2022.106562>
- Jones, K.E. (2022). Quantifying co-seismic and post-seismic erosion using geomorphic change detection for the Mw 7.8 Kaikōura earthquake, New Zealand. Victoria University of Wellington, Wellington, New Zealand.
- Kiernan, G. (2016). Repairing Kaikoura: the size, the speed, and the cost of delays. *Infometrics* <https://www.infometrics.co.nz/article/2016-11-repairing-kaikoura-size-speed-cost-delays>
- Klimeš, J., Benešová, M., Vilímek, V., Bouška, P., & Rapre, A. C. (2014). The reconstruction of a glacial lake outburst flood using HEC-RAS and its significance for future hazard assessments: an example from Lake 513 in the Cordillera Blanca, Peru. *Natural Hazards*, 71(3), 1617-1638. <https://doi.org/10.1007/s11069-013-0968-4>
- Korup, O. (2002). Recent research on landslide dams; a literature review with special attention to New Zealand. *Progress in Physical Geography*, 26(2), 206-235. <https://doi.org/10.1191/0309133302pp333ra>
- Korup, O. (2004). Geomorphometric characteristics of New Zealand landslide dams. *Engineering Geology*, 73(1-2), 13-35. <https://doi.org/10.1016/j.enggeo.2003.11.003>
- Korup, O. (2005). Geomorphic hazard assessment of landslide dams in South Westland, New Zealand: fundamental problems and approaches. *Geomorphology*, 66(1-4), 167-188. <https://doi.org/10.1016/j.geomorph.2004.09.013>
- Kougkoulos, I., Cook, S. J., Edwards, L. A., Clarke, L. J., Symeonakis, E., Dortch, J. M., & Nesbitt, K. (2018). Modelling glacial lake outburst flood impacts in the Bolivian Andes. *Natural Hazards*, 94(3), 1415-1438. <https://doi.org/10.1007/s11069-018-3486-6>

- Lancaster, S. T. (2008). Evolution of sediment accommodation space in steady state bedrock-incising valleys subject to episodic aggradation. *Journal of Geophysical Research: Earth Surface*, 113(F4). <https://doi.org/10.1029/2007JF000938>
- Langston, A. L., & Temme, A. J. (2019). Impacts of lithologically controlled mechanisms on downstream bedrock valley widening. *Geophysical Research Letters*, 46(21), 12056-12064. <https://doi.org/10.1029/2019GL085164>
- Lee, C., & Dai, F. (2011). The 1786 Dadu River Landslide Dam, Sichuan, China. In *Natural and artificial rockslide dams* (pp. 369-388). Springer. [https://doi.org/10.1007/978-3-642-04764-0\\_13](https://doi.org/10.1007/978-3-642-04764-0_13)
- Li, M.-H., Sung, R.-T., Dong, J.-J., Lee, C.-T., & Chen, C.-C. (2011). The formation and breaching of a short-lived landslide dam at Hsiaolin Village, Taiwan—Part II: Simulation of debris flow with landslide dam breach. *Engineering Geology*, 123(1-2), 60-71. <https://doi.org/10.1016/j.enggeo.2011.05.002>
- Lifton, Z. M., Thackray, G. D., Van Kirk, R., & Glenn, N. F. (2009). Influence of rock strength on the valley morphometry of Big Creek, central Idaho, USA. *Geomorphology*, 111(3-4), 173-181. <https://doi.org/10.1016/j.geomorph.2009.04.014>
- LINZ data service New Zealand <https://data.linz.govt.nz/>
- Liu, W., Carling, P. A., Hu, K., Wang, H., Zhou, Z., Zhou, L., Liu, D., Lai, Z., & Zhang, X. (2019). Outburst floods in China: A review. *Earth-Science Reviews*, 197, 102895. <https://doi.org/10.1016/j.earscirev.2019.102895>
- LRIS Portal. (2022) Land Cover Database version 5.0, Mainland, New Zealand <https://iris.scinfo.org.nz/layer/104400-lcdb-v50-land-cover-database-version-50-mainland-new-zealand/>
- Macara, G.R. 2016. The climate and weather of West Coast. NIWA Science and Technology Series 72, 40 pp. [https://niwa.co.nz/our-science/climate/publications/regional-climatologies/west\\_coast](https://niwa.co.nz/our-science/climate/publications/regional-climatologies/west_coast)
- Massey, C., Townsend, D., Dellow, S., Lukovic, B., Rosser, B., Archibald, G., Villeneuve, M., Davidson, J., Jones, K., & Morgenstern, R. (2018). Kaikoura Earthquake Short Term Project: Landslide inventory and landslide dam assessments. *GNS Science report*, 19, 45.
- Massey, C., Townsend, D., Jones, K., Lukovic, B., Rhoades, D., Morgenstern, R., Rosser, B., Ries, W., Howarth, J., & Hamling, I. (2020). Volume characteristics of landslides triggered by the MW 7.8 2016 Kaikōura Earthquake, New Zealand, derived from digital surface difference modeling. *Journal of Geophysical Research: Earth Surface*, 125(7), e2019JF005163. <https://doi.org/10.1029/2019JF005163>
- Morgenstern, R., Massey, C., Rosser, B., & Archibald, G. (2020). Landslide dam hazards: assessing their formation, failure modes, longevity and downstream impacts. Workshop on World Landslide Forum, [https://doi.org/10.1007/978-3-030-60319-9\\_12](https://doi.org/10.1007/978-3-030-60319-9_12)
- Morgenstern et al., (in prep) The New Zealand Landslide Dam Database, v. 1.0.
- Nash, T., Bell, D., Davies, T., & Nathan, S. (2008). Analysis of the formation and failure of Ram Creek landslide dam, South Island, New Zealand. *New Zealand Journal of Geology and Geophysics*, 51(3), 187-193. <https://doi.org/10.1080/00288300809509859>
- Nelson City Council. (2022) One month on, where are we? <https://our.nelson.govt.nz/stories/one-month-on-where-are-we/>
- NIWA. (2019) River Environment Classification <https://niwa.co.nz/freshwater/management-tools/river-environment-classification-0>
- Nikon. (2011) Nikon Introduces New Laser Rangefinder Forestry Pro. [https://www.nikon.com/news/2011/0909\\_foresty-pro\\_01.htm](https://www.nikon.com/news/2011/0909_foresty-pro_01.htm)
- Nobes, D., Jol, H., & Duffy, B. (2016). Geophysical imaging of disrupted coastal dune stratigraphy and possible mechanisms, Haast, South Westland, New Zealand. *New Zealand Journal of Geology and Geophysics*, 59(3), 426-435. <https://doi.org/10.1080/00288306.2016.1168455>
- O'Connor, J., & Beebee, R. A. (2009). Floods from natural rock-material dams. *Megaflooding on Earth and Mars*, 128-171.

- Ollett, P. P. (2001). *Landslide dambreak flooding in the Callery River, Westland*. Lincoln University
- Orchiston, C., Davies, T., Langridge, R., Wilson, T., Mitchell, J., & Hughes, M. (2016). Alpine Fault magnitude 8 hazard scenario. *Report Commissioned by Project AF8, Environment Southland, Invercargill*, 45. <http://projectaf8.co.nz/wordpress/wp-content/uploads/2016/11/project-af8-hazard-model-report-final-october-2016.pdf>
- Peng, M., & Zhang, L. (2012a). Analysis of human risks due to dam-break floods—part 1: a new model based on Bayesian networks. *Natural Hazards*, 64(1), 903-933. <https://doi.org/10.1007/s11069-012-0275-5>
- Peng, M., & Zhang, L. M. (2012b). Analysis of human risks due to dam break floods—part 2: application to Tangjiashan landslide dam failure. *Natural Hazards*, 64(2), 1899-1923. <https://doi.org/10.1007/s11069-012-0336-9>
- Peng, M., & Zhang, L. M. (2011). Breaching parameters of landslide dams. *Landslides*, 9(1), 13-31. <https://doi.org/10.1007/s10346-011-0271-y>
- Perrin, N., & Hancox, G. (1992). Landslide-dammed lakes in New Zealand-preliminary studies on their distribution, causes and effects. *Landslides*. International symposium, <http://pascal-francis.inist.fr/vibad/index.php?action=getRecordDetail&idt=6464378>
- Robinson, T., & Davies, T. (2013). Potential geomorphic consequences of a future great (M w= 8.0+) Alpine Fault earthquake, South Island, New Zealand. *Natural Hazards and Earth System Sciences*, 13(9), 2279-2299. <https://doi.org/10.5194/nhess-13-2279-2013>
- Robinson, T., Davies, T., Wilson, T., & Orchardson, C. (2016). Coseismic landsliding estimates for an Alpine Fault earthquake and the consequences for erosion of the Southern Alps, New Zealand. *Geomorphology*, 263, 71-86. <https://doi.org/10.1016/j.geomorph.2016.03.033>
- Robinson, T. R., Rosser, N. J., Davies, T. R., Wilson, T. M., & Orchardson, C. (2018). Near-Real-Time Modeling of Landslide Impacts to Inform Rapid Response: An Example from the 2016 Kaikōura, New Zealand, Earthquake. *Bulletin of the Seismological Society of America*, 108(3B), 1665-1682. <https://doi.org/10.1785/0120170234>
- Shan, Y., Chen, S., & Zhong, Q. (2020). Rapid prediction of landslide dam stability using the logistic regression method. *Landslides*, 17(12), 2931-2956. <https://doi.org/10.1007/s10346-020-01414-6>
- Shrestha, A., Ezee, G., Adhikary, R., & Rai, S. (2012). *Resource manual on flash flood risk management. Module 3: structural measures*. International Centre for Integrated Mountain Development (ICIMOD). <https://www.cabdirect.org/cabdirect/abstract/20133037688>
- Stirling, M., McVerry, G., Gerstenberger, M., Litchfield, N., Van Dissen, R., Berryman, K., Barnes, P., Wallace, L., Villamor, P., & Langridge, R. (2012). National seismic hazard model for New Zealand: 2010 update. *Bulletin of the Seismological Society of America*, 102(4), 1514-1542. <https://doi.org/10.1785/0120110170>
- Statistics New Zealand. (2018). 2018 Census Data- West Coast Region <https://www.stats.govt.nz/tools/2018-census-place-summaries/west-coast-region>
- Tacconi Stefanelli, C., Casagli, N., & Catani, F. (2020). Landslide damming hazard susceptibility maps: a new GIS-based procedure for risk management. *Landslides*, 17(7), 1635-1648. <https://doi.org/10.1007/s10346-020-01395-6>
- Tacconi Stefanelli, C., Catani, F., & Casagli, N. (2015). Geomorphological investigations on landslide dams. *Geoenvironmental Disasters*, 2(1). <https://doi.org/10.1186/s40677-015-0030-9>
- Tacconi Stefanelli, C., Segoni, S., Casagli, N., & Catani, F. (2016). Geomorphic indexing of landslide dams evolution. *Engineering Geology*, 208, 1-10. <https://doi.org/10.1016/j.enggeo.2016.04.024>
- Takayama, S., Miyata, S., Fujimoto, M., & Satofuka, Y. (2021). Numerical simulation method for predicting a flood hydrograph due to progressive failure of a landslide dam. *Landslides*, 18(11), 3655-3670. <https://doi.org/10.1007/s10346-021-01712-7>
- Tasman District Council. (2022), Rain Event Recovery Page <https://www.tasman.govt.nz/my-property/building-and-alteration/rain-event-recovery-page/>

- Townend, J., Sutherland, R., Toy, V., Eccles, J., Boulton, C., Cox, S., & McNamara, D. (2013). Late-interseismic state of a continental plate-bounding fault: Petrophysical results from DFD-1 wireline logging and core analysis, Alpine Fault, New Zealand. *Geochemistry, Geophysics, Geosystems*, 14(9), 3801-3820. <https://doi.org/10.1002/ggge.20236>
- Weiss, A. (2001). Topographic position and landforms analysis. Poster presentation, ESRI user conference, San Diego, CA, [http://www.jennessent.com/downloads/tpi-poster-tnc\\_18x22.pdf](http://www.jennessent.com/downloads/tpi-poster-tnc_18x22.pdf)
- Wells, A., & Goff, J. (2007). Coastal dunes in Westland, New Zealand, provide a record of paleoseismic activity on the Alpine fault. *Geology*, 35(8), 731-734. <https://doi.org/10.1130/G23554A.1>
- Westoby, M. J., Glasser, N. F., Brasington, J., Hambrey, M. J., Quincey, D. J., & Reynolds, J. M. (2014). Modelling outburst floods from moraine-dammed glacial lakes. *Earth-Science Reviews*, 134, 137-159. <https://doi.org/10.1016/j.earscirev.2014.03.009>
- Wolter, A., Gasston, C., Morgenstern, R., Farr, J., Rosser, B., Massey, C., Townsend, D., & Tunnicliffe, J. (2022). The Hapuku Rock Avalanche: Breaching and evolution of the landslide dam and outflow channel revealed using high spatiotemporal resolution datasets. *Frontiers in Earth Science*, 1280. <https://doi.org/10.3389/feart.2022.938068>
- Wu, H., Trigg, M. A., Murphy, W., & Fuentes, R. (2022). A new global landslide dam database (RAGLAD) and analysis utilizing auxiliary global fluvial datasets. *Landslides*, 19(3), 555-572. <https://doi.org/10.1007/s10346-021-01817-z>
- Xu, C., Xu, X., Tian, Y., Shen, L., Yao, Q., Huang, X., Ma, J., Chen, X., & Ma, S. (2016). Two comparable earthquakes produced greatly different coseismic landslides: The 2015 Gorkha, Nepal and 2008 Wenchuan, China events. *Journal of Earth Science*, 27(6), 1008-1015. <https://doi.org/10.1007/s12583-016-0684-6>
- Xu, Q., Fan, X.-M., Huang, R.-Q., & Westen, C. V. (2009). Landslide dams triggered by the Wenchuan Earthquake, Sichuan Province, south west China. *Bulletin of engineering geology and the environment*, 68(3), 373-386. <https://doi.org/10.1007/s10064-009-0214-1>
- Zheng, H., Shi, Z., Shen, D., Peng, M., Hanley, K. J., Ma, C., & Zhang, L. (2021). Recent advances in stability and failure mechanisms of landslide dams. *Frontiers in Earth Science*, 9, 659935. <https://doi.org/10.3389/feart.2021.659935>
- Zhong, Q., Wang, L., Chen, S., Chen, Z., Shan, Y., Zhang, Q., Ren, Q., Mei, S., Jiang, J., & Hu, L. (2021). Breaches of embankment and landslide dams-State of the art review. *Earth-Science Reviews*, 216, 103597. <https://doi.org/10.1016/j.earscirev.2021.103597>
- Zhou, G. G., Cui, P., Chen, H., Zhu, X., Tang, J., & Sun, Q. (2013). Experimental study on cascading landslide dam failures by upstream flows. *Landslides*, 10(5), 633-643. <https://doi.org/10.1007/s10346-012-0352-6>
- Zhou, G. G. D., Zhou, M., Shrestha, M. S., Song, D., Choi, C. E., Cui, K. F. E., Peng, M., Shi, Z., Zhu, X., & Chen, H. (2019). Experimental investigation on the longitudinal evolution of landslide dam breaching and outburst floods. *Geomorphology*, 334, 29-43. <https://doi.org/10.1016/j.geomorph.2019.02.035>
- Zhu, Y., Peng, M., Cai, S., & Zhang, L. (2021). Risk-Based Warning Decision Making of Cascade Breaching of the Tangjiashan Landslide Dam and Two Smaller Downstream Landslide Dams. *Frontiers in Earth Science*, 9. <https://doi.org/10.3389/feart.2021.648919>